DEVELOPMENT OF GENERAL ELECTRO-MAGNETIC RESPONSE FUNCTION OF DIELECTRIC MATERIAL

THESIS SUBMITTED FOR THE DEGREE OF

DOCTOR OF PHILOSOPHY (SCIENCE)

OF

JADAVPUR UNIVERSITY

By

ANANYA BANERJEE

BIJOY KRISHNA GIRLS' COLLEGE

HOWRAH 711 101

WEST BENGAL, INDIA

MAY, 2019

DEVELOPMENT OF GENERAL ELECTRO-MAGNETIC RESPONSE FUNCTION OF DIELECTRIC MATERIAL

Ananya Banerjee

CERTIFICATE FROM THE SUPERVISORS

This is to certify that the thesis entitled "**DEVELOPMENT OF GENERAL ELECTRO-MAGNETIC RESPONSE FUNCTION OF DIELECTRIC MATERIAL**" submitted by **Ananya Banerjee** who got her name registered on 10 / 05 / 2012 for the award of **Ph.D. (Science) degree** of **Jadavpur University**, is absolutely based upon her own work under the supervision of Dr. Aloke Kr. Sarkar and Prof. Sujata Tarafdar and neither this thesis nor any part of its has been submitted for any degree / diploma or any other academic award anywhere before.

Aloke Kumar Sarkar 25.4.2019

Dr. Aloke Kr. Sarkar

Ex- Associate Professor
Department of Physics
Bijoy Krishna Girls' College
5/3, M.G. Road
Howrah-711 101

Dr. Aloke Kumar Sarkar
Associate Professor, Physics
Bijoy Krishna Girls' College
5/3, M. G. Road, Howrah-711 101

S. Tarafdar 07/05/2019

Prof. Sujata Tarafdar

Ex- Professor
Department of Physics
Jadavpur University
Kolkata-700 032

Professor
Department of Physics
Jadavpur University
Kolkata – 700 032

(Signature fo the Supervisors & date with official seal)

CONTENTS

PREFACE

The advancement of material research on soft materials and many complex materials have been encountered in material research so far. The investigation of dielectric aspect of the materials demand more studies on structure and dynamics of the material. Dielectric Spectroscopy (DS) has established its own advantages in this field compared other techniques especially when one involve in investigating electrical transport or characterization of bulk properties of the mentioned system. When an external electro-magnetic field is applied on dielectric material, the electrical polarization of the material reaches to a steady value, after a period of time. Similarly when the applied electric field is withdrawn the polarization decay due interaction with phonons and follows the identical law as the growth or decay function of dielectric polarization. The phenomenon is the basic relaxation process in a dielectric.

The thesis is started with the demonstration of general Debye response and a proposed simple nonlinear form of dielectric response function. Then it describes the dielectric spectroscopy and instrumentation used in this research work. Then it covers the theoretical development to calculate effective permittivity in case of metal dielectric composite like Dilute Magnetic Dielectric (DMD). The proposed theoretical formulation of DMD like composites (pearl and mica) with coupling term and its comparison with experimental result by UV-VIS spectroscopy shows a good qualitative agreement. Next an Experimental Investigation of Electrical, Optical Properties of DMS under external Magnetic Field is done and magnetoresistance is also calculated. In this work another indigenous optical experimental setup for investigation of magnetism in a DMD is attempted following Maxwell's EM theory. An improved version of the instrumentation could be a cost effective one for determination magnetism in such DMD specimens. Finaly, to investigate the magnetic nature of Dilute Magnetic Dielectrics (DMD) at low temperature, SQUID-magnetometry is used over the developed nano sized Gadolinium system. In this work magnetic moment is measured and magnetocalcaloric effect is also shown. Further, simple synthesis, high chemical stability, absence of magnetic and thermal hysteresis and insulating nature suggest them as potential magnetic refrigerants below the liquid hydrogen temperatures.

ACKNOWLEDGEMENTS

I owe my special debt of gratitude to my respected supervisors, Dr. Aloke Kr. Sarkar, Associate Professor, Dept. of Physics, B.K. Girls' College, Howrah not only for completion of my research work but also for constant support in times of difficulty. I offer my sincere gratitude to my other supervisor Prof. Sujata Tarafdar, Professor, Dept. of Physics, Jadavpur University, Kolkata, for constructive suggestion and encouragement and also spearheading the research activity by constant directive. I am indebted to my loving parents late Biswanath Banerjee and late Aparna Banerjee for their tireless support and encouragement above and beyond my work. I am thankful to the Department of Physics, B.K. Girls' College and Jadavpur University for their constant support. I express my sincere thanks to my colleagues, Mr. Arnab Ganguly, Mr. Arup Dutta,Mr. Somnath Paul and Ms. Aditi Sarkar who have extended their co-operation and technical assistance in an uncounted number of ways. I take this opportunity to sincerely acknowledge the Indian Institute of Technology (IIT), Kharagpur for offering its CRF facilities for SQUID VSM measurement.

I also wish to convey my special thanks to my brother Anirban Banerjee and sister-in-law Rommani Banerjee and friends for their love and support. Last but not the least; I would like to thank my dear husband Santanu Ghosal for his constant encouragement. Without his cooperation, I could not have completed my thesis work.

OBJECTIVE OF THE WORK

The electrical conductivity of ion-conducting solid is mostly dependent on dielectric behavior of the material. The nature of frequency dispersion of electrical conductivity of the solid may be determined by a.c. dielectric function or dielectric response. This thesis is dedicated towards the development of a simple nonlinear non Debye form of dielectric response function. The proposed function of dielectric response is capable to reproduce other existing response function along with some new features. Hence, following Maxwell Garnett Theory (MGT) and using the modified Clausius-Mossotti relation, the effective relative permittivity of the composite medium is formulated. Effect of electromagnetic coupling in case of dielectric composite like Dilute Magnetic Dielectric (DMD) is introduced. The work of the thesis is also concerned with synthesis of DMD like composites and its comparison with experimental result by UV-VIS spectroscopy with theoretical formulation shows a good qualitative agreement. In this work another indigenous optical experimental setup for investigation of magnetism in a DMD is designed. Authors have investigated dielectric response for four DMD sulfide sample. All samples were synthesized following chemical and green techniques. An improved version of the instrumentation could be a cost effective one for determination magnetism in such DMD specimens. Finally, to investigate the magnetic nature of DMD at low temperature, SQUID-magnetometry is used over the developed sample. One of them is Gadolinium oxide nanoparticles which play a central role in multimodal imaging, targeting the cancer cells and drug delivery in medical science. In this work bulk magnetic moment is measured and magnetocalcaloric effect is also shown, which may be potential magnetic refrigerants below the liquid hydrogen temperatures.

LIST OF FIGURES

LIST OF TABLES

LIST OF PUBLICATIONS

---

1. Ananya Banerjee and A Sarkar ,General Dielectric Response and A.C. Conductivity, *Asian .J. Chemistry*, Vol 23,No 12,2011,5561-62, ISBN ISSN. 0970-7077

2. Ananya Banerjee and A. Sarkar Formulation of Dielectric Behaviour of Composite Material, *Advanced Material Research*, vol 665,168-171,2012 Trans Tech Publication Switzerland, ISSN: 1662-8985

3. Ananya Banerjee and A. Sarkar, Effective Dielectric Constant of Dilute Magnetic Dielectrics**,** *International Journal of Engineering Research and Technology*, 2013 **1**, 1, 2013, 18-19.

4. Ananya Banerjee and A.Sarkar, Variation of Effective Dielectric Constant of Dilute Magnetic Dielectrics with Magnetic Field, *AIP Conf. proc* , 1591, (2014),1583-1585.

5. Ananya Banerjee and A.Sarkar, Optical Investigation of Effective Permeability of Dilute Magnetic Dielectrics with Magnetic Field, *AIP Conf. proc* , 1728, 020391 (2016),

6. Ananya Banerjee and A.Sarkar, An Experimental Investigation of Electrical, Optical Properties Of DMS Under External Magnetic Field (ICC 2017) *AIP Conf. proc* 1953(1):050019(2018).

7. Ananya Banerjee and A.Sarkar, Investigation of Effective Permeability and dielectric aspect of Dilute Magnetic Dielectrics by Optical Method, *Indian Journal of Physics* (communicated) 2019.

8. Ananya Banerjee S Paul and A.Sarkar, Low Temperature Study of Magnetism in Gd system using SQUID magnetometry, Adv .in App.Sci.Res (communicated) 2019.

CHAPTER 1

INTRODUCTION

1.1 Classification of material in regards of electrical conduction

On the basis of electrical conductivity, the materials can be classified into the following categories:

a) Conductors/Metals

Metals in general have high electrical conductivity and thermal conductivity along with high density. Typically they are malleable and ductile, deforming under stress without cleaving. In terms of optical properties, metals are shiny and lustrous.

The electrical and thermal conductivities of metals originate from the fact that their outer electrons are delocalized. This situation can be visualized by seeing the atomic structure of a metal as a collection of atoms embedded in a sea of highly mobile electrons. The electrical conductivity, as well as the electrons' contribution to the heat capacity and heat conductivity

of metals can be calculated from the free electron model, which does not take into account the detailed structure of the ion lattice.

When considering the electronic band structure and binding energy of a metal, it is necessary to take into account the positive potential caused by the specific arrangement of the ion cores which is periodic in crystals. The most important consequence of the periodic potential is the formation of a small band gap at the boundary of the Brillouin zone. Mathematically, the potential of the ion cores can be treated by various models, the simplest being the nearly free electron model.

b) Semiconductor

A semiconductor material has an electrical conductivity value falling between that of a conductor (e.g. copper), and an insulator (e.g. glass). Their resistance decreases as their temperature increases, which is behavior opposite to that of a metal. Their conducting properties may be altered in useful ways by the deliberate, controlled introduction of impurities ("doping") into the crystal structure. Where two differently-doped regions exist in the same crystal, a semiconductor junction is created. The behavior of charge carriers which include electrons, ions and electron holes at these junctions is the basis of diodes, transistors and all modern electronics.

Semiconductor devices can exhibit a range of useful properties such as passing current more easily in one direction than the other, showing variable resistance and sensitivity to light or heat. Because the electrical properties of a semiconductor material can be modified by doping, or by the application of electrical fields or light, devices made from semiconductors can be used for amplification, switching, and energy conversion.

The modern understanding of the properties of a semiconductor relies on quantum physics to explain the movement of charge carriers in a crystal lattice [1]. Doping greatly increases the number of charge carriers within the crystal. When a doped semiconductor contains mostly free holes it is called "p-type", and when it contains mostly free electrons it is known as "n-type". The semiconductor materials used in electronic devices are doped under precise

conditions to control the concentration and regions of p- and n-type dopants. A single semiconductor crystal can have many p- and n-type regions; the p–n junctions between these regions are responsible for the useful electronic behavior.

c) Dielectric

A dielectric (or dielectric material) is in general an electrical insulator that can be polarized by an applied electric field. When a dielectric is placed in an electric field, electric charges do not flow through the material as they do in an electrical conductor, but only slightly shift from their average equilibrium positions causing dielectric polarization. Because of dielectric polarization, positive charges are displaced toward the field and negative charges shift in the opposite direction. This creates an internal electric field that reduces the overall field within the dielectric itself [1]. If a dielectric is composed of weakly bonded molecules, those molecules not only become polarized, but also reorient so that their symmetry axes align to the field [1].The study of dielectric properties concerns storage and dissipation of electric and magnetic energy in materials dielectrics [2] and are important for explaining various phenomena in electronics, optics, solid-state physics, and cell biophysics.

Although the term insulator implies low electrical conduction, dielectric typically means materials with a high polarizability. The latter is expressed by a number called the relative permittivity (also known as dielectric constant). The term insulator is generally used to indicate electrical obstruction while the term dielectric is used to indicate the energy storing capacity of the material (by means of polarization). A common example of dielectric is the electrically insulating material between the metallic plates of a capacitor. The polarization of the dielectric [1] by the applied electric field increases the capacitor's surface charge for the given electric field strength.

1.2 Dielectrics and their characteristics

Dielectric parameters play a critical role in many technological areas. These areas include electronics, microelectronics, remote sensing, radiometry, and dielectric heating. When an Electro-Magnetic (EM) field is applied to a material, the atoms, molecules, free charge, and defects adjust positions. If the applied field is static, then the system will eventually reach an equilibrium state. However, if the applied field is time dependent then the material will continuously relax in the applied field, but with a time lag. The time lag is due to screening, coupling, friction, and inertia. A number of processes are occurring during relaxation, such as heat conversion processes, lattice phonon, and photon phonon coupling. Dielectric relaxation can be a result of dipolar and induced polarization, lattice-phonon interactions, defect diffusion, higher multipole interactions or the motion of free charges. Time-dependent fields produce in equilibrium behavior in the materials due to the heat generated in the process and the constant response to the applied field. However, for linear materials and time-harmonic fields, the response is averaged over a cycle, if heating is appreciable; non-equilibrium effects such as entropy production relate more to temperature effects than the driving field stimulus. The dynamic readjustment of the molecules in response to the field is called relaxation and is distinct from resonance. For example, if a dc electric field is applied to a polarizable dielectric and then the field is suddenly turned off, then the dipoles will relax over a characteristic relaxation time into a more random state. The response of materials depends strongly on material composition and lattice structure. The relationship between the electric field **E** and the electric dipole moment **P** gives rise to the behavior of the dielectric, which, for a given material, can be characterized by the relation:

$$\mathbf{P} = \alpha \mathbf{E} \tag{1.1}$$

Where, α is the polarizability.

1.2.1 Macroscopic and Local Electro-magnetic Fields in Materials

The microscopic description of the EM fields in a material is complicated. As a field is applied to a material, charges reorient to form new fields that oppose the applied field. In

addition, a dipole tends to polarize its immediate environment, which modifies the field that dipole experiences. The field that polarizes a molecule is the local field E_l and the induced dipole moment is $p = \alpha.E_l$. In order to use this expression in Maxwell's equations, the local field [4] needs to be expressed in terms of the macroscopic field. Calculation of this relationship is a rigorous one. To the first approximation, the macroscopic field, is related to the external or applied field ($\mathbf{E}_a$), and the depolarization field, given by

$$\mathbf{E} = \mathbf{E_a} - \frac{\mathbf{P}}{3\varepsilon_0} \tag{1.2}$$

Where, ε_0 is the electric permittivity of free space and P is the polarization. The local field is composed of the macroscopic field and a material-related field. In the literature, the effective local field is commonly modeled by the Lorentz field, which is defined as the field in a small cavity that is carved out of a material around a specific site, but excludes the field of the observation dipole. A well known example of the relationship between the applied, macroscopic, and local fields is given by an analysis of the Lorentz spherical cavity in a static electric field. For a Lorentz sphere the local field is the sum of applied, depolarization, Lorentz, and atomic fields [3,4]

$$\mathbf{E} = \mathbf{E_a} + \mathbf{E_{depol}} + \mathbf{E_l} + \mathbf{E_{atom}} \tag{1.3}$$

For cubic lattices in a spherical cavity, the Lorentz local field is related to the macroscopic field and polarization by

$$\mathbf{E_l} = \mathbf{E} + \frac{\mathbf{P}}{\mathbf{3\varepsilon_0}} \tag{1.4}$$

In the case of a sphere, the local field in Eq. (1.4) equals the applied field. For induced dipoles,

$$\mathbf{P} = N\alpha\mathbf{E_l} \tag{1.5}$$

Where, N is the density of dipoles, and Eq. (1.4) yields

$$\mathbf{E_l} = \mathbf{E}/(1 - N\alpha/3\varepsilon_0) = \mathbf{P}/N\alpha. \tag{1.6}$$

Onsager [5] generalized the Lorentz theory by distinguishing between the internal field that acts on induced dipoles and the directing field that acts on permanent dipoles. If we use $P = \varepsilon_0 (\varepsilon_r - 1)E$ in Eq. (1.4), we find $\mathbf{E_l} = ((\varepsilon_r + 2)/3)E$. Therefore, for normal materials the Lorentz field exceeds the macroscopic field. For a material where the permittivity is negative we can have $\mathbf{E_l} \leq \mathbf{E}$. In principle, we can null out the Lorentz field when $\varepsilon_r = -2$. Some of the essential problems encountered in microscopic constitutive theory center around the local field. Note that for some materials, recent research indicates that the Lorentz local field does not always lead to the correct polarizabilities [6]. We expect the Lorentz local field expression to break down near interfaces.

A rigorous expression for the static local field created by a group of induced dipoles can be obtained by an iterative procedure [7] using $p_i = \alpha_i E_l (r_i)$ and

$$\mathbf{E_i}(\mathbf{r_j}) = \mathbf{E_a} + \sum_{\mathbf{i=1, i\neq j}}^{\mathbf{n}} \mathbf{E_{ij}}(\mathbf{r_j}) \tag{1.7}$$

Where,
$$\mathbf{E_{ij}}(\mathbf{r_j}) \approx \frac{\mathbf{1}}{\mathbf{4\pi\varepsilon_0}} \left[\frac{\mathbf{3(r_j - r_i)P(r_i)}}{|\mathbf{r_j - r_i}|^{\mathbf{5}}} - \frac{\mathbf{P(r_i)}}{|\mathbf{r_j - r_i}|^{\mathbf{5}}} \right] \tag{1.8}$$

If there are also permanent dipoles, they need to be included as $p(r_i) = p_p(r_i) + \alpha_i E_l(r_i)$.

Over the years, many models of polar and non polar materials have been developed that use different approximations to the local field. The Clausius- Mossotti equation was developed for Non-interacting, non-polar molecules governed by the Lorentz equation for the internal field. This equation works well for non-polar gases and liquids. Debye introduced a generalization of the Clausius-Mossotti equation for the case of polar molecules. Onsager developed an extension of Debye's theory by including the reaction field and a more comprehensive local field expression [5]. For a dielectric composed of permanent dipoles, the polarization is written in terms of the local field as Eq. (1.6) There are electronic, ionic, and permanent dipole polarizability contributions, so that $\mu_d = (\alpha_{el} + \alpha_{ion} + \alpha_p)\mathbf{E_l}$, $\alpha_{el} = 4\pi\varepsilon_0 R^3 / 3$, $\alpha_{ion} = e^2 / Yd_0$. Here, Y is Young's modulus, R is the radius and d_0 is the equilibrium separation of the ions, and $\alpha_p = \mu e^2/3kBT$, where μ_e is the permanent dipole moment.

There may also be a contribution to the polarizability due to excess charge at microscopic interfaces. Using the Lorentz expression for the local field, the polarization can be written as

$$\mathbf{P} = \mathrm{N}\alpha(\mathbf{E} + \frac{\mathbf{P}}{3\varepsilon_0}) \tag{1.9}$$

$$\boldsymbol{P} = \frac{\mathrm{N}\alpha\mathbf{E}}{1-\mathrm{N}\alpha/3\varepsilon_0} = \varepsilon_0(\varepsilon_\mathrm{r} - 1)\mathbf{E} \tag{1.10}$$

This is the Clausius-Mossotti relation that is commonly used to estimate the permittivity of non-polar materials from atomic polarizabilities

$$\frac{\varepsilon_r - 1}{\varepsilon_r + 2} = \frac{N\alpha}{3\varepsilon_0} \tag{1.11}$$

$$\varepsilon_r = \frac{3\varepsilon_0 + 2N\alpha}{3\varepsilon_0 - N\alpha} \tag{1.12}$$

The Clausius-Mossotti relation relates the permittivity to the polarizability. The polarizability is related to the vector dipole moment μ_d of a molecule or atom and the local field $\mathrm{E_l}$, $\mu_\mathrm{d} = \alpha.\mathrm{E_l}$. In principle, once the polarizability is determined for a group of molecules, then the permittivity of the ensemble can be calculated with the implicit assumption that there are many molecules located over the distance of a wavelength. Typical polarizabilities of atoms are between 0.1 and 100 Fm^2 [8]. Polarizabilities of molecules can be higher than for atoms. The local field for a sphere is related to the polarization by Eq. (1.14). A generalization of the Clausius-Mossotti equation to include a permanent moment μ_e is summarized in what is called the Debye equation that is valid for gases and dilute solutions

$$\frac{\varepsilon_r - 1}{\varepsilon_r + 2} = \frac{N(\mu_e^2)}{3KT} \tag{1.13}$$

1.2.2 Dielectric polarization

In the classical approach to the dielectric model, a material is made up of atoms. Each atom consists of a cloud of negative charge (electrons) bound to and surrounding a positive point charge at its center. In the presence of an electric field the charge cloud is distorted, as shown in the top right of the figure 1.1.

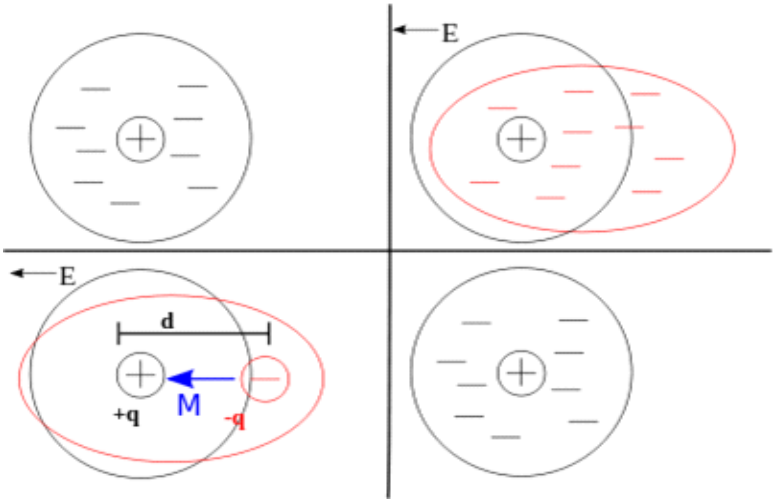

Figure 1.1: Electric field interaction with an atom under the classical dielectric model.

This can be reduced to a simple dipole using the superposition principle. A dipole is characterized by its dipole moment, a vector quantity shown in the figure as the blue arrow labeled M. It is the relationship between the electric field and the dipole moment that gives rise to the behavior of the dielectric. (Note that the dipole moment points in the same direction as the electric field in the figure. This isn't always the case, and is a major simplification, but is true for many materials.)

When the electric field is removed the atom returns to its original state. The time required to do so is the so-called relaxation time; an exponential decay.

1.2.2.1 Dipolar polarization

Dipolar polarization is a polarization that is either inherent to polar molecules (orientation polarization), or can be induced in any molecule in which the asymmetric distortion of the nuclei is possible (distortion polarization). Orientation polarization results from a permanent dipole, e.g., that arising from the 104.45° angle between the asymmetric bonds between oxygen and hydrogen atoms in the water molecule, which retains polarization in the absence of an external electric field. The assembly of these dipoles forms a macroscopic polarization.

When an external electric field is applied, the distance between charges within each permanent dipole, which is related to chemical bonding, remains constant in orientation polarization; however, the direction of polarization itself rotates. This rotation occurs on a timescale that depends on the torque and surrounding local viscosity of the molecules. Because the rotation is not instantaneous, dipolar polarizations lose the response to electric fields at the highest frequencies. A molecule rotates about 1 radian per pico second in a fluid, thus this loss occurs at about 10^{11} Hz (in the microwave region). The delay of the response to the change of the electric field causes friction and heat.

When an external electric field is applied at infrared frequencies or less, the molecules are bent and stretched by the field and the molecular dipole moment changes. The molecular vibration frequency is roughly the inverse of the time it takes for the molecules to bend, and this distortion polarization disappears above the infrared.

1.2.2.2 Ionic polarization

Ionic polarization is polarization caused by relative displacements between positive and negative ions in ionic crystals (eg, NaCl). If a crystal or molecule consists of atoms of more than one kind, the distribution of charges around an atom in the crystal or molecule leans to positive or negative. As a result, when lattice vibrations or molecular vibrations induce relative displacements of the atoms, the centers of positive and negative charges are also displaced. The locations of these centers are affected by the symmetry of the displacements. When the centers don't correspond, polarizations arise in molecules or crystals. This polarization is called ionic polarization.

Ionic polarization causes the ferroelectric effect as well as dipolar polarization. The ferroelectric transition, which is caused by the lining up of the orientations of permanent dipoles along a particular direction, is called an order-disorder phase transition. The transition caused by ionic polarizations in crystals is called a displacive phase transition.

1.2.3 Electric susceptibility

The electric susceptibility χ_e of a dielectric material is a measure of how easily it polarizes in response to an electric field. This, in turn, determines the electric permittivity of the material and thus influences many other phenomena in that medium, from the capacitance of capacitors to the speed of light.

It is defined as the constant of proportionality (which may be a tensor) relating an electric field **E** to the induced dielectric polarization density **P** such that

$$\mathbf{P} = \varepsilon_0 \chi_e \mathbf{E} \tag{1.14}$$

Where, ε_0 is the electric permittivity of free space. The susceptibility of a medium is related to its relative permittivity ε_r by

$$\chi_e = \varepsilon_r - 1 \tag{1.15}$$

So in the case of a vacuum,

$$\chi_e = 0 \tag{1.16}$$

The electric displacement **D** is related to the polarization density **P** by

$$\boldsymbol{D} = \varepsilon_0 \boldsymbol{E} + \boldsymbol{P} = \varepsilon_0 \varepsilon_r \boldsymbol{E} \tag{1.17}$$

1.2.4 Dispersion and causality

In physics, dielectric dispersion is the dependence of the permittivity of a dielectric material on the frequency of an applied electric field. Because there is a lag between changes in polarization and changes in the electric field, the permittivity of the dielectric is a complicated function of frequency of the electric field. Dielectric dispersion is very important for the applications of dielectric materials and for the analysis of polarization systems. This is one instance of a general phenomenon known as material dispersion that is a

frequency-dependent response of a medium for wave propagation. When the frequency becomes higher, dipolar polarization can no longer follow the oscillations of the electric field in the microwave region around 10^{10} Hz, ionic polarization and molecular distortion polarization can no longer track the electric field past the infrared or far-infrared region around 10^{13} Hz and electronic polarization loses its response in the ultraviolet region around 10^{15} Hz. In the frequency region above ultraviolet, permittivity approaches the constant ε_0 in every substance, where ε_0 is the permittivity of the free space. Because permittivity indicates the strength of the relation between an electric field and polarization, if a polarization process loses its response, permittivity decreases.

In general, a material cannot polarize instantaneously in response to an applied field. The more general formulation as a function of time is

$$\boldsymbol{P}(t) = \varepsilon_0 \int_{-\infty}^{t} \chi_e\,(t-\tau)\boldsymbol{E}(\tau)d\tau \tag{1.18}$$

The polarization is a convolution of the electric field at previous times with time-dependent susceptibility given by $\chi_e(\Delta t)$. The upper limit of this integral can be extended to infinity as well if one defines $\chi_e(\Delta t) = 0$ for $\Delta t < 0$. An instantaneous response corresponds to Dirac delta function susceptibility $\chi_e(\Delta t) = \chi_e\delta(\Delta t)$. It is more convenient in a linear system to take the Fourier transform and write this relationship as a function of frequency. Due to the convolution theorem, the integral becomes a simple product,

$$\mathbf{P} = \varepsilon_0\chi_e\mathbf{E} \tag{1.19}$$

Note the simple frequency dependence of the susceptibility, or equivalently the permittivity. The shape of the susceptibility with respect to frequency characterizes the dispersion properties of the material. Moreover, the fact that the polarization can only depend on the electric field at previous times (i.e., $\chi_e(\Delta t) = 0$ for $\Delta t < 0$, a consequence of causality, imposes Kramers–Kronig constraints on the real and imaginary parts of the susceptibility $\chi_e(\omega)$.

1.3 Dielectric response (Debye and Non-Debye)

Overview of Linear-Response Theory Models of relaxation that are based on statistical mechanics can be developed from linear-response theory. Linear-response theory uses an approximate solution of Liouville's equation and a Hamiltonian that contains a time-dependent relationship of the field parameters based on a perturbation expansion. This approach shows how the response functions and relaxation are related to time dependent polarization correlation functions. The polarization P (t), is related to the response function Φ(t) and the external field E, is given by

$$\mathbf{P}(\mathrm{t}) = \int_{-\infty}^{\mathrm{t}} \phi(\mathrm{t}-\tau)\mathbf{E}(\tau)\mathrm{d}\tau \tag{1.20}$$

Where, $\varphi(t - \tau) = 0$ for $t - \tau < 0$. The susceptibility is defined as,

$$\chi(\omega) = \int_0^{\infty} \phi(t) e^{-i\omega\tau} d\tau = \chi'(\omega) - \chi''(\omega) \tag{1.21}$$

In many solids, such as solid polyethylene, the molecules are not able to appreciably rotate or polarize in response to applied fields, indicating a low permittivity and small dispersion. The degree of crystallinity, existence of permanent dipoles, dipole-constraining forces, mobility of free charge and defects all contribute to dielectric response.

The electrical/optical conductivity of ion-conducting solid is mostly dependent on dielectric behavior [12] of the material. The nature of frequency dispersion of electrical conductivity and or dielectric constant of the solid may be determined by a.c. dielectric function or dielectric response. The simplest form of the linear response is the Debye response theory [12].

It is known that when an external field is applied to the dielectric, polarization of the material reaches its equilibrium value, not instantly, but over a period of time. By analogy, when the field is removed suddenly, the polarization decay caused by thermal motion follows the same law as the relaxation or decay function of dielectric polarization

$$\phi(t) = \frac{P(t)}{P(t)} \tag{1.22}$$

Where, P is a polarization vector of a sample unit. The relationship for the dielectric displacement vector D(t) in the case of time dependent fields may be written as follows [8,9]:

$$\mathrm{D(t)} = \varepsilon_\infty \mathbf{E(t)} + \int_{-\infty}^{\mathrm{t}} \frac{\mathrm{d}\Phi(\mathrm{t}')}{\mathrm{d}(\mathrm{t}')} \mathbf{E}(\mathrm{t}-\mathrm{t}')\mathrm{d}(\mathrm{t}') \tag{1.23}$$

$$\mathbf{D(t)} = \varepsilon_0 \mathbf{E(t)} + \mathbf{P(t)} \tag{1.24}$$

Where, ε_0 is the dielectric permittivity of free space, ε_∞ is the high frequency limit of the complex dielectric permittivity$\varepsilon^*(\omega)$, and $\phi(t)$ is the dielectric response function

$\Phi(t) = (\varepsilon_s - \varepsilon_\infty)[1 - \phi(t)]$, where ε_0 is the low-frequency limit of the complex dielectric permittivity. The complex dielectric permittivity $\varepsilon^*(\omega)$, is connected with the relaxation function by a very simple relationship [8,9]

$$\frac{\varepsilon^*(\omega)-\varepsilon_\infty}{\varepsilon_s-\varepsilon_\infty} = \hat{L}[-\frac{d}{dt}\phi(t)] \tag{1.25}$$

Where, $\hat{L}$is the operator of the Laplace transform, which is defined for the arbitrary time-dependent function f(t) as

$$\hat{L}[f(t)] = \int_0^\infty e^{-pt} f(t) dt \tag{1.26}$$

Where, $P = i\omega$. If

$$\phi(t) = \exp(-t/\tau_m) \tag{1.27}$$

Where, τ_m represents the characteristic dielectric relaxation time, then the relation first obtained by Debye is true for the frequency domain [8-10].

$$\frac{\varepsilon^*(\omega)-\varepsilon_\infty}{\varepsilon_s-\varepsilon_\infty} = \frac{1}{1+i\omega\tau_m} \tag{1.28}$$

For most of the systems being studied, the relationship above does not sufficiently describe the experimental results. This causes the necessity for empirical relationships, which formally take into account the distribution of the relaxation of a continuous distribution of relaxation times τ. In the most general way such Non-Debye dielectric behavior can be

described in terms, g(τ) [9]. This implies that the complex dielectric permittivity can be presented as follows:

$$\frac{\varepsilon^*(\omega)-\varepsilon_\infty}{\varepsilon_s-\varepsilon_\infty} = \int_0^\infty \frac{g(\tau)}{i\omega\tau}\, d\tau \qquad (1.29)$$

Where, distribution function g(τ) satisfies normalization condition

$$\int_0^\infty g(\tau)\, d\tau = 1 \qquad (1.30)$$

The corresponding expression for the decay function is

$$\phi(t) = \int_0^\infty g(\tau)\, e^{-t/\tau} d\tau \qquad (1.31)$$

Frequency and time representation the g(τ) calculation does not by itself provide anything more than another way of describing the dynamic behavior of the dielectric in time domain [11]. Moreover, such a calculation is a mathematically ill-posed problem [12-13], which can provide a clearer physical interpretation [13-14]. In most cases of non-Debye dielectric spectrums the data have been described by the so called Havriliak–Negami (HN) relationship [9-10,15]

$$\varepsilon^*(\omega) = \varepsilon_\infty + \frac{\varepsilon_s-\varepsilon_\infty}{[1+(i\omega\tau_m)^\alpha]^\beta} \quad 0 < \alpha, \beta < 1 \qquad (1.32)$$

Where α and β are empirical exponents. The specific case α =1; β=1 gives the Debye relaxation law, β=1, ≠1 corresponds to the so-called Cole– Cole (CC) [16] equation 1.32, whereas the case α =1, β ≠1 corresponds to the Cole–Davidson (CD) formula [17].

Sometimes in the case of superposition of relaxation processes with dc and ac conductivities the high and low frequency asymptotic forms are usually assigned to Jonscher power-law wings $(i\omega\tau_i)^{(n_i-1)}$ (n_i is a Jonscher stretch parameter, and τ_i is the correspondent characteristic relaxation time) [15,16]. Notice that the real part $\varepsilon'\omega$) of the complex dielectric permittivity is proportional to the imaginary part $\sigma''(\omega)$ of the complex ac-conductivity$\sigma^*(\omega)$, $\varepsilon'(\omega) \infty -\sigma''(\omega)/(\omega)$, and the dielectric losses ε'' is proportional to the real part $\sigma'(\omega)$ of the ac conductivity, $\varepsilon''(\omega) \infty \sigma'(\omega)/(\omega)$, The latter arises from the Jonscher term

and has the form, $\sigma'(\omega) \infty \omega^{u}j$, which has been termed ‘‘universal’’ due to its appearance in many types of disordered systems [18,19].

1.3.1 The response function developed and presented in this work

A simple nonlinear form of dielectric response function is proposed. The proposed form is an essential extension of Debye linear response and simple one following L-C-R electric analogue of material to depict a non-Debye response function. The function of dielectric response is capable to reproduce existing other response function along with some new features. The corresponding form of a.c. electrical conductivity is also extracted.

1.3.1.1 Theory

For the case of ideal dielectrics, Debye (1924) has formulated a relaxation model [1]

$$\varepsilon^*(\omega) = \varepsilon_\infty + \frac{\varepsilon_s - \varepsilon_\infty}{1+i\omega\tau} \tag{1.33}$$

Where ε^* is the complex dielectric constant ε_s and ε_∞ are respectively, dielectric permittivity at the frequencies ω=0 which is Static dielectric permittivity and ω=∞ which is optic dielectric permittivity. The single relaxation time τ corresponds to single relaxation process.

In general, such relaxations are really observed in practice. Multiple relaxation or distribution of relaxations is found in real materials. The most commonly observed simple Non Debye relaxation distributions are the Cole-Cole [16], Davidson Cole [17], Havriliak Negami [15] distribution.

According to our model, let us introduce a Differential equation,

$$\frac{d^2P}{dt^2} + \frac{A}{\tau}\frac{dP}{dt} + \frac{Bp}{\tau^2} = \frac{\alpha E}{\tau^2} \tag{1.34}$$

Solution of this differential equation is,

$$P = \frac{\alpha E}{(B-\omega^2\tau^2 + j\omega A\tau)} \tag{1.35}$$

Using the above equations one may express, the real and imaginary parts of the dielectric constant, and hence the a.c. conductivity in terms of frequency ω and relaxation timeτ.

$$\varepsilon^* = \varepsilon_\infty + \frac{(\varepsilon_S-\varepsilon_\infty)}{(B-\omega^2\tau^2+j\omega A\tau)} \tag{1.35}$$

$$\varepsilon' = \varepsilon_\infty + \frac{(\varepsilon_S-\varepsilon_\infty)(B-\omega^2\tau^2)}{(B-\omega^2\tau^2)^2+(A\omega\tau)^2} \tag{1.36}$$

$$\varepsilon'' = \frac{(\varepsilon_S-\varepsilon_\infty)A\omega\tau}{(B-\omega^2\tau^2)^2+(A\omega\tau)^2} \tag{1.37}$$

$$\sigma^*(\omega) = \sigma(0) + \frac{\varepsilon_0(\varepsilon_S-\varepsilon_\infty)A\omega^2\tau}{(B-\omega^2\tau^2)^2+(A\omega\tau)^2} \tag{1.38}$$

$\omega \ll 1/\tau$ $$\sigma^*(\omega) = \sigma(0) + \frac{\varepsilon_0(\varepsilon_S-\varepsilon_\infty)A\omega^2\tau}{B^2} \tag{1.39}$$

For $\omega \gg 1/\tau$ $$\sigma^*(\omega) = \sigma(0) + \frac{\varepsilon_0(\varepsilon_S-\varepsilon_\infty)}{\omega^2\tau^3} \tag{1.40}$$

1.3.1.2 Results and Discussion

The result obtained from this elementary is quite reasonable. The obtained expression for σ(ω) given in equation (1.38) has a singularity at $\omega\tau = \sqrt{B}$ and precisely at $\omega\tau = 1$ with $B^2=1+A$

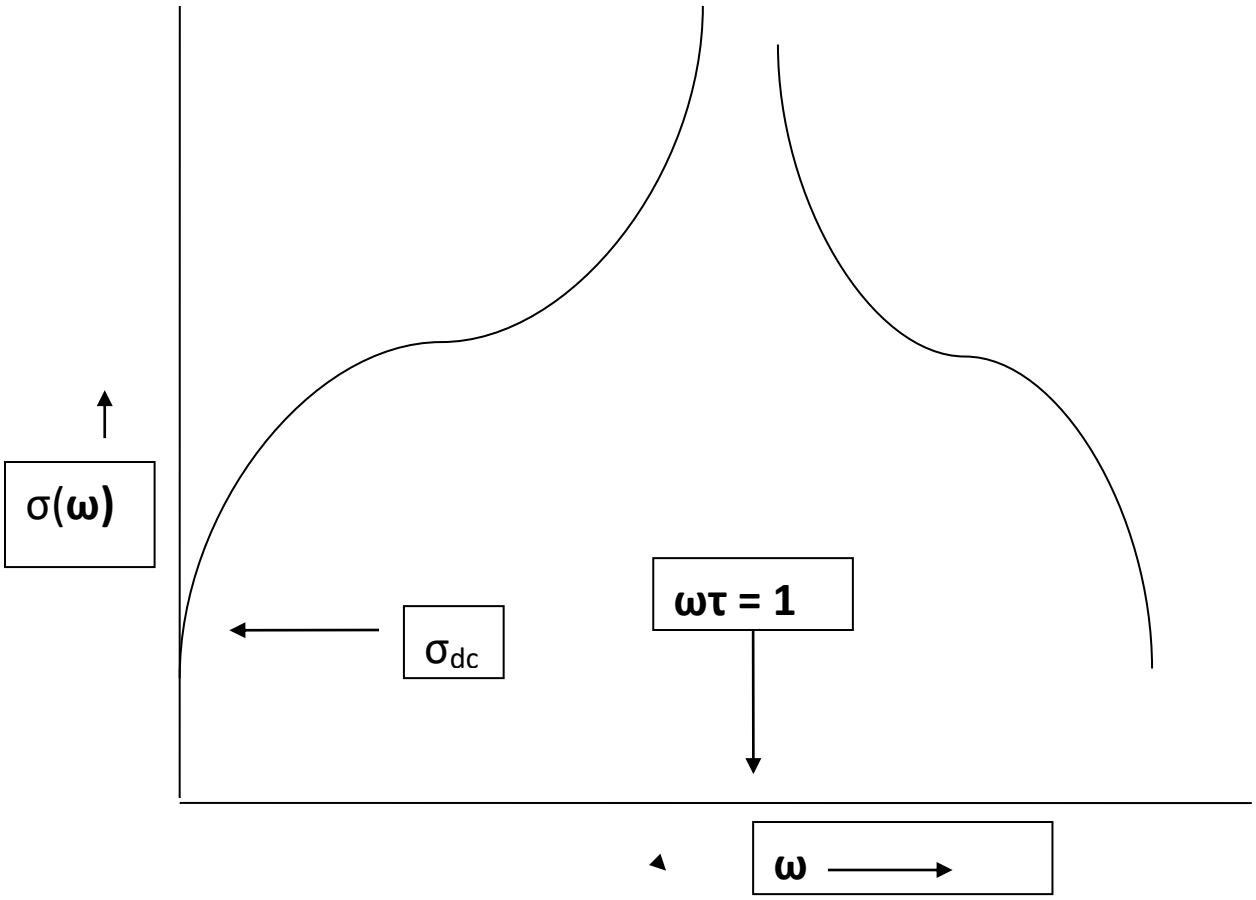

Figure.1.2: Variation of a.c. conductivity σ(ω) with frequency ω of electric field

In fact it limits, the choice of parameter A and B, moreover A and B may be determined theoretically with physical consistency condition. The overall nature of real ε may be compared with that of complex functional material.

$\omega \ll \frac{1}{\tau}$, $\omega^2\tau^2$ may be neglected and reduces to Debye case. With increase in $\omega\tau$ so that $\omega^2\tau^2$ has a contribution comparable to $\omega\tau$, gives a new result may explain many anomalous $\varepsilon(\omega)$ or $\sigma(\omega)$ dispersion. For $\omega\tau=1$or $\omega \gg \frac{1}{\tau}$ the term $\omega\tau$ may be neglected**.**

Figure 1.2 shows variation of $\sigma(\omega)$ with ω following equation (1.38).The equation (1.38) is the outcome of this present theoretical calculation. The low frequency part of a.c. conductivity $\sigma(\omega)$ shows about ω^2 variation and $\frac{1}{\omega^2}$ variation in the high frequency domain. In frequency domain $\omega\tau \approx 1$, $\sigma(\omega)$ has singularities, representing physical phenomenon in charge transport mechanism in solid. The obtained response function in the frequency region $\omega\tau \gg 1$ corresponds to frequencies higher than phonon frequencies of system. The nature of $\sigma(\omega)$ in the mentioned region is the optical conductivity in a dielectric system. The proposed dielectric response and hence the calculated a.c. conductivity $\sigma(\omega)$ account the overall spectrum very well. The high frequency region provides a good qualitative account of optical conductivity showing Drude nature [20, 21].

The proposed dielectric constant provides a fair account of a.c. conductivity in both low and high frequency limit. In low frequency limit it can reproduce the pioneer Debye response however in the high frequency limit it provides more physical aspect of optical conductivity.

1.4 Magnetic Response

In this section, overview the basic elements of magnetic phenomena needed in our applications to EM interactions. Magnetism has a quantum-mechanical origin intimately related to the spin and angular momentum and currents of electrons, nuclei, and other particles. Stern and Gerlach [3] proved the existence of discrete magnetic moments by observing the quantized deflection of silver atoms passing through a spatially varying magnetic field. Electrons orbiting a nucleus form a magnetic moment as well as the intrinsic spin of the electron. Magnetic moments are caused either by intrinsic quantum mechanical spin or by currents flowing in closed loops m $\propto$ (current)(area). Spins react to a magnetic

field by precessing around the applied field with damping [22]. For spins of the nucleus, this precession forms the study of nuclear magnetic resonance (NMR); for paramagnetic materials it is called electron-spin or ESR or electron-paramagnetic resonance or EPR; and for ferromagnetic materials it is called ferromagnetic resonance or FMR. The dynamics in spin systems are tied phenomena such as spin precession, relaxation, eddy currents, spin waves, and voltages induced by domain-wall movements. [7-9, 23].

Paramagnetism originates from spin alignment in an applied magnetic field and relates to the competition between thermal versus magnetic energy (**m.B**/ k_BT). Paramagnets do not retain significant magnetization in the absence of an applied magnetic field, since thermal motion tend to randomize the spin orientations.

The origin of diamagnetism in materials is the orbital angular momentum of the electrons in applied fields. Diamagnetic materials usually do not have a strong magnetic response, although there are exceptions. In ferromagnetic materials, exchange coupling allows regions of aligned spins to be formed [24].

Ferromagnetic and ferrimagnetic materials may have spin resonances in microwave to millimeter wave frequencies [25]. Ferrimagnetic materials consist of two overlapping lattices whose spins are oppositely directed, but with a larger magnetic moment in one lattice than the other. Antiferromagnetism is a property of many transition elements and some metals. In these materials the atoms form an array with alternating spin moments, so the average spin and magnetic moment are zero. Antiferromagnetic materials are composed of two interpenetrating lattices. Each lattice has all spins more or less aligned, but the lattices, as a whole, are inverse. Resonances in antiferromagnetic materials may occur at millimeter wave frequencies and above. Antiferromagnetic materials are paramagnetic above the Neel temperature.

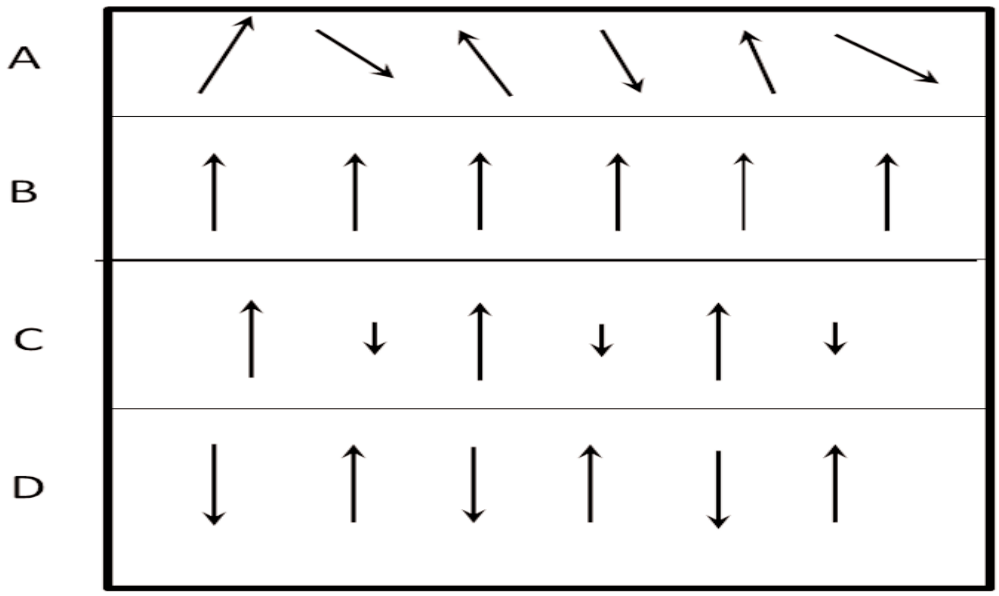

Figure 1.3 Simplistic summary of spin orientations for A) paramagnetic B) ferromagnetic C) ferrimagnetic D) antiferromagnetic materials.

For anisotropic and gyrotropic media with an applied magnetic field, the permittivity and permeability tensors are hermitian and can be expressed in the general form

$$\varepsilon(\omega) = \begin{bmatrix} \varepsilon_{xx} & \varepsilon_{xy} - ig_z & \varepsilon_{xz} + ig_y \\ \varepsilon_{xy} + ig_z & \varepsilon_{yy} & \varepsilon_{yz} - ig_x \\ \varepsilon_{xz} - ig_y & \varepsilon_{yz+}ig_x & \varepsilon_{zz} \end{bmatrix}$$

The off-diagonal elements are due to gyrotropic behavior in an applied field.

1.5 Experimental analysis of Dielectric response

The interaction between electromagnetic waves and dielectric materials can be determined by broadband measurement techniques. Dielectric relaxation spectroscopy allows the study of molecular structure, through the orientation of dipoles under the action of an electric field. In linear systems the time-dependent response to a step function field and the frequency-dependent response to a sinusoidal electric field are related through Fourier transforms.

Time domain spectroscopy

To cover the lowest frequency range (from 10^{-4} to 10^{1} Hz), time domain spectrometers have recently been developed.

In these devices, a voltage step Vo is applied to the sample placed between the plates of a plane parallel capacitor, and the current I(t) is recorded.

$C_{0=}e_0S/d=e_0\pi R^2/d$

$I(t)/v_{0\,=}C_0d\varepsilon(t)/dt$

$d\varepsilon(t)/dt=I(t)/e_0S\ E_0$

$\varepsilon(t)=1/c_0v_0$

Measurement Techniques' in the frequency domain

In the intermediate frequency range 10^{-1}- 10^{6} Hz, capacitance bridges have been the common tools used to measure dielectric permittivities. The devices are based on the Wheatstone bridge principle where the arms are capacitance-resistance networks. The principle of measurement of capacitance bridges is based on the balance of the bridge placing the test sample in one of the arms. Here sample is represented by an RC network in parallel or series. When the null detector of the bridge is at its minimum value (as close as possible to zero), the equations of the balanced bridge provide the values of the capacitance and loss factor (or conductivity) for the test sample. Frequency response analyzers have proved to be very useful in measuring dielectric permittivities in the frequency range 10^{-2} - 10^{6} Hz. An a.c. voltage V_1 is applied to the sample, and then a resistor R, or alternatively a current-to-voltage converter for low frequencies, converts the sample current I_s, into a voltage V_2.

Experimental data (ε'' vs ε') rarely fit to a Debye semicircle. Studying several organic crystalline compounds, Cole and Cole found that the centers of the experimental arcs were displaced below the real axis, the experimental data thus having the shape of a depressed arc shown in figure 1.4.

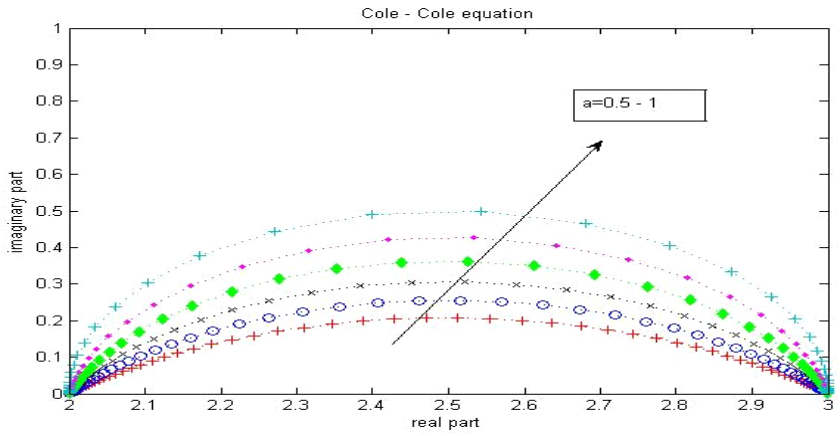

Figure.1.4: Cole Cole plot

At frequencies above 1 GHz the technique often used to obtain dielectric spectra is reflectometry.

The technique is based on the reflection of an electric wave, transported through a coaxial line, in a dielectric sample cell attached at the end of the line.

In this case, the reflective coefficient is a function of the complex permittivity of the sample, and the electric and geometric cell lengths.

The dielectric loss is also represented by $\tan\delta = \frac{\varepsilon''}{\varepsilon'}$

1.6 Principle of Dielectric Spectroscopy

Dielectric spectroscopy (which falls in a subcategory of impedance spectroscopy) measures the dielectric properties of a medium as a function of frequency. It is based on the interaction of an external field with the electric dipole moment of the sample, often expressed by permittivity.

It is also an experimental method of characterizing electrochemical systems. This technique measures the impedance of a system over a range of frequencies, and therefore the frequency response of the system, including the energy storage and dissipation properties, is revealed. Impedance is the opposition to the flow of alternating current (AC) in a complex system. A passive complex electrical system comprises both energy dissipater (resistor) and energy storage (capacitor) elements. If the system is purely resistive, then the opposition to AC or direct current (DC) is simply resistance. All measure the impedance spectrum $Z^*(\omega)$ of a sample material arranged between 2 or 4 more electrodes. The main interest here is on materials properties - contributions due to electrode effects are typically tried to be avoided. The intrinsic electric material properties like, e.g., the complex permittivity $\varepsilon^*(\omega)$ or conductivity $\sigma^*(\omega)$ spectra are easily evaluated from $Z^*(\omega)$ with the help of sample dimensions. The magnetic permeability spectra $\mu^*(\omega)$ can be determined if the sample electrodes are replaced by an inductive coil filled with sample material.

Beyond frequency, electrical materials properties depend on additional parameters, the most important one being temperature. Time, DC bias (superimposed static electrical field), AC field strength and pressure dependence are frequently determined as well. The measured spectra are further processed with special procedures depending on the sample type.

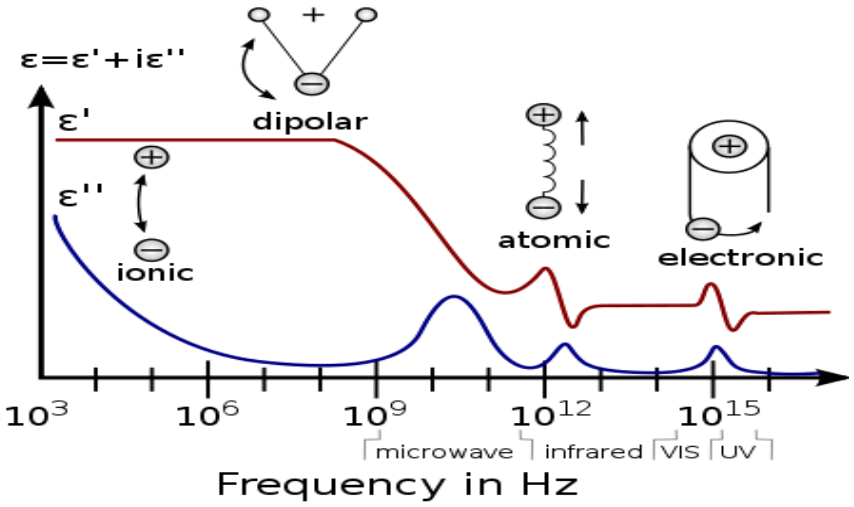

Figure 1.5: Broadband permittivity variation for materials

Generally, material specific models are matched by non linear curve fitting procedures to the measured data. As the models may include results from other material characterization methods, a link between the several techniques can be established in order to get more general information.

Permittivity $\varepsilon^*(\omega)$, conductivity $\sigma^*(\omega)$ and permeability $\mu^*(\omega)$ spectra are fundamental material parameters. With modern equipment, they can be accurately and automatically determined from some mHz up to several GHz (15 decades) for nearly all kind of materials. Sample preparation requires only little effort. Equipment costs are low compared to other material analysis methods.

Impedance analyzers measure the complex impedance $Z^*(\omega) = Z'(\omega) + j\ Z''(\omega)$ between electrical ports of a system under test in dependence of frequency $\omega/(2\pi)$. For materials analysis, the $Z^*(\omega)$ spectrum of 2 or 4 more electrodes with the sample material in between is measured. Depending on the sample material, the requirements to the impedance analyzer are extraordinary high and the result quality and availability strongly depends on its performance. In practice one is generally not so much interested in extreme high accuracy, but to measure both components of $Z^*(\omega)$, permittivity $\varepsilon^*(\omega)$ or conductivity $\sigma^*(\omega)$ at all. Beside the frequency range, the impedance range and the tan (δ) or phase accuracy are the most important performance parameters.

D.C. measurement

Electrical conductivity of materials is a material property which may vary over wide range. Material is a subclass of organic conductors. The electrical conductivity in an otherwise material originates from motion of either electrons or ions or both. The electrical conductivity of material is given by,

$\sigma=\Sigma\ q_i n_i \mu_i$

q_i, n_i and μ_i are the respective charge, concentration and mobility of the i-th species of conduction carrier. The mobility is the carrier drift velocity in the field direction per unit electric field.The band theory also explained electron and hole conduction in a system. The electrical conductivity of a material is

$$\sigma = \frac{d}{RA}\ \text{S(cm)}^{-1}$$

R= resistance of the sample(Ohm)of thickness d (cm). and cross-sectional area A cm^2. The total bulk electrical conductivity in a material is the sum of electronic and ionic contributions. i.e.

$$\sigma = \sigma_{\text{electronic}} + \sigma_{\text{ion}}$$

Study of volt-Ampere (I-V) characteristics of a material is important in regard of electronic conduction in it. The nature of I-V characteristics provides information about electron and 'hole' contribution to the total electronic conductivity.

A.C Measurements

AC measurement is generally done by impedance spectroscopy measurement. It measures the dielectric properties of a medium as a function of frequency. It is based on the interaction of an external field with the electric dipole moment of the sample, often expressed by permittivity. This technique measures the impedance of a system over a range of frequencies, and therefore the frequency response of the system, including the energy storage and dissipation properties.

Impedance spectroscopy plays an important role in fundamental and applied electro-chemistry and material science in the coming years. It is the method of choice for characterizing the electrical behavior of systems in which the overall system response is measured by strongly coupled processes. High quality impedance bridges and automatic measuring instrument can now measure the milihertz to megahertz of frequency range. It is a powerful method of characterizing many of the electrical materials and their interfaces with electronically conducting electrodes. It may be used to investigate the dynamics of bound or mobile charge in the bulk or interfacial regions of any kind of solid liquid material, ionic semiconducting, mixed (electronic+ ionic) and even insulators (dielectric).

Basic impedance spectroscopy experiment:

Electrical measurements to evaluate the electro-chemical behaviour of electrode and/or electrolyte materials are usually made with cells of two identical electrodes applied to the faces of a sample in the form of a circular cylinder or rectangular parallopiped. The general approach is to apply an electrical stimulus a known voltage or current to the electrodes and observe the response (the resulting current or voltage).

The experimental A.C. conductivities are calculated from the measured data, following relation, σ_{ac}= (d/RA)

Where R is the real part of the impedance, d is the sample thickness and A is the cross-sectional area (CSA) of the electrodes. The variation of A.C. conductivity with frequency may be described following Jonscher's power law [17] viz.

$$\sigma_\omega = \sigma_{dc} + K\,\omega^n$$

$$\text{Or, } \log(\sigma_\omega - \sigma_{dc}) = n \log \omega + \log K$$

Where, K and n are temperature dependent and frequency independent material parameters. Value of n may be directly estimated from the slope of the above equation.

The goal of impedance spectroscopy is to map out the complex impedance (a complex generalization of resistance that includes capacitive and inductive effects as well) Z of the sample as a function of frequency ω. This is done by applying a small oscillatory voltage to the sample and measuring the resulting oscillatory current through the sample. The phase and amplitude difference between the voltage across and the current through the sample determines the impedance of the sample at that frequency. By varying the frequency we can map out the impedance spectrum. Once the impedance spectrum is known, it can be fit against analytical formulas for impedance derived from circuit models, yielding an equivalent resistance and capacitance, which can be converted into resistivity and dielectric constant.

Dielectric Spectroscopy is a powerful experimental method to investigate the dynamical behaviour of a sample through the analysis of its frequency-dependent dielectric response. This technique is based on the measurement of the capacitance as a function of frequency of

a sample sandwiched between two electrodes. The tan δ, and capacitance (C) was measured as a function of frequency in the range 10 Hz to 50 kHz at variant temperatures for all the test samples. The measurements were made using high-resolution dielectric spectroscopy.

Electrical Polarization and A.C Conductivity

Let a dielectric material containing permanent dipole moment μ is connected by two plane parallel electrodes of area A, separation d. So the conductivity σ and dielectric constant ε are connected to conductance G and capacitance C by $\sigma = G\,(d/A)$ and $\varepsilon = C\,(d/\varepsilon_0 A)$.

Without an external electric field the dipoles are oriented at random and possesses only electronic polarizability α_e due to electronic displacements within the composing ions or atoms and polarizability α_a due to atomic or ionic displacement within the molecule. An external electric field E orients the dipoles in the direction of the field, creating average dipole moment along the field direction at temperature T is $(\mu^2/3kT)E$ for $\mu E << kT$. Hence the dipole moment per unit volume is

$$P_s = N\left(\alpha_e + \alpha_a + \frac{\mu^2}{3kT}\right)E = P_e + P_a + P_d$$

Impedance Spectroscopy

Impedance Spectroscopy describes the response of a circuit to an alternating current or voltage as a function of frequency.
In d.c. theory where the frequency equals 0 Hz., resistance is defined by Ohm's law E = I R Resistor R is the only element that impedes the flow of electrons in a d.c. circuit.

In a.c. theory, where the frequency is non-zero, the analogous equation is E = I Z.

Z is defined as impedance, the a.c. equivalent of resistance. In addition to resistors, capacitors and inductors impede the flow of electrons in a.c. circuits. Also slow electrode kinetics, diffusion can impede electron flow and can be considered analogous to the resistors, capacitors and inductors.

The real and imaginary components of an alternating current or voltage waveform are defined w.r.t some reference waveform. The real component is in phase with the reference waveform and the imaginary component (or quadrature component) is exactly 900 out of phase.

The impedance of a resistor $Z = R + j\,0$ has no imaginary component. When an alternating voltage $e = E_0 \sin \omega t$ is connected across a resistor the phase shift is zero degree – the current $i = e / R = (E_0 \sin \omega t) / R$ is in phase with the voltage. Both current and impedance are independent with the frequency.

A capacitor is a two terminal device consisting of two conducting bodies separated by a non-conducting material called dielectric. Charges are not permitted to move from one conducting body to the other within the device, they are transported via external circuitry.
Let a small number of electrons, $-\Delta q$ is transported from upper plate to the lower plate via external circuit (Figure 16). This leaves a charge $+\Delta q$ on the top plate and $-\Delta q$ on the bottom plate. A work is performed for separation of these charges which raises the potential of the upper plate by $+\Delta v$ with respect to the bottom plate. So potential difference between the plates is proportional to the charge being transformed so $q = C\,v$, where C is known as Capacitance in coulombs per volt, the unit is Farad.
Hence current $i = (dq / dt) = C (dv / dt)$

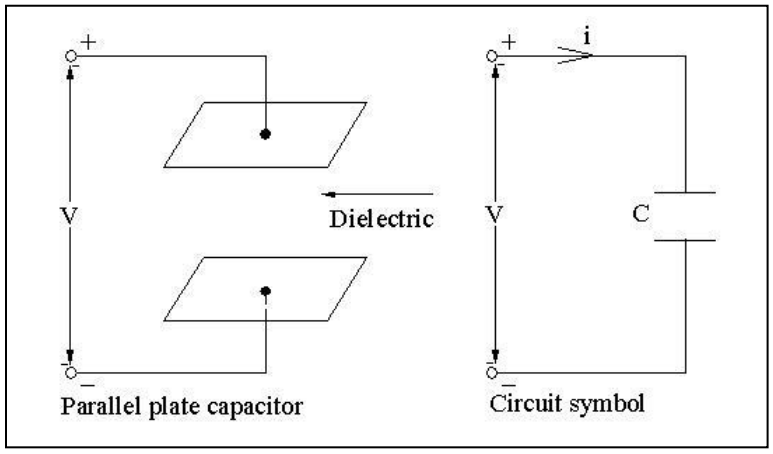

Figure 1.6: Capacitor Circuit

The energy stored in the capacitor

$$w_C(t) = \int_0^t v\, i\, dt = \int_0^t v\, C \frac{dv}{dt} dt = C \int_0^t v\, dv = \frac{1}{2} C v^2(t) = \frac{1}{2} \frac{q^2}{C} \text{ Joule}$$

An ideal capacitor cannot dissipate energy. Equivalent series capacitance is

$$\frac{1}{C_S} = \frac{1}{C_1} + \frac{1}{C_2} + \cdots\cdots\cdots + \frac{1}{C_N} = \sum_i \frac{1}{C_i}$$

Equivalent parallel capacitance is

$C_P = C_1 + C_2 + \cdots\cdots\cdots\cdots + C_N = \sum C_i$

The impedance of a capacitor $Z = 0 - (j / \omega C)$ has no real component. Its imaginary component is a function of both capacitance and frequency and varies inversely with frequency. At high frequencies a capacitor acts as a short circuit – it's impedance tends towards zero. At low frequencies (approaching d.c.) a capacitor acts as an open circuit, and the impedance tends towards infinite.

When an alternating voltage is connected across a capacitor (Figure 1.7), the phasor of current I through the capacitor would be ahead of phasor of voltage e precisely by 90^0 and the current would be purely reactive i.e., ideal dielectric.

$$q = Ce = CE_0 \sin \omega t \quad \& \quad i = \frac{dq}{dt} = C\omega E_0 \sin \omega t = \frac{E_0}{1/\omega C} \sin \omega t = I_0 \cos \omega t = I_0 \sin (\omega t + \frac{\pi}{2})$$

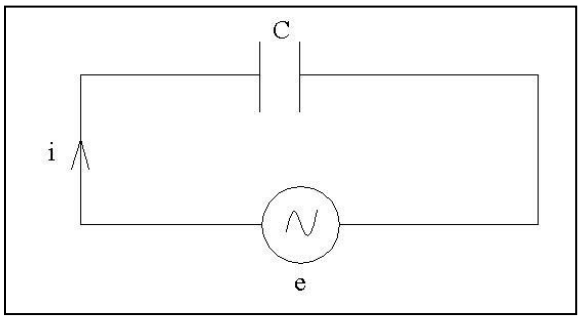

Figure 1.7: Alternating voltage applied to a capacitor

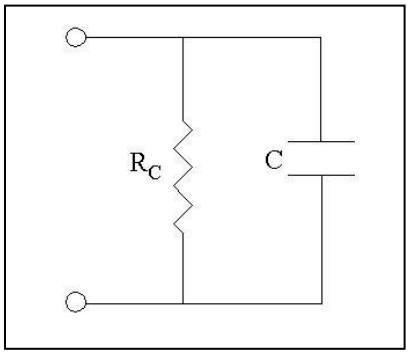

Figure 1.8: Equivalent circuit of a lossy capacitor

1

Practical capacitors, unlike ideal capacitors, dissipate a small amount of power. This is due to leakage currents that occur within the dielectric material. Practical dielectrics have a non-zero conductance, which allows an ohmic current to flow between the capacitor plates. This current is included in an equivalent circuit by placing a resistance R_C in parallel with an ideal capacitance (Figure 1.8). The leakage resistance R_C is inversely proportional to the capacitance C.In this practical situation the phase angle φ is less than 90^0. The total current I through the capacitor can be resolved into two components, active I_a and reactive I_r and $\delta = 90^0 - \varphi$, the angle φ is called dielectric loss angle (Figure 1.9). Tangent of this angle is equal to the ratio between the active and reactive currents; $\tan \delta = I_a / I_r$ or the ratio of active power (power loss) P to the reactive power P_q, therefore $\tan \delta = P / P_q$(loss tangent).

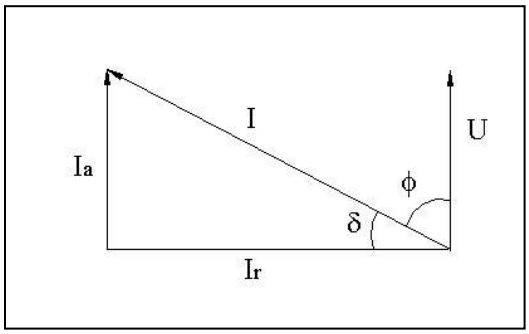

Figure 1.9: Currents in a lossy dielectric

A sinusoidal excitation is given by $v(t) = V_m \sin \omega t$ or $V_m \cos \omega t$

$= \text{Re}\,[V_m \exp(j\omega t)]$ or $\text{Im}\,[V_m \exp(j\omega t)]$

ωis angular frequency measured in radians per second (rad/s).

The current response is given by $i(t) = I_m \sin(\omega t + \phi)$ or $I_m \cos(\omega t + \phi)$

$= \text{Re}\,[I_m \exp(j\omega t + \phi)]$ or $\text{Im}\,[I_m \exp(j\omega t + \phi)]$

ϕis the phase difference .

Phasors

Let $v = V_m \cos(\omega t + \theta) = V_m \exp j(\omega t + \theta)$

A phasor is defined by a complex number $\mathbf{V} = V_m \exp j\theta = V_m \angle \theta$. Similarly for current $i = I_m \cos(\omega t + \phi) = I_m \exp j(\omega t + \phi)$ $\mathbf{I} = I_m \exp j\phi = I_m \angle \phi$.

Putting the value of v and i in Voltage - current relation for the resistor $v = Ri$ we obtain

$V_m \exp j(\omega t + \theta) = R\, I_m \exp j(\omega t + \phi) \Rightarrow V_m \exp j\theta = I_m \exp j\phi \Rightarrow \mathbf{V} = R\,\mathbf{I}$ hence $\theta = \phi$

Thus the sinusoidal voltage and current for a resistor have the same phase angle they are said to be in phase.

For a capacitor the voltage current relation is $i = C\,(dv/dt)$

$$\mathbf{I}_m\, e^{\,j(\omega t + \varphi)} = C \frac{d}{dt}[\,\mathbf{V}_m\, e^{\,j(\omega t + \theta)}] = j\omega C\, \mathbf{V}_m\, e^{\,j(\omega t + \theta)}$$

$$\text{or } \mathbf{I}_m\, e^{\,j\varphi} = j\omega C\, \mathbf{V}_m\, e^{\,j\theta} = \omega C\, \mathbf{V}_m\, e^{\,j(\theta + 90^0)} = \omega C\, \mathbf{V}_m \angle \theta + 90^0$$

In the case of a capacitor the current and voltage are out of phase with the current leading the voltage by 90^0.

From the phasor voltage $\mathbf{V} = V_m \angle \theta$ and phasor current $\mathbf{I} = I_m \angle \phi$, define the ratio of the phasor voltage to the phasor current as the impedance $\mathbf{Z}$ of the circuit $\mathbf{Z} = (\mathbf{V} / \mathbf{I})$

$$\text{or, } |Z| \angle \theta_z = \frac{V_m \angle \theta}{I_m \angle \varphi} = \frac{V_m}{I_m} \angle (\theta - \varphi) \qquad \text{hence } |Z| = \frac{V_m}{I_m} \text{ and } \theta_z = \theta - \varphi$$

Impedance is a complex number, being the ratio of two complex numbers, but it is not a phasor. The unit is ohms.

Impedance $\mathbf{Z}$ written in polar form $\mathbf{Z} = |Z| \angle \theta_z$ is written in rectangular form as $\mathbf{Z} = R + jX$ $R = \text{Re}\,\mathbf{Z}$ = resistance and $X = \text{Im}\mathbf{Z}$ = Reactive component or reactance.

$\mathbf{Z} = \mathbf{Z}(j\omega)$ is a complex function of $j\omega$ but $R = R(\omega)$ and $X = X(\omega)$ are real functions of ω.

Comparing polar and rectangular form of $\mathbf{Z} \Rightarrow$ $|Z| = (R^2 + X^2)^{1/2}$; $\theta_z = \tan^{-1}(X/R)$ and

$R = |Z| \cos\theta_z$ and

$X = |Z| \sin\theta_z$

We can also write

$$Z_R = R, \qquad Z_C = \frac{1}{j\omega C} = -\frac{j}{\omega C} = \frac{1}{\omega C} \angle -90^0$$

The capacitive reactance is denoted by $X_C = -(1/\omega C) \Rightarrow$ thus $Z_C = j\,X_C$

Reciprocal of Impedance is $\mathbf{Y} = (1/\mathbf{Z})$ is called admittance

$$\mathbf{Y} = G + jB = \frac{1}{\mathbf{Z}} = \frac{1}{R + jX} = \frac{R - jX}{R^2 + X^2}\ ; \quad \text{where } G = \frac{R}{R^2 + X^2} = \text{conductance} \text{ and } B = \frac{-X}{R^2 + X^2}$$

Phasor Diagram

For a series LCR circuit the current **I** is common to all elements and taken as a reference phasor. The Voltage phasors of the circuit are

$\mathbf{V_R}$= R **I** = R | **I** | $\angle 0^0$;$\mathbf{V_L}$= jωL **I** = ωL | **I** | $\angle$ 90^0 ; $\mathbf{V_C}$= (-j / ωC) **I** = (1/ωC) | **I** | $\angle$-90^0 and

$$\mathbf{V_G} = \mathbf{V_R} + \mathbf{V_L} + \mathbf{V_C}$$

Different cases may occur.

In case a) the net reactance is inductive and the current lags the source voltage by the angleθ. In b) the circuit has a net capacitive reactance and the currents lead the voltage. In c) the current and voltage are in phase, since the inductive and capacitive reactance components exactly cancel each other.

$$\mathbf{I} = \frac{\mathbf{V_G}}{\mathbf{Z}} = \frac{\mathbf{V_G}}{R + j(\omega L - \frac{1}{\omega C})}$$

Impedance Plot

The plot is a popular format for evaluating impedance data, is the Nyquist plot. This format is also known as Cole-Cole plot or a Complex Impedance plot. The imaginary impedance component Z'' is plotted against real impedance component Z' at each excitation frequency.

The basic test cell circuit of two blocking electrodes

A polymer acts as a resistor R_b in parallel with geometric capacitance C_g and in series with the double layer capacitor C_{dl} at the interface. Total impedance is [27]

$$Z = -\frac{j}{\omega C_{dl}} + \frac{R(1 - j\omega C_g R)}{1+(\omega C_g R)^2} = Z' - jZ''$$

$$\therefore Z' = \frac{R}{1+(\omega C_g R)^2}$$

$$Z'' = \frac{1}{\omega C_{dl}} + \frac{\omega C_g R^2}{1+(\omega C_g R)^2} = \frac{1+(\omega C_g R)^2 + \omega^2 C_g C_{dl} R^2}{\omega C_{dl}[1+(\omega C_g R)^2]}$$

$$= \frac{1+(\omega C_g R)^2 \left(1+ \frac{C_{dl}}{C_g}\right)}{\omega C_{dl}[1+(\omega C_g R)^2]}$$

Varying with temperature the impedance plot covers different regions of full semi circle spike curve. When the temperature is low and the resistance is high only the semicircle is seen whereas when the temperature is high and the resistance is low, only the spike and the small fail of the semi-circle are seen.

To understand why the frequency window lies over a particular part of the curve, consider the value of frequency at the top of the semicircle.

At the top of the semi-circle $\frac{dZ''}{dZ'} = 0$; $\frac{dZ''}{dZ'} = \frac{dZ''/d\omega}{dZ'/d\omega}$

$$\frac{dZ''}{d\omega} = \frac{d}{d\omega}\left[\frac{\omega C_g R^2}{1+(\omega C_g R)^2}\right] = \frac{C_g R^2[1+(\omega C_g R)^2] - 2\omega^2 C_g^3 R^4}{[1+(\omega C_g R)^2]^2}$$

$$= \frac{C_g R^2 - \omega^2 C_g^3 R^4}{[1+(\omega C_g R)^2]^2} = \frac{C_g R^2(1 - \omega^2 C_g^2 R^2)}{[1+(\omega C_g R)^2]^2}$$

$$\frac{dZ'}{d\omega} = \frac{d}{d\omega}\left[\frac{R^2}{1+(\omega C_g R)^2}\right] = \frac{-R.2\omega C_g^2 R^2}{[1+(\omega C_g R)^2]^2}$$

$$\therefore \frac{dZ''}{dZ'} = \frac{C_g R^2(1 - \omega^2 C_g^2 R^2)}{-2\omega C_g^2 R^3} = \frac{1 - \omega^2 C_g^2 R^2}{-2\omega C_g^2 R^3}$$

From $\frac{dZ''}{dZ'} = 0 \quad \Rightarrow \quad 1 - \omega^2 C_g^2 R^2 = 0$

$$\therefore \quad \omega C_g R = 1 \quad \Rightarrow \quad \omega = \frac{1}{C_g R}$$

As the resistance falls, provided that the change in capacitance is relatively small, the value of ω at the top of the semicircle increases. The movement of the frequency window across the impedance plot occurs for all solid electrolysis.

Series CR circuit

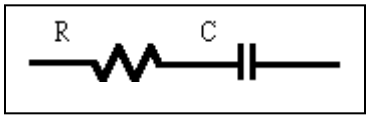

Figure 1.10**:** Series C-R circuit.

Total impedance is

$$Z = R + \frac{1}{j\omega C} = R - \frac{j}{\omega C} = Z' - jZ'' \quad \Rightarrow \quad Z' = R \text{ and } Z'' = \frac{1}{\omega C}$$

Therefore real value is constant but the imaginary y axis value varies. The impedance plot is a vertical line, intersecting the real z axis at a value R.

When $\omega = 0$ $Z'' = \infty$,

When $\omega = \infty$ $Z'' = 0$,

low frequency values are near the top of the line.

Parallel C R circuit

Using the phasor diagram, the parallel CR circuit is analyzed.

$$\frac{1}{Z_P} = \frac{1}{R} + j\omega C = \frac{1 + j\omega C R}{R}$$

$$\Rightarrow \quad Z_P = \frac{R}{1 + j\omega C R} = \frac{R\,(1 - j\omega C R)}{1 + (\omega C R)^2} = \frac{R}{1 + (\omega C R)^2} - j\,\frac{\omega C R^2}{1 + (\omega C R)^2} = Z' - j Z''$$

where $Z' = \dfrac{R}{1 + (\omega C R)^2}$ and $Z'' = \dfrac{\omega C R^2}{1 + (\omega C R)^2}$

From Z' and Z'' $\Rightarrow$ $\dfrac{Z''}{Z'} = \omega C R$; Putting this value in $Z' = \dfrac{R}{1 + (\omega C R)^2}$

$$\Rightarrow \quad Z' = \frac{R}{1 + \dfrac{Z''^2}{Z'^2}} = \frac{Z'^2 R}{Z'^2 + Z''^2} \qquad \Rightarrow \quad Z'^2 + Z''^2 = Z' R$$

$$\Rightarrow \quad Z'^2 - Z' R + Z''^2 = 0$$

$$\Rightarrow \quad Z'^2 - 2.\, Z'.\, \frac{R}{2} + (\frac{R}{2})^2 + Z''^2 = (\frac{R}{2})^2$$

$$\Rightarrow \quad (Z' - \frac{R}{2})^2 + (Z'' - 0)^2 = (\frac{R}{2})^2$$

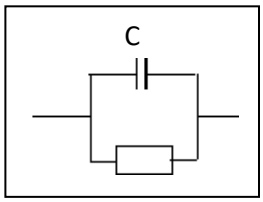

Figure 1.11: Parallel C-R circuit

This is the equation of a circle with center at [R/2, 0] and radius R/2.

As $\omega = 0$ $\Rightarrow$ $Z' = R$, $Z'' = 0$, $\omega \to \infty$ $\Rightarrow$ $Z' \to 0$, $Z'' \to 0$

The impedance plot is a semicircle (Figure 1.12) and as ω varies from 0 to ∞ the locus moves counterclockwise along the circle with its ends at the origin (infinite frequency) and at R (zero frequency).

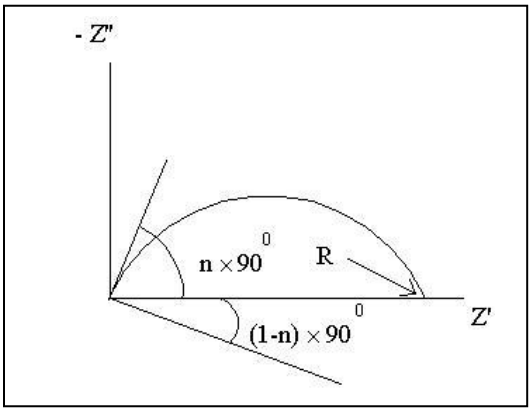

Figure 1.12: Complex impedance plot

Practical CR circuit

For polymer electrolytes, in impedance plot, the semicircle is depressed and the spike tilts. No C-R circuit produces such depression or tilting. These are natural consequences of constant phase elements.

Constant Phase Element

The Constant Phase Element (CPE) is a non-intuitive circuit element featuring the response of real – world systems. A polymer electrolyte can be thought as a 'leaky capacitor' containing the constant phase element. The Nyquist plot of such a system is not a semicircle with the center on the X axis, rather it is the arc of a circle and the center is at some distance below the X axis. A CPE's impedance is given by

$$Z_{CPE} = K(j\omega)^{-n} \qquad \text{where } 0 \le n \le 1, \qquad K = \text{constant}$$

$$= \frac{K}{(\omega)^n}(j)^{-n} = \frac{K}{(\omega)^n}(j^2)^{-\frac{n}{2}} = \frac{K}{(\omega)^n}(-1)^{-\frac{n}{2}}$$

$$= \frac{K}{(\omega)^n}[\exp(j\pi)]^{-\frac{n}{2}} = \frac{K}{(\omega)^n}\exp(-\frac{jn\pi}{2})$$

$$= \frac{K}{(\omega)^n}[\cos(\frac{n\pi}{2}) - j\sin(\frac{n\pi}{2})]$$

K is the numerical value of the impedance $|\mathbf{Z}|$ at $\omega = 1$ rad / sec.

A consequence of this equation is that the phase angle of the CPE impedance is independent of frequency and has a value of $(90\times n)^0$, this gives the CPE its name.

When $n = 0$, $Z_{CPE} = K$, the impedance is therefore frequency independent and the CPE behaves as a resistor for which $R = K$.

When $n = 1$, $Z_{CPE} = (K / j\omega)$. This is the same equation for that of the impedance of a capacitor, where $K = (1 / C)$.

When n is close to 1, the CPE resembles a capacitor, but the phase angle is not 90^0 at all frequencies. For a solitary CPE a straight line makes an angle $(90\times n)^0$ with the X axis. The center of the semicircle is depressed by an angle of $(1 - n)\,90^0$.

When $n = \frac{1}{2}$

$$Z_{CPE} = \frac{K}{(\omega)^{\frac{1}{2}}}[\cos(\frac{\pi}{4}) - j\sin(\frac{\pi}{4})] = \frac{K}{(2\omega)^{\frac{1}{2}}}(1-j)$$

This particular CPE is called Warburg impedance. The current is 45^0 out of phase with the imposed potential. The real and imaginary components of the impedance vector are equal at all frequencies. The behavior of Warburg impedance (a 45^0 phase shift) is midway between that a resistor (0^0 phase shift) and a capacitor (90^0 phase shift).

Causes of CPE

Roughness at the electrode–electrolyte interface causes the CPE behavior. For a rough, fractal surface the fractal dimension (D) of the surface is between 2 and 3. For this electrodes the interfacial impedance (electron transfer or double layer capacitance) is modified by an exponent n = 1 / (D-1).For a smooth surface D = 2 and hence n = 1, so the impedance is unchanged. For a highly contorted surface D = 3 and n = 0.5.

For a great many real metal or solid electrodes the measured impedance in the double layer region follows a power law. For CPE with a value of n between 0.9 to 1.0, the phase angle of this 'capacitance' is not 90^0 but $(90 \times n)^0$.

Electrical Polarization and A.C Conductivity

Let a dielectric material containing permanent dipole moment μ is connected by two plane parallel electrodes of area A, separation d. So the conductivity σ and dielectric constant ε are connected to conductance G and capacitance C by $\sigma = G\,(d/A)$ and $\varepsilon = C\,(d/\varepsilon_0 A)$.

Without an external electric field the dipoles are oriented at random and possesses only electronic polarizability α_e due to electronic displacements within the composing ions or atoms and polarizability α_a due to atomic or ionic displacement within the molecule. An external electric field E orients the dipoles in the direction of the field, creating average dipole moment along the field direction at temperature T is $(\mu^2/3kT)E$ for $\mu E << kT$. Hence the dipole moment per unit volume is

$$P_s = N(\alpha_e + \alpha_a + \frac{\mu^2}{3kT})E = P_e + P_a + P_d$$

Where, the material contains N molecules per unit volume. P_e and P_a reaches their final value instantaneously but the time required for P_d to teach its static value varies.

This equation leads to the Debye formula for the static dielectric constant of the material

$$\varepsilon_s - 1 = \frac{4\pi P}{E} = 4\pi N(\alpha_e + \alpha_a + \frac{\mu^2}{3kT})$$

When an alternating field $E(t) = E_0 \exp(j\omega t)$ is applied, the previous equation is converted to

Total polarization $P(t) = P_e + P_a + P_d(t)$. After a few simple calculations,

$$P(t) = \frac{\varepsilon_\infty - 1}{4\pi} E(t) + \frac{1}{4\pi} \cdot \frac{\varepsilon_s - \varepsilon_\infty}{1 + j\omega\tau} E(t)$$

Where, ε_∞ be instantaneous dielectric constant. Hence displacement current

$$D(t) = \varepsilon^* E(t) = E(t) + 4\pi P(t) = [\varepsilon_\infty + \frac{\varepsilon_s - \varepsilon_\infty}{1 + j\omega\tau}] \cdot E(t)$$

$$\Rightarrow \varepsilon^*(\omega) = \varepsilon'(\omega) - j\varepsilon''(\omega) = \varepsilon_\infty + \frac{(\varepsilon_s - \varepsilon_\infty)(1 - j\omega\tau)}{1 + \omega^2\tau^2}$$

$$\therefore \varepsilon'(\omega) = \varepsilon_\infty + \frac{(\varepsilon_s - \varepsilon_\infty)}{1 + \omega^2\tau^2} \quad \text{and} \quad \varepsilon''(\omega) = \frac{\omega\tau}{1 + \omega^2\tau^2}$$

$\varepsilon'(\omega)$ and $\varepsilon''(\omega)$ represents dispersion and loss characteristics.

The dielectric loss, which is proportional to $\varepsilon''(\omega)$ exhibits a maximum for $\omega\tau = 1$, i.e. for angular frequency $\omega = 1/\tau$.

When $\omega << 1/\tau$, i.e. $\omega\tau << 1 \Rightarrow \varepsilon'(\omega) \approx \varepsilon_s$. At low frequencies, dipoles have time to orient and are accompanied by a displacement current and dipoles contribute their full share to polarization.

When $\omega\tau >> 1 \Rightarrow \varepsilon'(\omega) \approx \varepsilon_\infty$. The dipoles could not follow the electric field variation and approach ε_∞.

Rewriting from previous equation $\varepsilon^*(\omega) - \varepsilon_\infty = \frac{\varepsilon_s - \varepsilon_\infty}{1 + j\omega\tau}$

This is known as Debye dielectric function where ε_s and ε_∞ are low and high frequency dielectric constant, τ is time constant.

Many materials display non-Debye dielectric behavior by a broader asymmetric loss peak. This non-Debye a.c response can be described by a combination of Cole-Cole and Davidson-Cole functions, an empirical expression proposed by Havrilink-Negami [29].

When $\alpha = 0,\ \beta = 1$ $\quad \varepsilon^*(\omega) - \varepsilon_\infty = \dfrac{\varepsilon_s - \varepsilon_\infty}{1 + j\omega\tau} \quad \Rightarrow$ Debye Funcion

When $\beta = 1$ $\quad \varepsilon^*(\omega) - \varepsilon_\infty = \dfrac{\varepsilon_s - \varepsilon_\infty}{1 + (j\omega\tau)^{1-\alpha}} \quad \Rightarrow$ Cole - Cole Function

When $\alpha = 0$ $\quad \varepsilon^*(\omega) - \varepsilon_\infty = \dfrac{\varepsilon_s - \varepsilon_\infty}{(1 + j\omega\tau)^{\beta}} \quad \Rightarrow$ Davidson - Cole Function

Debye function corresponds to a relaxation process with a single time constant, while H-N function is assumed to represent a superposition of many Debye functions with various relaxation times.

The frequency dependent dielectric constant $\varepsilon^*(\omega) = \varepsilon'(\omega) - j\,\varepsilon''(\omega)$ is related to frequency dependent conductivity $\sigma(\omega) = \sigma'(\omega) + j\,\sigma''(\omega)$ by ,

$$\varepsilon_0\,\varepsilon^*(\omega) = \frac{\sigma(\omega) - \sigma(0)}{j\omega}$$

Where, $\sigma'(\omega)$ and $\sigma''(\omega)$ are real and imaginary part of the complex conductivity. The real part follows the expression of Jonscher $\sigma'(\omega) = \sigma(0) + A\,\omega^s$, where $0<s<1$.

All disordered solids show a strong dispersion of the conductivity. At low frequency a constant conductivity is observed while at higher frequency the conductivity becomes strongly frequency dependent, varying approximately as a power of frequency.

CHAPTER 2

ELECTROMAGNETIC RESPONSE OF A DIELECTRIC

2.1 Maxwell's equations and different material medium

Maxwell's electromagnetic field equations [25] are the most fundamental laws to realize the matter wave interaction. The familiar four equations are given below.

$$\nabla \cdot \mathbf{B} = 0 \tag{2.1}$$

$$\nabla \cdot \mathbf{D} = \rho \tag{2.2}$$

$$\nabla \times \mathbf{E} = -\frac{\partial \mathbf{B}}{\partial t} \tag{2.3}$$

$$\nabla \times \mathbf{H} = \mathbf{J} + \frac{\partial \mathbf{D}}{\partial t} \tag{2.4}$$

The EM wave interacts with matter through the material parameters, like relative permittivity ε, relative permeability μ, charge density ρ (if any) and current density **J** (if any). Complete solutions of the above field vectors **E**, **H**, **B** and **D** are possible using above equations. Two more constitutive relations are also necessary to get the relation between four field vectors in the material.

$$c\bar{D} = \bar{\bar{P}}.\bar{E} + \bar{\bar{L}}.c\bar{B} \tag{2.5}$$

$$\overline{H} = \overline{\overline{M}}.\overline{E} + \overline{\overline{Q}}.c\overline{B} \tag{2.6}$$

In a compact form, these equations can be written as

$$\begin{bmatrix} c\overline{D} \\ \overline{H} \end{bmatrix} = \bar{\bar{C}}.\begin{bmatrix} \overline{E} \\ c\overline{B} \end{bmatrix} \tag{2.7}$$

$$\text{Where } \bar{\bar{C}} = \begin{bmatrix} \bar{\bar{P}} & \bar{\bar{L}} \\ \overline{\bar{M}} & \bar{\bar{Q}} \end{bmatrix} \tag{2.8}$$

Equations (2.5) and (2.6) are written in the relativistic invariant form. Where, c is velocity of light. $\bar{\bar{P}}$, $\bar{\bar{L}}$, $\overline{\bar{M}}$ and $\bar{\bar{Q}}$ are used as coupling terms, they are tensor in nature.

The materials can be classified into four groups depending upon the inherent material property [24].

(a) The terms $\bar{\bar{L}}$, $\overline{\bar{M}}$ relates electric field to magnetic field.

If $\bar{\bar{L}}$, $\overline{\bar{M}}$ = 0 and

$$\bar{\bar{P}} = c\epsilon\bar{\bar{I}} \tag{2.9}$$

$$\bar{\bar{Q}} = \frac{1}{c\mu}\bar{\bar{I}} \tag{2.10}$$

$\bar{\bar{I}}$ is the 3× 3 unit matrix used in the above equation.

$$\text{Hence, } \overline{D} = \epsilon\overline{E} \tag{2.11}$$

$$\overline{B} = \mu\overline{H} \tag{2.12}$$

The medium is known as isotropic.

(b) If there is no coupling between electric and magnetic field

$\bar{\bar{L}}$ = $\overline{\bar{M}}$ =0 and ε, μ are tensor.

$$\bar{\bar{P}} = c\bar{\bar{\epsilon}} \tag{2.13}$$

$$\bar{\bar{Q}} = \frac{1}{c}\bar{\bar{\mu}}^{-1} \tag{2.14}$$

$$\text{Hence, } \overline{D} = \bar{\bar{\epsilon}}\overline{E} \tag{2.15}$$

$$\overline{B} = \bar{\bar{\mu}}\overline{H} \tag{2.16}$$

The medium is known as anisotropic.

(c) If $\bar{\bar{L}}$, $\bar{\bar{M}}$ is not identically zero and not tensor and the coupling terms relate electric field to magnetic field, the medium is known as Biisotropic.

i.e.

$$c\bar{D} = P\bar{E} + Lc\bar{B} \tag{2.17}$$

Example: Pasteur medium

$$\bar{D} = \epsilon\bar{E} - ik\sqrt{\epsilon\mu}\bar{H} \tag{2.18}$$

k is known as chirality parameter.

Tellegen media

$$\bar{B} = \mu\bar{H} + \mathcal{X}\sqrt{\epsilon\mu}\bar{E} \tag{2.19}$$

$\mathcal{X}$ is Tellegen or reciprocity parameter.

(d) If magneto electric coupling constants $\bar{\bar{L}}$, $\bar{\bar{M}}$ is not zero and take tensor form, the medium is known as Bianisotropic.

On the microscopic level we know that the electromagnetic field is modeled as a collection of photons [26]. In theory, the electromagnetic field interactions with matter may be modeled on a microscopic scale by solving Schrödinger's equation, but generally other approximate approaches are used. At larger scales the interaction with materials is modeled by macroscopic Maxwell's equations together with constitutive relations and boundary conditions. Typical scales of various objects are shown in Fig 2.1

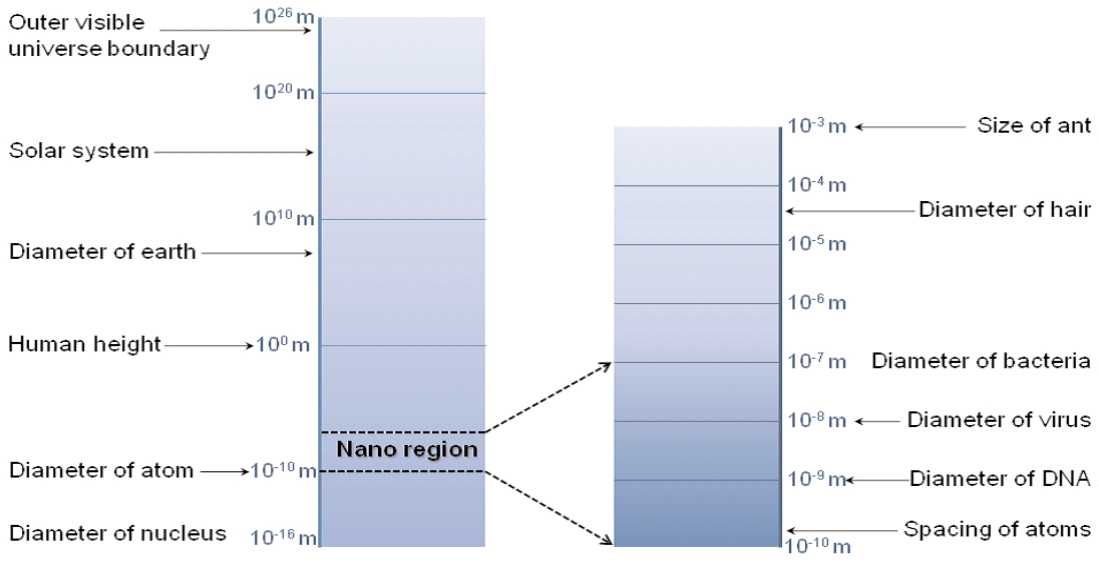

Figure 2.1 Scales of objects.

The interaction of the radiation field with atoms is described by quantum electrodynamics. From a quantum-mechanical viewpoint the radiation field is quantized, with the energy of a photon of angular frequency. Photons exhibit wave duality and quantization. This quantization also occurs in mechanical behavior where lattice vibrational motion is quantized into phonons.

Polarization in atoms and molecules can be due to permanent electric moments or induced moments, caused by the applied field and spins or spin moments. The response of induced polarization is usually weaker than that of permanent polarization, because the typical radii of atoms are on the order of 0.1 nm. On application of a strong external electric field, the electron cloud will displace the bound electrons only about 10^{-16} m. This is a consequence of the fact that the atomic electric fields in the atom are very intense.

In modeling EM interactions at macroscopic scales, a homogenization process is usually applied and the classical Maxwell field is treated as an average of the photon field. There also is a homogenization process that is used in deriving the macroscopic Maxwell equations from the microscopic Maxwell equations. The macroscopic Maxwell's equations in materials are formed by averaging the microscopic equations over a unit cell. In this averaging procedure, the macroscopic charge and current densities, the magnetic field H, the magnetization M, the displacement field D, and the electric polarization field P are formed. At these scales, the molecule dipole moments are averaged over a unit cell to form continuous dielectric and magnetic polarizations P and M. The constitutive relations for the polarization and magnetization are used to define the permittivity and permeability. At macroscopic to mesoscopic scales the permittivity, permeability, refractive index, and impedance are used to model the response of materials to applied fields. Quantities such as permittivity, permeability, refractive index, and wave impedance are not microscopic quantities, but are defined through an averaging procedure. This averaging works well when the wavelength is much larger than the size of the molecules or atoms and when there are a large number of molecules. In theoretical formulations for small scales and wavelengths near molecular dimensions, the dipole moment and polarizability tensor of atoms and molecules can be used rather than the permittivity or permeability.

In some materials, such as magnetoelectric and chiral materials, there is a coupling between the electric and magnetic responses. In such cases the time-harmonic constitutive relations are

$$B(\omega) = \mu H(\omega) + \eta 1 E(\omega)$$

and $$D(\omega) = \varepsilon E(\omega) + \eta 2 H(\omega). \quad (2.20)$$

In most materials the constitutive relations we use the relation

$$B(\omega) = \mu_0 (M(\omega) + H(\omega))$$

$$\text{and } D(\omega) = \varepsilon_0 E(\omega) + P(\omega). \quad (2.21)$$

In any complex lossy system, energy is converted from one form to another, such as the transformation of EM energy to lattice kinetic energy and thermal energy through photon-phonon interactions. Some of the energy in the applied fields that interact with materials is transferred into thermal energy as infrared phonons. In a waveguide, there is a constant exchange of energy between the charge in the guiding conductors and the fields [27].

When the electromagnetic field interacts with material degrees of freedom, a collective response may be generated. The term polariton relates to bosonic quasiparticles resulting from the coupling of EM photons or waves with an electric or magnetic dipole-carrying excitation [4, 5]. The resonant and non-resonant coupling of EM fields in phonon scattering is mediated through the phonon-polariton transverse-wave quasiparticle. Phononpolaritons are formed from photons interacting with terahertz to optical phonons. Ensembles of electrons in metals form plasmas and high-frequency fields applied to these electron gases produce resonant quasi-particles, commonly called plasmons. Plasmons are a collective excitation of a group of electrons or ions that simultaneously oscillate in the field. An example of a plasmon is the resonant oscillation of free electrons in metals and semiconductors in response to an applied high-frequency field. Plasmons may also form at the interface of a dielectric and a metal and travel as a surface wave with most of the EM energy confined to the low-loss dielectric. A surface Plasmon polariton is the coupling of a photon with surface plasmons. Whereas transverse plasmons can couple to an EM field directly, longitudinal plasmons couple to the EM field by secondary particle collisions. In the

microwave and millimeter wave bands artificial structures can be machined in metallic surfaces to produce plasmons-like excitations due to geometry. Magnetic coupling is mediated through magnons and spin waves. A magnon is a quantum of a spin wave that travels through a spin lattice. A polaron is an excitation caused by a polarized electron traveling through a material together with the resultant polarization of adjacent dipoles and lattice distortion [4]. All of these effects are manifest at the mesoscale through macroscale in the constitutive relations and the resultant permittivity and permeability.

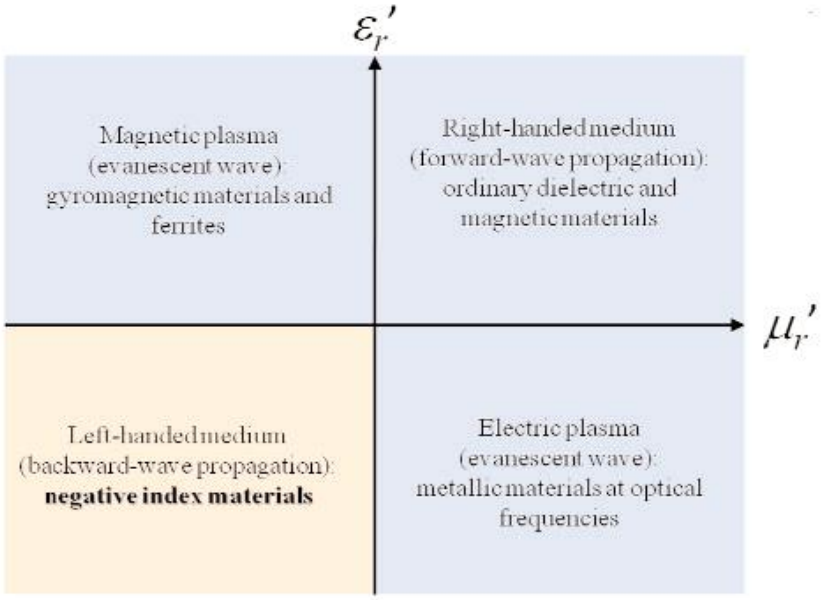

Figure2.2 The regions of the permittivity-permeability space for different material behaviors.

If we immerse a specimen in an applied field and the response is recorded by a measurement device, the data obtained are usually in terms of a digital readout or a needle deflection indicating the phase and magnitude of a voltage or current, a difference in voltage and current, power, force, temperature, or an interference fringe. For example, we deduce electric and magnetic field strengths and phase through Ampere's and Faraday's laws by means of voltage and current measurements. The scattering parameters measured on a network analyzer relates to the phase and magnitude of a voltage wave. The detection of a photon's energy is sensed by an electron cascade current. Cavities and microwave evanescent probes sense material characteristics through shifts in resonance frequency from the influence of the specimen under test. The shift in resonance frequency is again determined by voltage and power measurements on a network analyzer.

Magnetic interactions are also determined through measurements of current and voltage or forces [4, 7–9]. These measurement results are usually used with theoretical models, such as Maxwell's equations, circuit parameters, or the Drude model, to obtain material properties.

High-frequency electrical responses include the measurement of the phase and magnitude of guided waves in transmission lines, fields from antennas, resonant frequencies and quality factors (Q) of cavities or dielectric resonators, voltage waves, movement of charge or spin, temperature changes, or forces on charge or spins. These responses are then combined through theoretical models to obtain approximations to important fundamental quantities such as: power, impedance, capacitance, inductance, conductance, resistance, conductivity, resistivity, dipole and spin moments, permittivity, and permeability, resonance frequency, Q, antenna gain, and near-field response [10–16].

The homogenization procedure used to obtain the macroscopic Maxwell equations from the microscopic Maxwell equations is accomplished by averaging the molecular dipole moments within a unit cell and constructing an averaged continuous charge density function. Then a Taylor series expansion of the averaged charge density is performed, and, as a consequence, it is possible to define the averaged polarization vector. The spatial requirement for the validity of this averaging is that the wavelength must be much larger than the unit cell dimensions. According to this analysis, the permittivity of an ensemble of molecules is valid for applied field wavelengths that are much larger than the dimensions of an ensemble of molecules or lattice, assuming one can isolate the effects of the molecules from the measurement apparatus. This metrology is not always easy because a measurement contains effects of electrodes, probes, and other environmental factors. The concepts of atomic polarizability and dipole molecular moment are valid on a smaller scale than permittivity and permeability.

The dielectric function can be expressed in a classical Helmholtz–Drudemodel[1]

$$\epsilon_h(\omega) = 1 - \omega_0^2/(\omega_0^2 - \omega^2 + i\omega\gamma) \tag{2.22}$$

Where, ω_0 is the resonance frequency, and γ is the damping factor.

Frequency dependence of the response function for the metal [5] can be expressed as,

$$\epsilon_m(\omega) = 1 - \frac{\omega_p^2}{\omega^2 + i\omega\Gamma} \tag{2.23}$$

Where, ω_p is the plasma frequency, Γ is relaxation time.

In case of metal dielectric composite like Dilute Magnetic Dielectric we have to consider the Debye like spin lattice relaxation that was developed by Gorter and Kronig[1], given by,

$$\chi_{m=}\chi/(1 + i\omega\tau) \tag{2.24}$$

For $\mu \neq 1$, we have combined the spin lattice relaxation effect with the dielectric behavior of composite and a new function Φe is assigned to consider the combine effect. The proposed form of Φe is taken to describe complex refractive index is [6]

$$n(\omega) = \sqrt{[\epsilon(\omega)\mu(\omega)]} = \sqrt{\varphi_{eff}(\omega)} \tag{2.25}$$

Where, $\mu(\omega) = 1 + \chi_m(\omega)$

$$\varphi_{eff}(\omega) = \left[1 + \chi_m(\omega)\right]\epsilon_{eff}(\omega) \tag{2.26}$$

2.2 Development and analysis of Metal Dielectric composite in present study

A simple form of dielectric behavior of composite material is offered. The effect of inclusion of metallic or magnetic atom in host dielectric is undertaken and modified form of the response is proposed. For some material like Dilute magnetic dielectric, DMD [29].The effect magnetic susceptibility is taken into account to describe the dielectric behavior under

external e. m. wave. The proposed form of effective function is taken to describe complex refractive index for DMD like system. In Maxwell's electro-magnetic field theory both$\epsilon(\omega)$ and μ (ω) have their own identity however this proposed theory apparently coupled them to describe for a better convenience. The optical absorbance of a non-magnetic material is related to its dielectric function only, however for DMD like system it should be related to effective dielectric function namely.

2.2.1 Theory

Following Maxwell Garnett Theory (MGT) [28] and using the modified Clausius-Mossotti relation, the effective relative permittivity of the composite medium becomes,

$$\epsilon_{\text{eff}} = \left[3\epsilon_{\text{h}}\left(1 + 2\frac{\epsilon_{\text{h}}}{\epsilon_{\text{m}}}\right)/(1-\text{f})\left(1 + \frac{2-\text{f}}{1-\text{f}}\frac{\epsilon_{\text{h}}}{\epsilon_{\text{m}}}\right)\right] - 2\epsilon_{\text{h}} \qquad (2.27)$$

Equation (2.27) describes the bulk effective permittivity of a composite in terms of the permittivity of the inclusion with filling factor *f* and the host dielectric constant. The variation of frequency domain can be found following in eqn. (2.22) and (2.23). For this metal-dielectric composite, the metal is used as an inclusion while the dielectric component serves as the host. The composite behaves as dielectric for small concentrations, less than one third i.e. f=1/3, of metal. Beyond the percolation threshold, the composite acts as a dilute metal with an effective permittivity proportional to (f=1/3) [29]. In fact, this peak can extend to an infinite bandwidth if the filling fraction approaches 1/3, which is the percolation threshold for a three-dimensional metal-dielectric composite. Electronically, the percolation threshold represents the minimum volume fraction of conducting particles needed for the formation of a continuous conducting pathway.

2.2.2 Result and Discussion

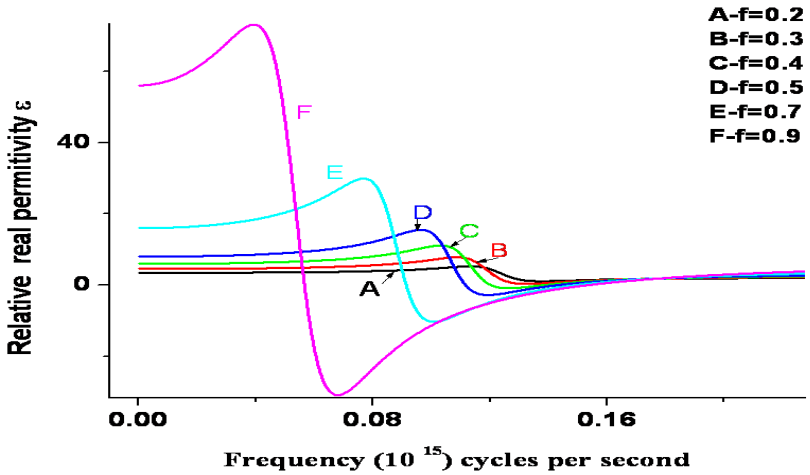

Figure 2.3 Frequency vs. relative real permittivity of composite with different filling factor

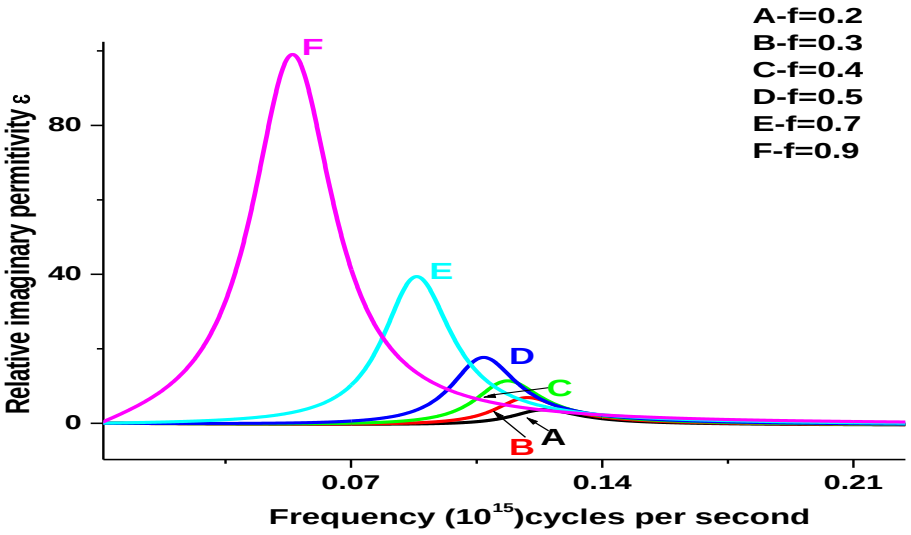

Figure 2.4 Plot of variation of Imaginary part Relative permittivity as a function of Frequency for different filling factor.

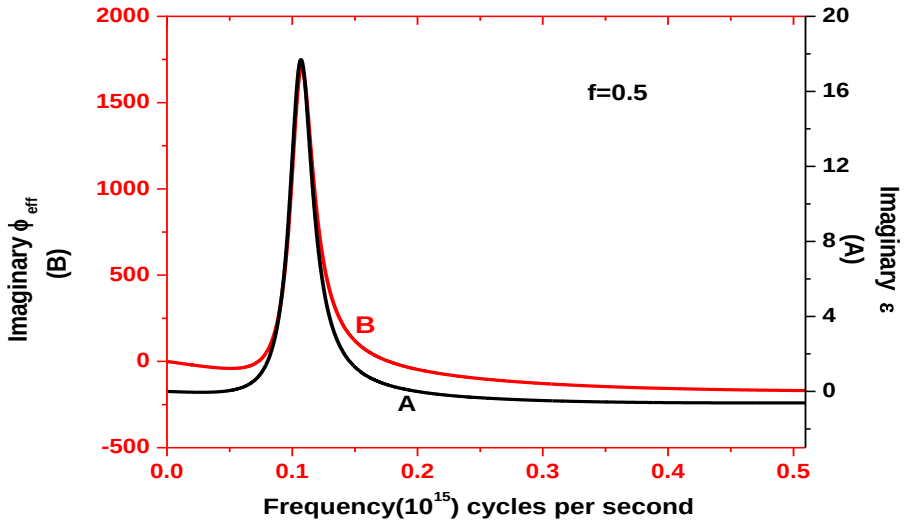

Figure 2.5 Frequency vs. Imaginary part of Relative permittivity of composite A-Frequency versus Imaginary part of Relative permittivity for Metal Dielectric Composite, B-Frequency versus Imaginary part of for magnetized Metal Dielectric Composite

Figure 2.3 shows the variation of real part of effective relative permittivity of the composite with frequency of e.m. wave following eq (2.27)Figure 2.4 shows the variation of imaginary part of effective relative permittivity of the composite with impressed frequency of e.m wave.

Figure 2.5 represent the double axis graph for filling factor f=0.5. From the curve A and B, It is clear that the dielectric behavior of a composite changes after applying the magnetic field.

The proposed theoretical formulation of DMD like composites and its comparison with experimental result shows a good agreement. The effective dielectric function may be exploited for composite material to study their optical behavior.

2.3 Effect of electro-magnetic coupling on dielectric Composite

Researchers have found that in magneto-electric, ferroic, and chiral materials the application of magnetic fields can produce a dielectric response and the application of an electric field can produce a magnetic response. These cross coupling behaviors can be found to occur in

specific material lattices, layered thin films, or by constructing composite materials. An origin of the intrinsic magneto-electric effect is from the strain-induced distortion of the spin lattice upon the application of an electric field. When a strong electric field is applied to a magneto-electric material such as chromium oxide, the lattice is slightly distorted, which changes the magnetic moment and therefore the magnetic response. Extrinsic effects can be produced by layering appropriate magnetic, ferroelectric, and dielectric materials in such a way that an applied electric field modifies the magnetic response and a magnetic field modifies the electric response.

Chiral materials can be constructed by embedding conducting spirals into a dielectric matrix. In artificial magneto-electric materials the calculated permittivity and permeability may be effective rather than intrinsic properties. The constitutive relations for the induction and displacement fields are not always simple and can contain cross coupling between fields.
In a continuous medium of composites with inclusion of magnetic atom the magneto-electric coupling is present in terms of the Tellegen parameters [30, 31],

$$D = \epsilon E + i\kappa\sqrt{\mu_0\epsilon_0}H$$

$$B = -i\kappa\sqrt{\mu_0\epsilon_0}E + \mu H \tag{2.28}$$

Where, ε_0 and μ_0 stand for the permittivity and permeability in free space, and κ denotes the coupling constant used in the Tellegen relations.

$$D = \epsilon E + \frac{i\omega\alpha}{c_0}H$$

$$B = -\frac{i\omega\alpha}{c_0}E + \mu H \tag{2.29}$$

Where, $c_0$is the speed of light in free space, and α stands for the rotatory parameter, which is frequency dependent.

$$D.E = \epsilon E^2 + ik\sqrt{\mu_0\epsilon_0}H.E \tag{2.30}$$

$$B.H = -ik\sqrt{\mu_0\epsilon_0}H.E + \mu.H^2 \tag{2.31}$$

$$D/E = \epsilon + \frac{ik}{c_0}\frac{H}{E} \tag{2.32}$$

In E.M. theory, the amplitude of electric and magnetic field are related by, $\beta(\omega)$= B_0/E_0.In case of pure dielectric the contribution $\beta(\omega)$ is very small, and the same is significant in conducting medium.

Hence, the imaginary part of $\epsilon(\omega)$ which directly related [8] to optical absorbance is given by

$$\epsilon''_{eff} = \epsilon'' + \frac{ik}{c_0}\beta(\omega) \tag{2.33}$$

Contribution lies Imϵ and Imμ for real k.

The values of Re and Im part ε(ω) may be estimated directly from Dielectric Spectroscopy data and are given by,

$$\mathrm{Re}\frac{\varepsilon(\omega)}{\varepsilon_0(\omega)} = \left[\frac{C_s(\omega)}{C_s(0)}\right]Cos(\theta) \quad \text{and,} \qquad \mathrm{Im}\frac{\varepsilon(\omega)}{\varepsilon_0(\omega)} = -\left[\frac{C_s(\omega)}{C_s(0)}\right]Sin(\theta) \tag{2.34}$$

Where, C_S is the series capacitance at frequency ω and C_0 (0) is the estimated d.c. capacitance at vacuum.

2.4 Effect of external field over DMD in present study

2.4.1 Experimental Detail

The Nickel acetate hydrate, analytical grade (Alpha Aesar) was heated (about 300 C) for 8h to pre-pare NiO powder. The developed NiO powder was grinding and strongly heated (about 350 C) for 10h. In this work Nickel oxide (NiO) powder is allowed to form pellets at pressure 10 ton/cm^2. The developed pellet was sandwiched between two high polished copper plates to form experimental parallel plate capacitor with known geometry. Copper being diamagnetic metal offers permeability to external magnetic field. In the measurement set up the mentioned capacitor was placed between pole-pieces of an electromagnet. Capacitance C(ω) and phase angle (θ) of the specimen were measured, between frequencies 5

Hz to 100 kHz with magnetic field as parameter, employing dielectric spectroscopy. The measurement was done at room temperature (RT) with HIOKI 3522-50 LCR Hi TESTER, (JAPAN). The applied equilibrium ac potential was 1V rms.

2.4.2 Result and Discussion

The developed anti-ferromagnetic Nio specimens contain nano-sized grain at a large fraction. In a nano-system magnetic parameters have their characteristics fluctuations [9].It has been found [10] that in magneto-electric, ferroic and chiral materials the application of magnetic field can produce a dielectric response and the application of an electric field can produce a magnetic response. These cross coupling behaviors can be found to occur in specific material lattices, layered thin films, or by constructing composite materials. Figure 2.6 shows the Variation of real part of dielectric constant as a function of frequency measured at different d.c. Magnetic field (H).

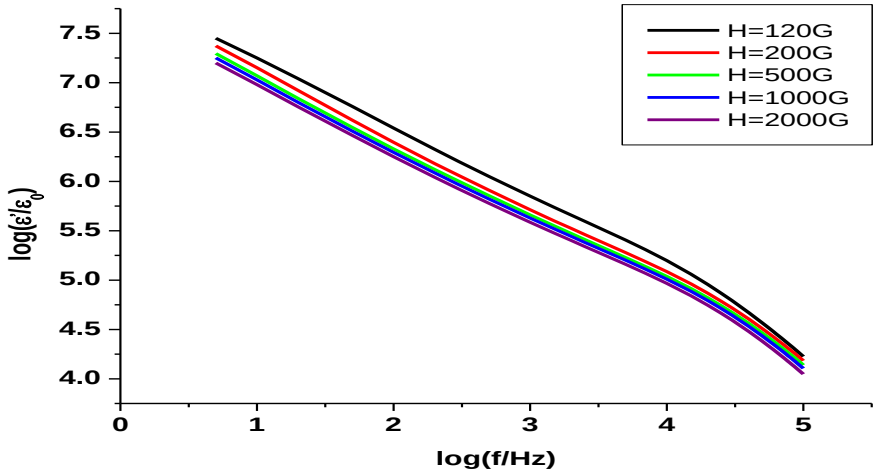

Figure 2.6 Variation of real part of dielectric constant ε as a function of frequency measured at different Magnetic field H.

The results show that a substantial change in real part of dielectric constant under variation of H in the measured frequency rage.Figure 2.7 depict the same for imaginary part of dielectric constant. DMD like NiO exhibits variation of magnetic susceptibility with external magnetic

field and hence variation of effective permittivity $\varphi_e(\omega) = [1+\chi_m(H)]\,\varepsilon(\omega)$ of the specimen. Both the figures show decrease in $\varepsilon(\omega)$ with increase in external field H.

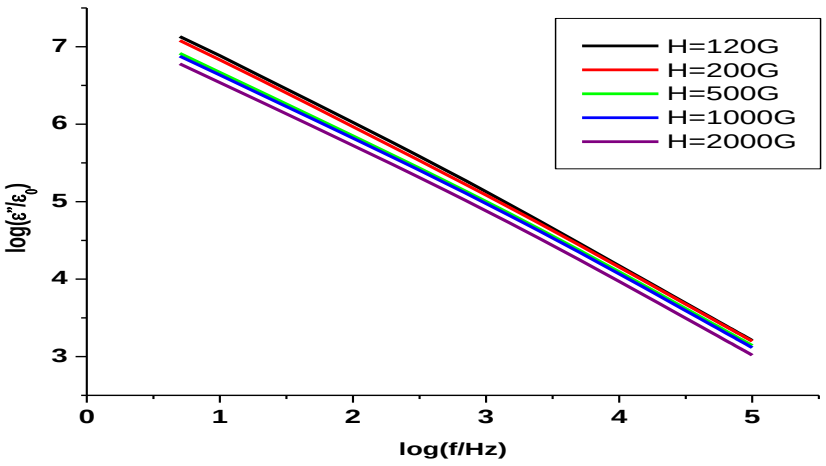

Figure 2.7 Variation of imaginary part of permittivity ε as a function of frequency measured at different Magnetic field.

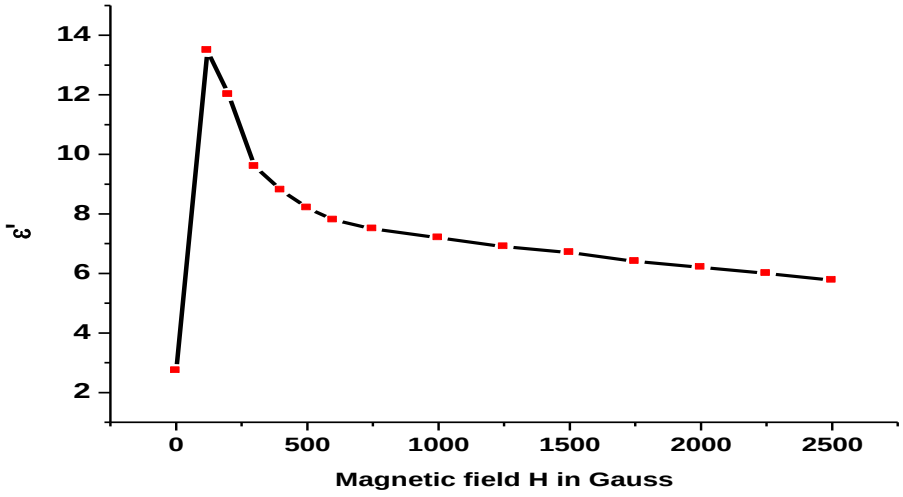

Figure 2.8 Variation of real part of permittivity with Magnetic field measured at 5KHz.

Figure 2.8 and 2.9 show the variation Re and Im part of $\varepsilon(\omega)$ respectively with external field H at frequency 5 kHz In both the cases $\varepsilon(\omega)$ exhibit an initial increase in its value from H=0

to H=120 Gauss and with further in increase in H, ε(ω) decreases with H. The observed nature is consistent with variation of χ_m (H) with H for the specimen NiO. The observed experimental results are consistent with effective dielectric constant given by equation (2.33).

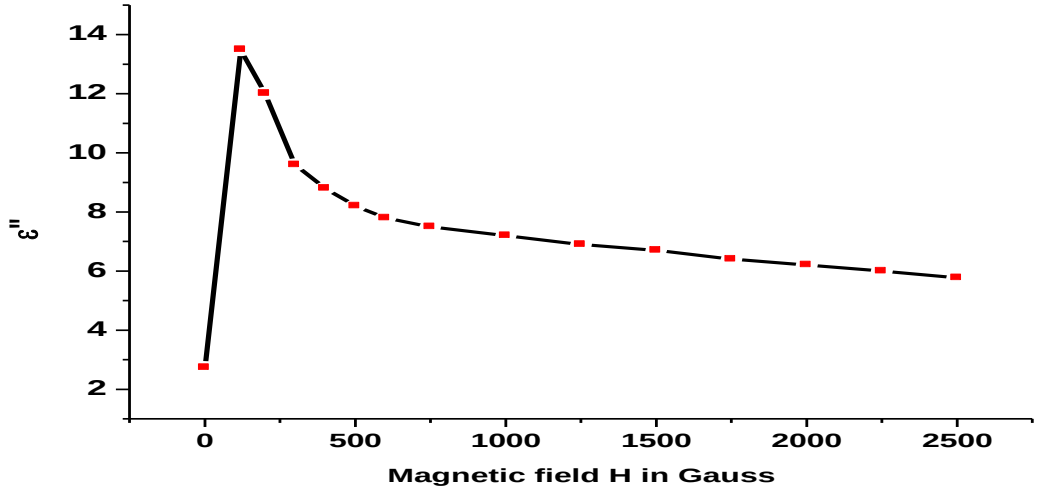

Figure 2.9 Variation of imaginary part of permittivity with Magnetic field measured at 5KHz.

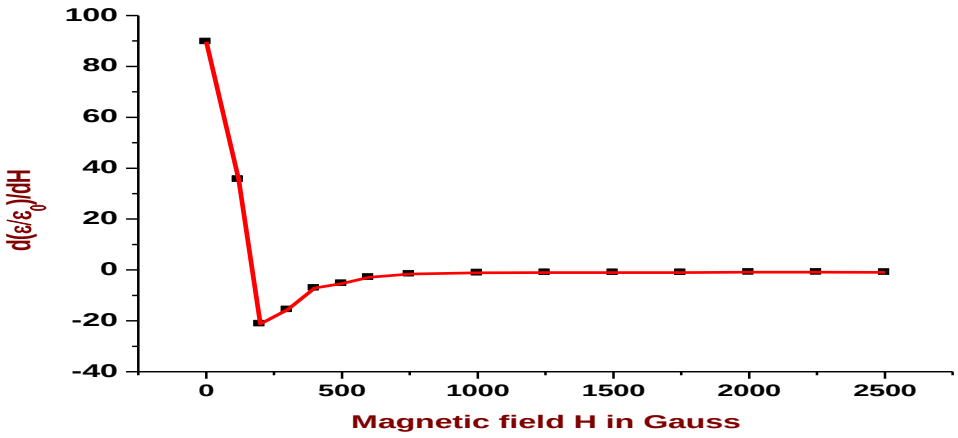

Figure 2.10 Variation of derivative of real part of permittivity with Magnetic field measured at 5KHz.

Figure 2.10 shows the rate of variation of Re ε(ω) with respect to H to external field H. It shows that sensitivity of ε(ω) on H is very high in the low field region between 0 to 100

Gauss. NiO is an antiferromagnetic system it attains a near saturation within very low field enhancement from no field state. In the high field region the observed variation rate is poor.

The non-linearity in variation curve shown figure 2.10 in high field region is due to non-linearity in χ_m (H) and the coupling term given by equation (2.33). The later has small and finite contribution in a dispersive medium. The qualitative agreement between theory and experiment is found to be encouraging. The overall results obtained are also good and consistent. The observed DMD characteristics may be applied to conventional electronics and spintronics. The developed NiO is a dielectric composite system. The effective dielectric constant of the system is dependent on external magnetic field also. The present work provides a good account of effective dielectric constant of the DMD system.

CHAPTER 3

DILUTED MAGNETIC SEMICONDUCTOR (DMS) AND DILUTED MAGNETIC DIELECTRIC (DMD)

3.1 What are DMS and DMD?

Spintronics [33-35], or spin electronics, involves the study of active control and manipulation of spin degrees of freedom in solid-state systems. It could make integrated use both charge and spin of electrons.

Diluted magnetic semiconductor (DMS) [33] is one of the key elements in spintronics. The idea of a DMS, where a small (<10%) concentration of magnetically active atoms (most often Mn although Co and Cr have also been used occasionally) is distributed at the cation sites of the host semiconductor, is appealing because such a system may have both semiconducting and ferromagnetic properties. However, making such materials has been problematic because the magnetic transition metal (i.e. Mn) is not thermodynamically stable in the semiconductor host (i.e.GaN) and tends to segregate.

Two basic approaches to understanding the magnetic properties of dilute magnetic semiconductors:

The mean-field model generally believed that the ferromagnetism in DMS is mediated by the itinerant carriers in the host semiconductor.

The clusters model suggests that the magnetic atoms form small (a few atoms) clusters that produce the observed ferromagnetism

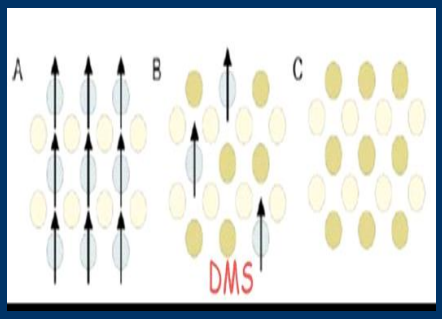

Three types of semiconductors:

A) a magnetic semiconductor, in which a periodic array of magnetic element is present; (B) a diluted magnetic semiconductor, an alloy between nonmagnetic semiconductor and magnetic element; and (C) a nonmagnetic semiconductor, which contains no magnetic ions.

Dilute magnetic semiconductors (DMS) have recently been a major focus of magnetic semiconductor research. These are based on traditional semiconductors, but are doped with transition metals instead of, or in addition to, electronically active elements. They are of interest because of their unique spintronics properties with possible technological applications.[36]

When, a dielectric material doped with transition metal this unique class of material, known as dilute magnetic dielectrics (DMD) [37]. The goal of a DMD is not to act as a spin injector, but rather to function as a spin filter for polarized injection. As both spin orientations of electrons reach the DMD from the metal, only those with the lower energy requirement for tunneling are capable of passing through into the semiconductor. Because of this, spin polarization and efficiency can increase drastically compared to other devices.

3.2 Importance of DMS and DMD in material science

Doped Wide band-gap metal oxides such as zinc oxide (ZnO) and titanium oxide (TiO2) are among the best candidates for industrial DMS due to their multi-functionality in optico-

magnetic applications. In particular, ZnO-based DMS with properties such as transparency in visual region and piezoelectricity have generated huge interest among the scientific community as a strong candidate for the fabrication of spin transistors and spin-polarized Light-emitting diodes.

The goal of a DMD is not to act as a spin injector, but rather to function as a spin filter for polarized injection. This works because the energy barrier for tunneling through DMDs varies directly with spin orientation. As both spin orientations of electrons reach the DMD from the metal, only those with the lower energy requirement for tunneling are capable of passing through into the semiconductor. Because of this, spin polarization and efficiency can increase drastically compared to other devices [38].

Much of the current interest surrounding DMDs is in regarding the mechanism behind their weak ferromagnetism. The desired state is one that results in intrinsic ferromagnetism. This kind of magnetism is characteristic of phase-pure material, where the magnetic material has substituted uniformly throughout the lattice. However, extrinsic magnetic behavior can also occur. This magnetism indicates that ferromagnetic dopant metal has not substituted into the lattice, but has formed magnetic clusters. In order to reiterate that the behavior seen is due to intrinsic doping, not extrinsic Prestgard et al [38] have reported the formation of non-phase-pure thin films.

3.3 Dielectric and magnetic aspect of DMS/DMD

Magnetic semiconductors are semiconductor materials that exhibit ferromagnetism (or a similar response) and useful semiconductor properties. If implemented in devices, these materials could provide a new type of control of conduction. Whereas traditional electronics are based on control of charge carriers (n- or p-type), practical magnetic semiconductors would also allow control of quantum spin state (up or down). This would theoretically provide near-total spin polarization (as opposed to iron and other metals, which provide only ~50% polarization), which is an important property for spintronics applications, e.g. spin transistors.

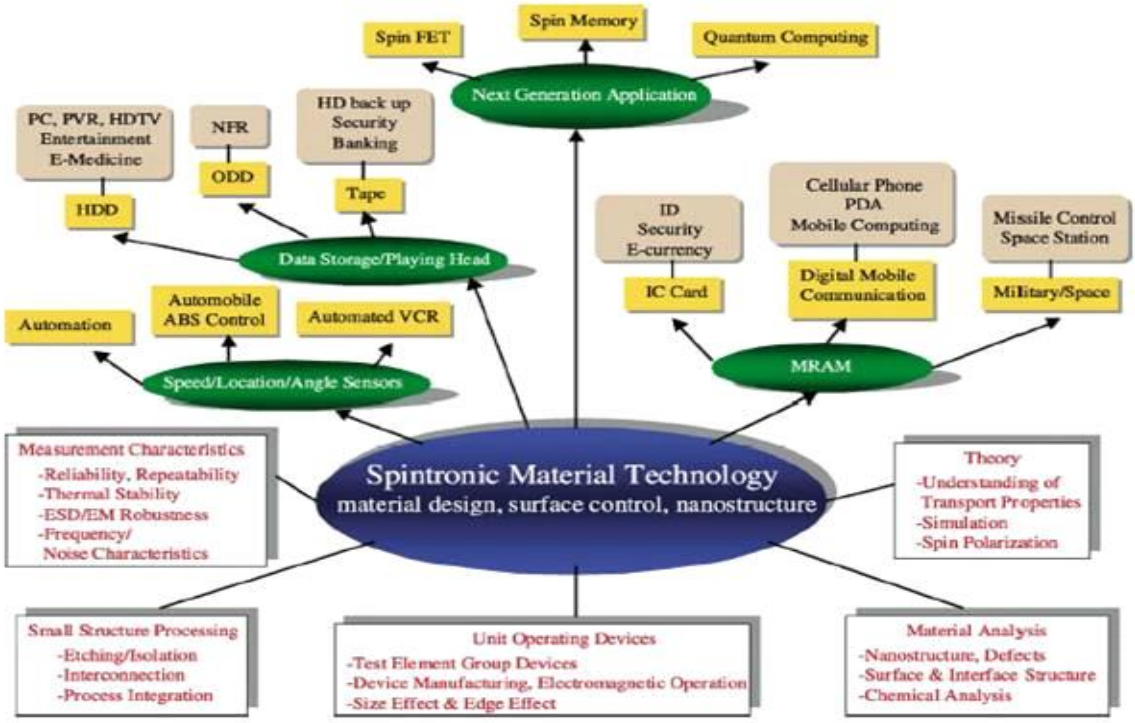

Figure 3.1 Applications of spintronic material

While many traditional magnetic materials, such as magnetite, are also semiconductors (magnetite is a semimetal semiconductor with bandgap 0.14 eV), materials scientists generally predict that magnetic semiconductors will only find widespread use if they are similar to well-developed semiconductor materials.

3.4 Method of characterization

Characterization is the process by which the structure and properties of the materials are probed and measured**.** UV-VIS spectroscopy is very important characterization method which refers to the ultra violet, optical part of the EM wave. For magnetic measurements SQUID-magnetometry is also used.

3.4.1 Principle of UV-VIS Spectroscopy

The first assumption in spectroscopic measurements is that Beers law relationship applies between a change in spectrometer response and the concentration of analyze material present

in a sample specimen. The Bouguer, Lambert and Beer relationship assumes that the transmission of a sample within an incident beam is equivalent to 10 exponent the negative product of the molar extinction coefficient (in L 1/mol.cm), multiplied by the concentration of a molecule in solution times the path length (in cm) of the sample in solution. So Beers relationship is

$$T=I/I_0=10^{-sec} \quad (3.1)$$

T is the transmittance, I_0 is the intensity of incident energy, I is the intensity of transmitted light, e is the molar extinction coefficient, c is the concentration and l is the path length. To simplify the equation in more standard form showing absorbance as a logarithmic term used to linearize the relationship between the spectrophotometer response and concentration, gives the following expressions as the relationship between absorbance and concentration.

$$Abs\ (A) = -\log(I/I_0)= -\log(T)=ecl \quad (3.2)$$

The goal in the design of an optical spectrometer is to maximize the energy (or radiant power) from a light source through the spectrometer to the detector. The optical throughput for a spectrometer is dependent on multiple factors, such as the light source area the apertures present within the light path lens transmittance and the mirror reflectance losses, the exit aperture and the detector efficiency.

3.4.2 UV-VIS Spectrophotometer

The ultraviolet-visible (UV-VIS) is an instrument commonly used in the laboratory that analyzes compounds in ultraviolet and visible region of the EM spectrum. Generally UV-VIS spectroscopy looks at electronic transition while infrared spectroscopy looks at vibrational motion. It determines the wavelength and maximum absorbance of compounds.

Many molecules absorb ultraviolet or visible light. The absorbance of a solution increases as attenuation of the beam increases. Different molecules absorb radiation of different wavelengths. An absorption spectrum will show a number of absorption bands corresponding to structural groups within the molecule. For example, the absorption that is observed in the

UV region for the carbonyl group in acetone is of the same wavelength as the absorption from the carbonyl group in diethyl ketone.

A molecule of any substance has an internal energy which can be considered as the sum of the energy of its electrons, the energy of vibration between its constituent atoms and the energy associated with rotation of the molecule. The electronic energy levels of simple molecules are widely separated and usually only the absorption of a high energy photon, that is one of very short wavelength, can excite a molecule from one level to another. In complex molecules the energy levels are more closely spaced and photons of near ultraviolet and visible light can affect the transition. These substances, therefore, will absorb light in some areas of the near ultraviolet and visible regions. The vibrational energy states of the various parts of a molecule are much closer together than the electronic energy levels and thus protons of lower energy (longer wavelength) are sufficient to bring about vibrational changes. Light absorption due to only to vibrational changes occurs in the infrared region. The rotational energy states of molecules are so closely spaced that light in the far infrared and microwave regions of the electromagnetic spectrum has enough energy to cause these small changes.

For ultraviolet and visible wavelengths, absorption spectrum of a molecule (i.e., a plot of its degree of absorption against the wavelength of the incident radiation) should show a few very sharp lines. Each line should occur at a wavelength where the energy of an incident photon exactly matches the energy required to excite an electronic transition. In practice it is found that the ultraviolet and visible spectrum of most molecules consists of a few humps rather than sharp lines. These humps show that the molecule is absorbing radiation over a band of wavelengths. One reason for this band, rather than line absorption is that an electronic level transition is usually accompanied by a simultaneous change between the more numerous vibrational levels. Thus, a photon with a little too much or too little energy to be accepted by the molecule for a 'pure' electronic transition can be utilized for a transition between one of the vibrational levels associated with the lower electronic state to one of the vibrational levels of a higher electronic state. The energy levels of a molecule shown in Fig 3.2.

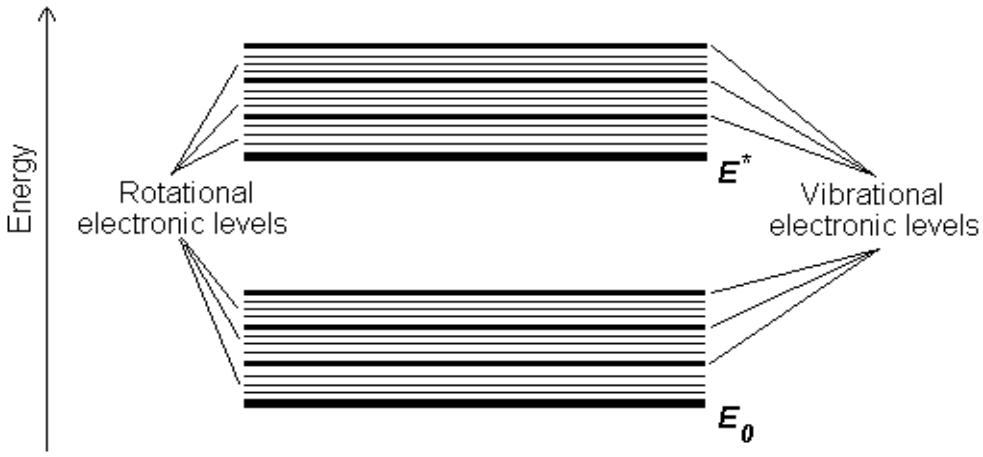

Figure 3.2 (a) Energy levels of a molecule.

A molecule or ion will exhibit absorption in the visible or ultraviolet region when radiation causes an electronic transition within its structure. Thus, the absorption of light by a sample in the ultraviolet or visible region is accompanied by a change in the electronic state of the molecules in the sample. The energy supplied by the light will promote electrons from their ground state orbitals to higher energy, excited state orbitals or antibonding orbitals. Potentially, three types of ground state orbitals may be involved [39]:

i) σ (bonding) molecular

ii) π (bonding) molecular orbital

iii) n (non-bonding) atomic orbital

In addition, two types of antibonding orbitals may be involved in the transition:

i) σ* (sigma star) orbital

ii) π* (pi star) orbital

(There is no such thing as an n* antibonding orbital as the n electrons do not form bonds).

A transition in which a bonding s electron is excited to an antibonding σ orbital is referred to as σ to σ* transition. In the same way π to π* represent the transition from one electron of a lone pair (non-bonding electron pair) to an antibonding π orbital. Thus the following electronic transitions can occur by the absorption of ultraviolet and visible light shown in Fig.3.3

σ to σ*,

n to σ*

n to π*

π to π*.

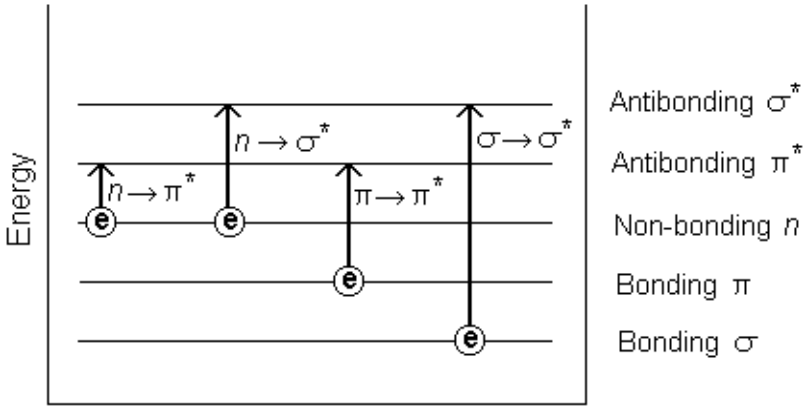

Figure 3.2(b) Energy and molecular transitions

Both s to σ* and n to σ* transitions require a great deal of energy and therefore occur in the far ultraviolet region or weakly in the region 180-240nm. Consequently, saturated groups do not exhibit strong absorption in the ordinary ultraviolet region. Transitions of the n to π* and π to π* type occur in molecules with unsaturated centers; they require less energy and occur at longer wavelengths than transitions to σ* anti-bonding orbitals. Many inorganic species show charge-transfer absorption and are called charge-transfer complexes. For a complex to demonstrate charge-transfer behavior one of its components must have electron donating properties and another component must be able to accept electrons. Absorption of radiation then involves the transfer of an electron from the donor to an orbital associated with the acceptor. Molar absorptivities from charge-transfer absorption are large (greater that 10,000

L mol^{-1} cm^{-1}). The details of the principle and application may be found in many literatures [39-40].

3.4.3 Principle of SQUID-VSM magnetometry

The quantum design magnetic property measurement system (MPMS) is a family of analytical instruments configured to study the magnetic properties of small experimental samples over a broad range of temperatures and magnetic fields. Computerized control and data collection are provided along with this system. Extremely receptive magnetic measurements are performed with superconducting pickup coils and a Superconducting Quantum Interference Device (SQUID). For this reason, the MPMS family of instruments is called SQUID magnetometers. To optimize speed and sensitivity, some analytic techniques are utilized in SQUID-VSM over conventional VSM. Specifically, the sample is vibrated at a known frequency and phase-sensitive detection is employed for rapid data collection and spurious signal rejection. Unlike traditional VSMs (non-superconducting), the strength of the signal produced by a sample independent on the frequency of vibration, but it depends only on the magnetic moment of the sample, the vibration amplitude and sensitive design of SQUID detection circuit. The MPMS SQUID VSM utilizes a superconducting magnet (a solenoid of superconducting wire) to subject samples to magnetic fields up to 7 Tesla (70 kOe). The SQUID and magnet both are cooled with liquid helium. The sample chamber is also cooled with liquid helium, providing temperature control of samples from 350 down to 10 K.

Figure 3.3 Image of SQUID-VSM used for magnetic characterization

The Quantum Design MPMS SQUID VSM EverCool system features an integrated pulse-tube cryocooler-dewar system that not only recondenses the liquid helium directly within the EverCool Dewar but also liquefies the initial charge of liquid helium directly from helium gas. This eliminates the need to use any liquid cryogens for the operation of the MPMS SQUID VSM [41].

The SQUID VSM utilizes a 7 Tesla, superconducting, helium-cooled magnet and accomplishes rapid switching between charging and discharging states and stable fields with a unique superconducting switching element called the Quick Switch, which changes, between superconducting and normal states in less than one second. This allows rapid collection of high precision data. Typical M-H loop up to 5T would take ~ 60 mins and M-T measurement would take ~70 mins.

Other Features:

Operating Range: 1.8 K to 1000 K

Cooling Rate: 30 K/min (300 K to 10 K stable in 15 min.);
10 K/min (10 K to 1.8 K stable in 5 min.)
Temperature Stability: +/- 0.5%
Temperature Accuracy: lesser of +/- 1% or 0.5 K

Magnetic field control
Feature: QuickSwitch
Magnetic Field Range: -70 kOe to +70 kOe
Field Uniformity: 0.01% over 4 cm
Field Charging Rate: 4 Oe/sec to 700 Oe/sec
Field Charging Resolution: 0.33 Oe
Remanent Field: ~5 Oe (typical) when oscillating from full field back to zero

Magnetization measurements
Feature: SQUID based VSM FastLab
Maximum DC moment: 10 emu
Sensitivity: < 2,500 Oe < 1 x 10-8 emu (with less than 10 second averaging) > 2,500 Oe < 8 x 10-8 emu (with less than 10 second averaging)
Variable drive amplitude: 0.1 to 5 mm (peak-to-peak**)**

3.5 Study of Effective Dielectric Constant of DMD using UV-VIS spectroscopy

The optical absorbance of a non-magnetic material is related to its dielectric function only, however for DMD like system it should be related to effective dielectric function, namely $\varphi_{eff}(\omega)$. In this present work UVVIS spectroscopy on some selected system is also undertaken. The said analysis is carried out to study the nature of optical absorbance of pure dielectric and metal-dielectric composite. The experimental results also show the effect of weak magnetization in the composite material comprising of magnetic element inclusion.

3.5.1 Experimental Detail

The fresh water pearl was collected from south India and it was taken in the powder form for the UV-VIS experiments as a dielectric sample. Fine micron sized grain of Al, Ni, Fe was used for preparation of different metal-composite. Sample ‘a’ for the UV-VIS study was only pearl powder. Pearl powder composite with Ni particle was marked as sample ‘b’. Pearl powder composite of Ni particle exposed under moderate magnetic field for about 48 hours was taken as sample ‘c’. Pearl powder composite with Fe particle was marked as sample‘d’. The weakly magnetized Pearl powder composite of Fe particle under magnetic field for 48 hours was taken as sample e. Sample f was the pearl powder composite of Al particle. The optical (UV-VIS) absorption spectra of the samples were recorded with 2450 UV-VIS spectrophotometer, Shimadzu, Japan in the range between 225 to 900 nm with sampling interval 0.5 nm and slit width 5 nm.

3.5.2 Results and Discussions

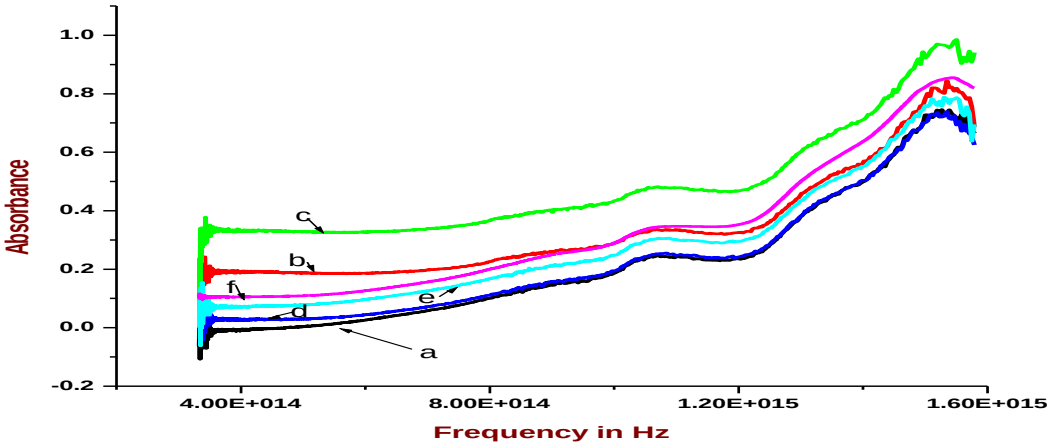

Figure 3.4. UV VIS absorbance spectra. a- Pearl, b- Pearl Ni composite, c- magnetized pearl - Ni composite, d- Pearl-Fe composite, e- magnetized Pearl-Fe composite, f- Pearl-Al composite

Figure 3.4 shows the changes of absorbance data with frequency of the dielectric material pearl due to inclusion of Al as metal particle and Ni and Fe as magnetic materials respectively. It also shows the effect of applied magnetic field on the respective composites. Optical absorbance is related to the imaginary part of $\varepsilon^*$and it has been found from UV-VIS absorption data.

3.6 Another study of Effective Dielectric Constant of DMD UV-VIS spectroscopy

Natural mica is a non-magnetic dielectric. Electro-deposition of Ni atoms over one surface of natural mica sheet (thickness 1.5 mm) is taken. The mentioned specimen was regarded as a DMD system.

3.6.1 Experimental Detail

The UV-VIS absorption spectra of the fabricated DMD specimen was recorded with model 2450 UV-VIS spectrophotometer, Shimadzu, Japan in the range between 225 to 900 nm.

3.6.2 Results and Discussions

The experimental result of UV-VIS spectroscopy is shown in Fig.3.5. It compares absorbance of the pure mica to that of fabricated DMD specimen. The absorbance of the Ni coated mica is greatly modified presence of magnetic layer on mica sheet. It has been found [32] that in magneto-electric, ferroic, and chiral materials the application of magnetic field can produce over its pure variant. The observed variation is due the coupling of EM field of the incident EM wave from the spectrometer and the said coupling is due to the over its pure variant. The experimental result of UV-VIS spectroscopy is shown in Figure.3.5. It compares absorbance of the pure mica to that of fabricated DMD specimen. The absorbance of the Ni coated mica is greatly modified.

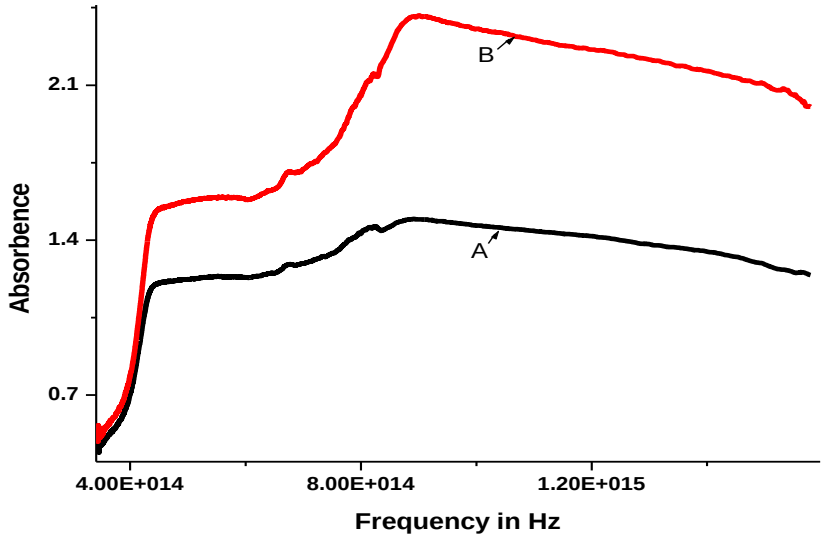

Figure 3.5 UV-VIS absorbance spectra for A- pure mica (thickness = 1.5 mm), B-Ni coated composite

A dielectric response and the application of an electric field can produce a magnetic response. These cross coupling behaviors can be found to occur in specific material lattices, layered thin films, or by constructing composite materials. When a strong electric field is applied to a magneto-electric material such as nickel / chromium oxide, the structure is slightly distorted, which changes the magnetic moment and therefore cross coupling.

The modification, of nature of optical absorbance of pure mica shown by graph A in Fig.3.5 , compared to that in DMD system represented B in the Fig.3.5. It is purely due magnetic layer over mica sheet. The over results obtained are in qualitative agreement

The proposed theoretical formulation of DMD like composites and its comparison with experimental result shows a good qualitative agreement. The effective dielectric function may be exploited for DMD composite material to study their optical and electrical behavior.

3.7 An Experimental Investigation of Electrical, Optical Properties of DMS under External Magnetic Field in Present Study

In this sub section magnetoresistance of a DMS system is analyzed. Diluted magnetic a (DMSs) have received considerable attention [41] due to the possible application of both charge and spin degrees of freedom in spintronics devices. Mn doped DMS leads to ferromagnetism and interesting magneto optical transport properties. Theoretical understanding of the physical properties of DMSs remains as a complicated topic. Recently large magnetoresistance effects in DMS have also been observed. A large positive MR effects in the DMS like (Zn, Mn) Se in the regime of electron hopping has also been reported [42].

The physical origin of the MR effect lies in the manifestation of spin orbit coupling. The electron cloud around each nucleus deforms slightly as the direction of the magnetization rotates, and this deformation changes the amount of scattering undergone by the conduction electrons when traversing the lattice. A heuristic explanation is that the magnetization direction rotates the closed orbit orientation with respect to the current direction. If the field and magnetization are oriented transverse to the current, then the electronic orbits are in the plane of the current, and there is a small cross-section for scattering, giving a low resistance state. Conversely for fields applied parallel to the current, the electronic orbits are oriented perpendicular to the current, and the cross-section for scattering is increased, giving a high resistance state

The Nickel oxide is known as magnetic semiconductor although its nature of magnetism is anti-ferromagnetic.

Magnetoresistance (δ_H) is a phenomena where value of the electrical resistivity of a material change under the application of an external magnetic field to it. This is also known as ordinary magnetoresistance (OMR) and is given by,

$$\delta_H = \frac{R(0) - R(H)}{R(H)}$$

R(0) is the no field electrical resistance of a specimen, R(H) is that under application of external field H. $R=Z\ Cos\theta$, for ac results, Z and θ are the impedance phase angle respectively.

Recently it has been observed that some materials and multilayer exhibit MR different from OMR type namely giant magneto resistance (GMR), colossal magnetoresistance (CMR) and tunnel magnetoresistance (TMR). Giant magnetoresistance (GMR) is a quantum phenomena at macroscopic scale. The type of MR is observed in structures consisting alternate thin-films of ferromagnetic and non-magnetic conducting layers.

3.7.1 Sample Preparation

The Nickel acetate hydrate and cobalt acetate hydrate, analytical grade (Alpha Aesar) was heated (about 300 ^{o}C) for 8h to prepare NiO and CoO powder. The developed NiO and CoO powder was grinding and strongly heated (about 350 ^{o}C) for 10h. Anhydrous NiO and CoO were taken in form of pellets prepared by mechanical pressing at pressure 12 ton/cm^2 followed by sintering.

3.7.2 Experimental Details

AC impedance measurements of the bulk specimen between two high polished copper electrodes were carried out using LCR meter, HIOKI 3522-50 (Japan) between frequency ranges 1to 100 kHz at the fixed input voltage 1V.

DC current voltage characteristics (CVC) of the developed pure and carbon doped Nio specimens were studied. The developed pellet was sandwiched between two high polished copper plate for such electrical measurement, the applied field direction are parallel to sample plane (L mode) and perpendicular to the sample plane (T mode). The DC CVC was recorded at room temperature (RT) by Keithley 2400(USA) Source meter unit and plotted by using characterization software.

UV-VIS absorption spectra of the specimens were studied with model UV-2450, UVVIS spectrophotometer, Shimadzu, Japan in the range between190nm to 900nm at adequate accuracy using integrating sphere attachment.

3.7.3 Result and Discussion

Figure.3.6 shows the variation of ac resistance R of CoO with frequency and B as parameter. Increase in R is observed in both L and T mode due to increase B over the corresponding no field R. Increase in R is more on L mode compare to that in T mode. Figure 3.7 provides the corresponding results on NiO and overall effects are less dominant. Figure 3.8 shows dc V-I characteristics of CoO with B as parameter.

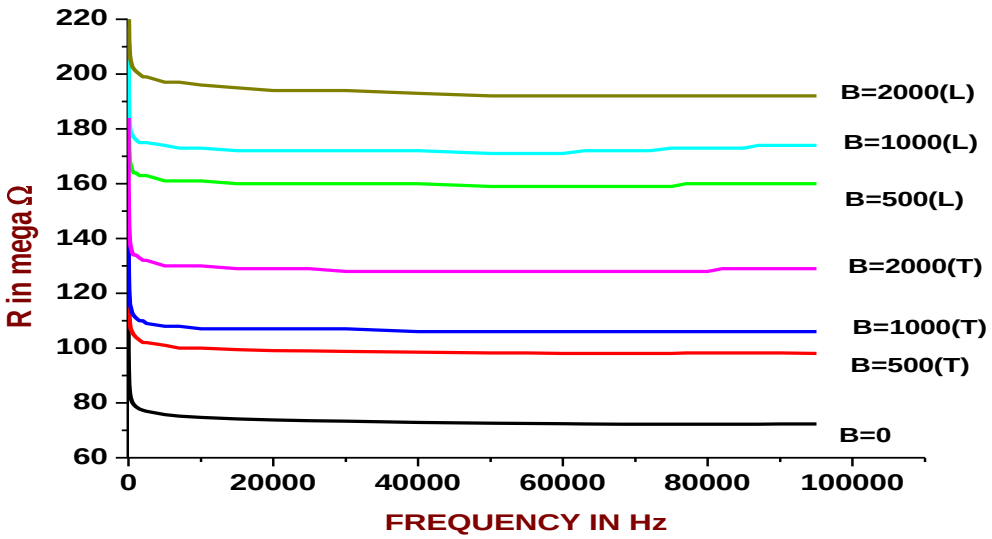

Figure 3.6 Plot of Variation of R as a function of frequency measured at different Magnetic field on CoO both for L mode and T mode.

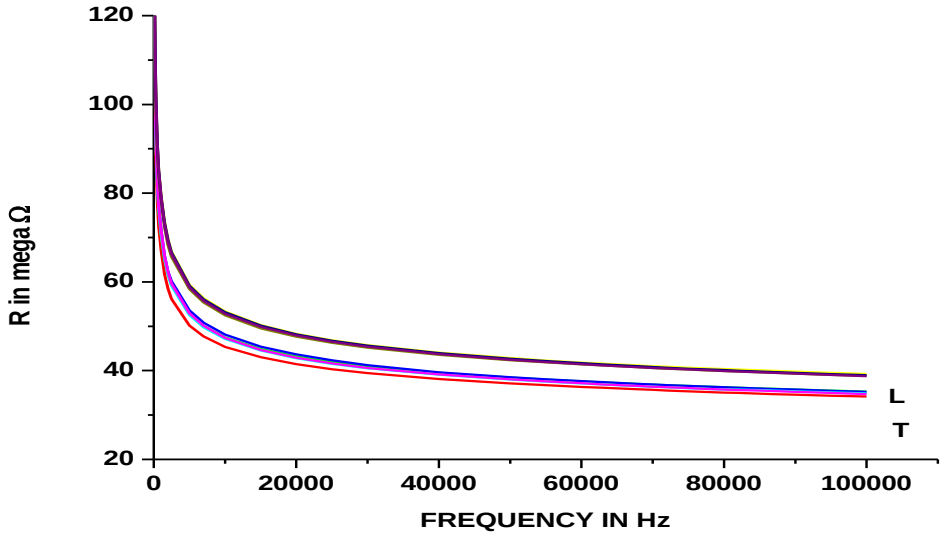

Figure 3.7 Variation of R as a function of frequency measured at different **B** on NiO both for L mode and T mode (black line is for without field)

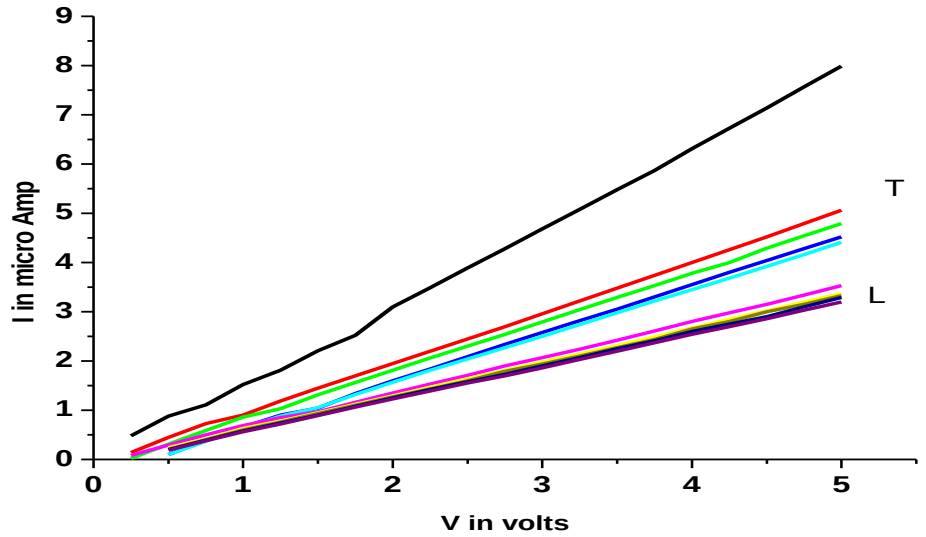

Figure 3.8: I -V characteristic of pure CoO with B as parameter

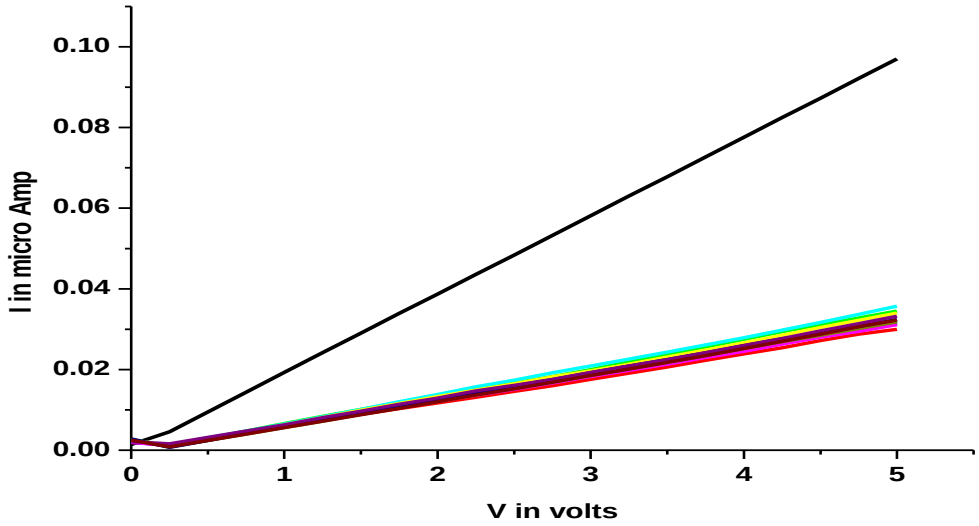

Figure 3.9: I-V characteristic of CoO with carbon with B as parameter.

Figure.3.9 compares the corresponding results on Carbon doped CoO. Fig. 3.10 is the dc V-I of NiO in L and T mode along with no field result. Figure.3.11 summarized the results of optical absorbance of CoO from UV-VIS study and it also compares the same with **B**. The Figure.3.11 shows a finite change in optical absorbance on application of **B**.

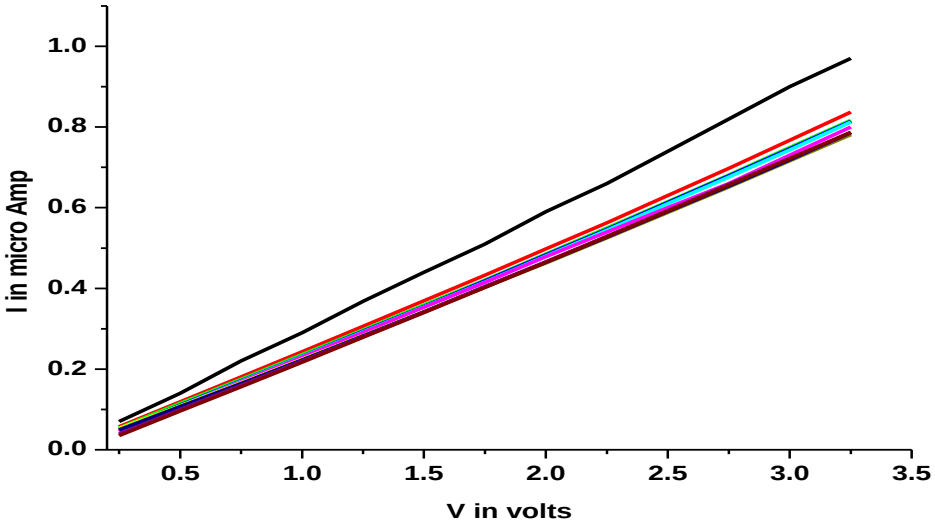

Figure 3.10: DC I-V characteristic of NiO with B as parameter

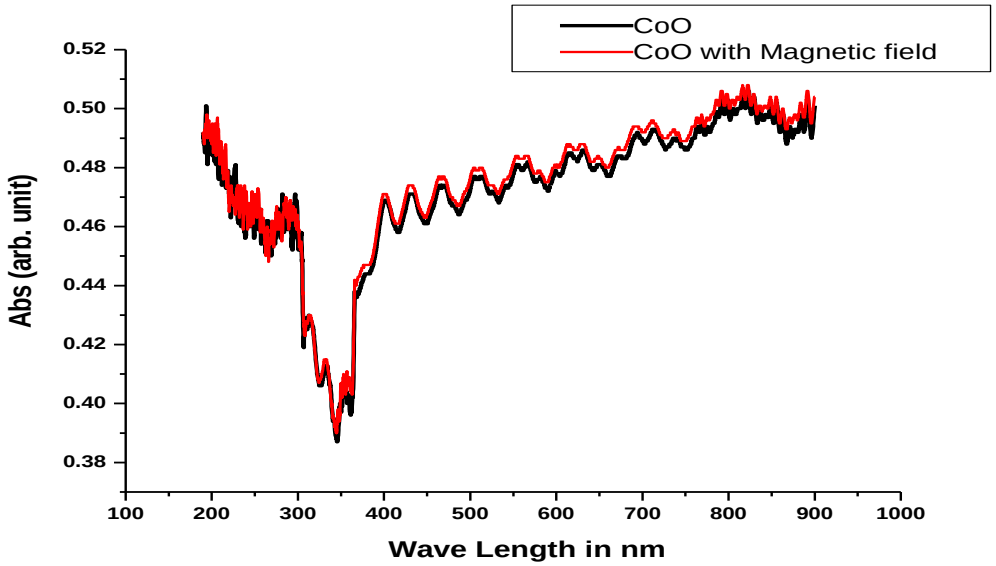

Figure 3.11.UV VIS absorbance spectra for CoO and CoO with Magnetic field.

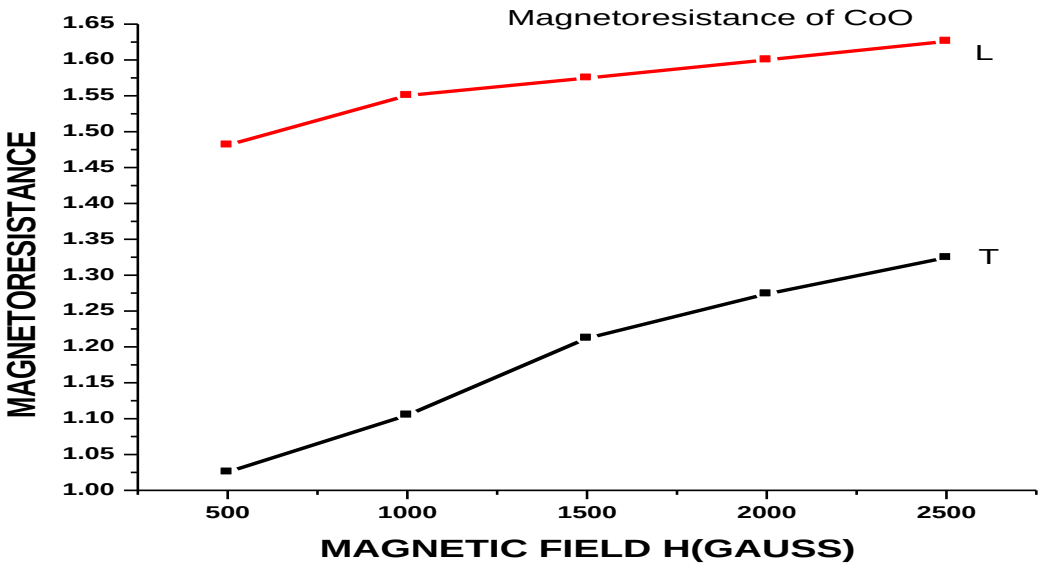

Figure 3.12 DC Magnetoresistance of CoO (L and T mode)

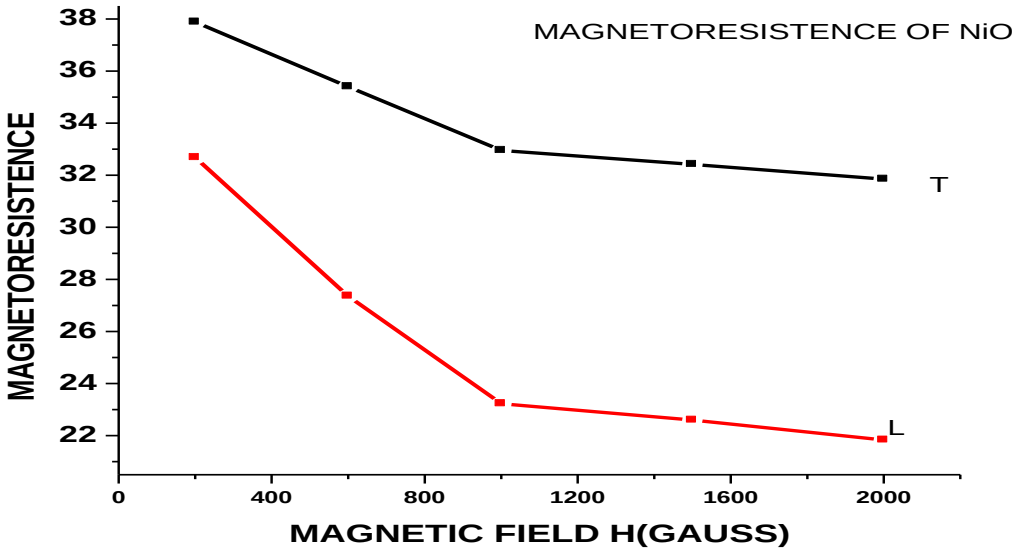

Figure 3.13 DC Magnetoresistance of NiO.

Figure.3.12 and Figure.3.13 provide the variation of MR for L and T modes of measurement on CoO and NiO respectively. Figure.3.13 exhibits a different feature of MR for NiO compared to that CoO shown in Figure.3.12.

The prepared DMS systems exhibit almost linear dc V-I characteristics. MR effects are found to prominent in both CoO and NiO. Later being anti-ferromagnetic at RT, exhibits decrease in MR with increase in B. A small change in optical absorbance of CoO was observed under application of B as the probable spin-orbit effect. A finite discontinuity in the slope of MR vs **B** for NiO was also observed.

CHAPTER 4

OPTICAL AND ELECTRONIC PROPERTIES OF DMD SYSTEM

When light moves from a medium of a given refractive index n_1, into a second medium with refractive index, n_2, both reflection and refraction of the light may occur. The Fresnel equations [43] describe what fraction of the light is reflected and what fraction is refracted (i.e., transmitted). They also describe the phase shift of the reflected light.

The equations assume the interface between the media is flat and that the media are homogeneous. The incident light is assumed to be a plane wave, and effects of edges are neglected.

S and p polarizations

The behaviour depends on the polarization of the incident ray, which can be separated into 2 cases:

s-polarized (perpendicular) or TE

The incident light is polarized with its electric field perpendicular to the plane containing the incident, reflected, and refracted rays. This plane is called the plane of incidence; it is the plane of the diagram below. The light is said to be s-polarized,

p-polarized (parallel) or TM

The incident light is polarized with its electric field parallel to the plane of incidence. Such light is described as p-polarized, from parallel.

According to Electromagnetic theory, at the interface of two dielectrics,

$$E_{0I} - E_{0R} = \beta E_{0T} \tag{4.1}$$

Where, E_{0I}, E_{0R} and E_{0T} are the amplitudes of incident, reflected and transmitted electric field of EM wave and

$$\beta = \frac{\mu_1 V_1}{\mu_2 V_1} = \frac{\mu_1 n_2}{\mu_2 n_1} \tag{4.2}$$

$$E_{0I} + E_{0R} = \alpha E_{0T} \tag{4.3}$$

Where,
$$\alpha = \frac{\cos\theta_T}{\cos\theta_I} \tag{4.4}$$

Solving eq (4.1) and (4.3) for the reflected and transmitted amplitude, we obtain

$$E_{OR} = \frac{(\alpha-\beta)}{(\alpha+\beta)} E_{OI} \tag{4.5}$$

$$E_{OT} = \frac{2}{(\alpha+\beta)} E_{OI} \tag{4.6}$$

These are known as Fresnel's equation for the case of polarization in the plane of incidence.

The amplitude of the transmitted and reflected waves depends on the angle of incidence.

Because α is a function of θ_I

$$\alpha = \frac{\sqrt{1-\left[\frac{n_1}{n_2}\sin\theta_I\right]^2}}{\cos\theta_I} \tag{4.7}$$

In case of normal incidence $\theta_I = 0$, α=1.At grazing incidence θ_I=90°, α diverges and the wave is totally reflected. There is an intermediate angle Brewster angle (θ_B) at which the reflected wave is completely extinguished. For Non magnetic dielectric

$$\mu_1 = \mu_2 = \mu_0 \tag{4.8}$$

Brewster angle (θ_B),

$$\theta_B = \tan^{-1}\beta = \tan^{-}\left(\frac{n_2}{n_1}\right) \tag{4.9}$$

Where, n_2 and n_1 are absolute refractive indices of the two medium.

For DMD system, in general

$$\tan\theta_B = \sqrt{\mu_r \varepsilon_r} \tag{4.10}$$

At zero field the relation given by equation (4.10) becomes,

$$\tan\theta_B(0) = \sqrt{\mu_r(0)\varepsilon_r} \tag{4.11}$$

And at the presence of field H. the same is,

$$\tan\theta_B(H) = \sqrt{\mu_r(H)\varepsilon_r} \tag{4.12}$$

Hence using equations (4.11) and (4.12),

$$\frac{\mu_r(H)}{\mu_r(0)} = \left[\frac{n(H)}{n(0)}\right]^2 \tag{4.13}$$

Ferromagnetic or super-paramagnetic [49] material exhibits a non linear magnetization curve and hence μ_r (H) is a non-linear function of H. Moreover as H→ H_K, the relative permittivity is $\mu_r \rightarrow 0$, where H_K is saturation field.

4.1 Optical Investigation of Effective Permeability of Dilute Magnetic Dielectrics with Magnetic Field on Gadolinium oxide

In an early work [44] the effective dielectric response of the system under external magnetic field was studied theoretically .The work provides a good account of effective dielectric

response of the DMD system. Debye formalism was simply extended by adding the coupling term to describe the general response of a dielectric in crossed magnetic and electric fields. Gadolinium (Gd) is a weak magnetic element [45] at room temperature. It has been demonstrated that the effective dielectric constant of the system is dependent on external magnetic field also.

Characterization techniques of magneto-optic Kerr Effect (MOKE)

One of most popular technique for detection and measurement of magnetism uses the optical method. The magneto-optic Kerr Effect (MOKE) [47] is a powerful spectroscopic tool in magnetic materials research Magneto-optic phenomenon play an important role in the development of Maxwell's electro-magnetic (EM) theory. Maxwell theory describes a macroscopic description of the MOKE involving the energy and material dependent dielectric tensor, and the magnetic aspects. The microscopic manifestation of the magneto – optic effect lies in the interaction between the electric field of the incident EM wave and the magnetic moments in the solid. Magneto Optical Kerr effects are generally described macroscopically by dielectric tensor theory or the effects can also be described microscopically, where the coupling between the electric field of the light and the magnetisation occurs by the spin-orbit interaction. To understand the magneto optical Kerr effects, one need to understand the terminologies associated with the effect, how the state of polarisation of reflected light is dependent upon the initial polarisation and the magneto optical geometry in which it is being used. The MOKE instrumentation is a very elite technology.

In this present work another simple optical techniques for investigation of magnetism in a DMD is employed. The technique exploited the Maxwell's EM theory. DMD with good reflecting surface to exhibit minimum reflectance of incident in plane polarized light. The corresponding angle of incidence is the Brewster angle [47]. Brewster's no reflection condition is one of the main features of the laws of reflection and refraction of electromagnetic waves at interface between two media. For a specific incident angle, known as the Brewster angle, the reflected wave vanishes. In dielectric media, this phenomenon exists only for transverse-magnetic (TM) waves (p waves), and not for transverse-electric (TE) waves (s waves). The influence of external out of plane magnetic field is to cause the variation of the Brewster

angle due change in magnetism of the specimen. The experimental realization Brewster's effect is applied metamaterials [46]. In the experiment designed an array of split ring resonators (SRRs) as a metamaterial was used with micro-wave. In this present work following the path of the light beam from its starting place to the photodetector, the setup involves a monochromatic light source which can be realized, e.g., by a stable laser diode. The latter provides a monochromatic, nearly parallel light beam of roughly linearly polarized light. Further elements are a polarizer P, the magnetic sample S, an analyzer A, and the photodetector. Gadolinium oxide (Gd_2O_3) is a poor semiconductor with magnetism is chosen as DMD. The details of underlying theory, material preparation, and experimental analysis are summarized in the following sub-sections.

According to Electro Magnetic Theory, light that is reflected from a magnetized surface can change in both polarization and reflected intensity. The effect is similar to the Faraday Effect. The Faraday Effect describes changes to light transmitted through a magnetic material, while the Kerr effect describes changes to light reflected from a magnetic surface. Both effects result from the off-diagonal components of the dielectric tensor $\boldsymbol{\varepsilon}$. These off-diagonal components give the magneto-optic material an anisotropic permittivity, meaning that its permittivity is different in different directions. The permittivity affects the speed of light in a material:

$$U=(\mu\boldsymbol{\varepsilon})^{-1/2} \tag{4.14}$$

Physically, Brewster's phenomena can be understood as follows, when electromagnetic waves is at the interface between two media, the direction of the induced electric dipole in second medium is perpendicular to the wave vector. With regard to TM waves, the dipole lies in the plane of incidence. A linearly vibrating dipole radiates transversally and cannot emit radiation in the direction of the vibration. This direction coincides with the wavevector of the reflected wave when the Brewster condition is satisfied. The oscillating dipoles in the medium 2 do not send any waves in the direction of the reflection. On the other hand, with regard to TE waves, each dipole is perpendicular to the plane of incidence and emits waves isotropically in the plane. Therefore, no special angles exist for TE waves. (The dipole model

also explains the sign change in the amplitude reflectivity when the angle is changed through the Brewster angle.)

In this present work another simple optical technique for investigation of magnetism in a DMD is attempted. The technique exploited the Maxwell's EM theory. DMD with good reflecting surface to exhibit minimum reflectance of incident in plane polarized light. The corresponding angle of incidence is the Brewster angle. Brewster's no reflection condition is one of the main features of the laws of reflection and refraction of electromagnetic waves at a boundary between two media. For a specific incident angle, known as the Brewster angle, the reflection wave vanishes. In dielectric media, this phenomenon exists only for transverse-magnetic (TM).

One of most popular techniques for detection and measurement of magnetism uses the optical method. The magneto-optic Kerr Effect (MOKE) is a powerful spectroscopic tool in magnetic materials research Magneto-optic phenomenon play an important role in the development of Maxwell's electro-magnetic (EM) theory. Maxwell theory describes a macroscopic description of the MOKE involving the energy and material dependent dielectric tensor, and the magnetic aspects. The microscopic manifestation of the magneto – optic effect lies in the interaction between the electric field of the incident EM wave and the magnetic moments in the solid. The MOKE instrumentation is very elite technology.

In this present work another simple optical technique for investigation of magnetism in a DMD is attempted. The technique exploited the Maxwell's EM theory. DMD with good reflecting surface to exhibit zero/ minimum reflectance of incident in plane polarized light. The corresponding angle of incidence is the Brewster angle. The influence of external out of plane magnetic field is to cause the variation of the Brewster angle due change in magnetism of the specimen. In this present Gadolinium oxide (Gd_2O_3) is a poor semiconductor with magnetism is chosen as DMD. The details of underlying theory, material preparation, and experimental analysis are summarized in the following subsections.

4.1.1 Sample Preparation

The Gadolinium (III) acetate hydrate, analytical grade (Alfa Aesar) was heated (about 200 ^{0}C) for 8h to prepare Gd_2O_3 powder. The developed Gd_2O_3 powder was grinding and heated (about 300 ^{0}C) for 20h. After heating a pellet is formed by mechanical pressing at pressure 12ton/cm^2. This applied pressure makes the specimen shiny enough to achieve optical reflection.

4.1.2 Experimental Details

The optical reflectance measurement was carried out using specially designed optical spectrometer, an indigenous set up in which a monochromatic He- Ne LASER (wave length 633 nm) was used as a source and a polarizer was used at the collimator end of the spectrometer to get plane polarized light. The cross-wire of the spectrometer was replaced by a photo transistor to produce equivalent current proportional to the light intensity. The electric current equivalent of reflected light intensity for different angle of incidence (at angular resolution of 20") of the plane polarized light was recorded by photo transistor based high sensitive detector along with Keithley 2400 (USA) source meter. Experiment was carried out for in plane polarized light namely polarization parallel to the plane of incidence. All measurements were done at room temperature, 300 K. Figure 4.1 shows Experimental setup for optical reflectivity measurement.

4.1.3 Results and Discussions

The optical reflectance measurements using the mentioned set were carried over the developed DMD specimen at five different external fields (excluding zero field).

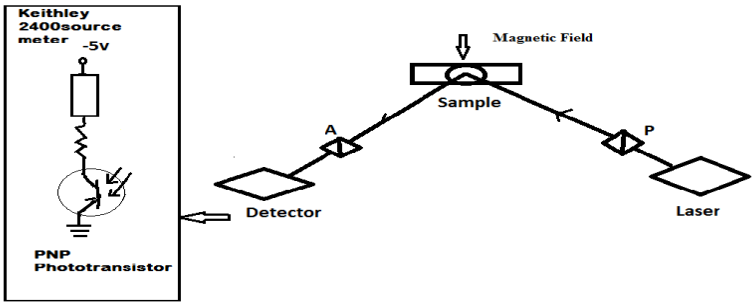

Figure.4.1 an indigenous Experimental setup for optical reflectivity measurement

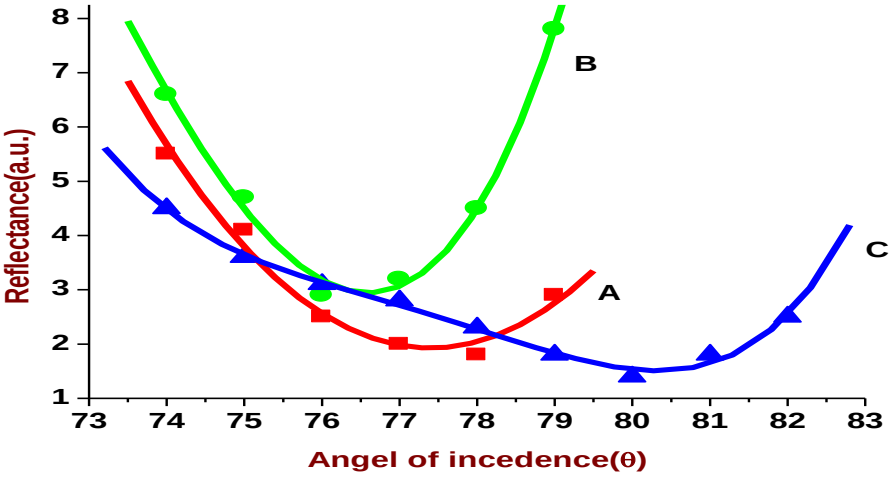

Figure 4.2: reflectance with angle of incidence (for Gd_2O_3) pellet with thickness 0.5 mm) for polarization vector of the field parallel to the plane of incidence. Experimental curve A - with zero magnetic field. B - with high magnetic field (200G), and C -with low (20G) magnetic field.

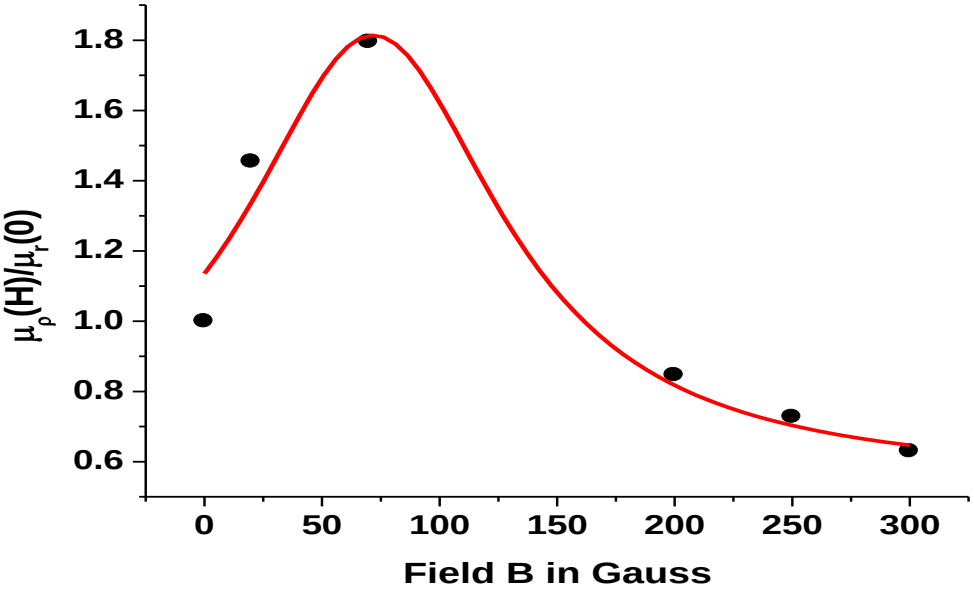

Figure 4.3 Variation of $\mu_r(H)/\mu_r(0)$ the specimen Gd_2O_3 with external field. Dots are the experimental points and solid red line is best fit curve for the relation.

Figure 4.2 shows the angular variation of intensity of the reflected light for mentioned external field including zero fields. The minimum of the intensity corresponds to the Brewster angle measured at an accuracy of about $\pm 1^0$.

Figure 4.3 Shows the variation of $\mu_r(H)/\mu_r(0)$ with H. The overall variation nature is that of Ferro-magnetic material. A knowledge of $\mu_r(0)$ or ε_r may be used in evaluation of $\mu_r(H)$. The same may be applied by neglecting small contribution from cross coupling effect. The results of variation of $\mu_r(H)/\mu_r(0)$ with H, shows the typical character of ferro-magnetic material. The graph also shows the tendency to assume the magnetic saturation of the material.

The variation of Brewster angle with external field on the developed DMD was recorded successfully. The experimental DMD has a Ferro-magnetic at room temperature, an improved version of the instrumentation could be a cost effective one for determination

magnetism in such DMD specimen. The overall success of this work is good and encouraging.

4.2 Optical Investigation of Effective Permeability of Dilute Magnetic Dielectrics with Magnetic Field on Sulfide samples developed by green synthesis

Long range magnetic order is mainly found in materials containing elements from the 3d transition metals (such as Co and Ni) and the 4f rare-earth metal series like Gd. Magnetic materials which contain 4f electrons usually have a saturation magnetization close to what has been predicted predicted by Hund's rule, but the moment configuration is quite complicated and spin reorientations are often observed. The saturation magnetization of the transition metals on the other hand very seldom follow Hund's rule and due to the itinerant nature of the 3d electrons, the saturation magnetisation can vary to a great extent. For applications, 3d materials are more often used due to their higher Curie temperatures. The materials are tailor-made to fit in the application. Whereas the coercivity has historically been the most important parameter and the growing interest of data storage has made the anisotropy and the magneto-resistive properties the most studied parameters.

In this work authors have investigated dielectric response for four DMD sample i.e. Gadolinium Nickel Sulfide Complex, Cobalt Sulfide, Nickel Sulfide and Titanium. All samples were synthesized following chemical and green techniques. Later process provides good stability of the nano clusters (NC) due to in-situ capping of sample NC. It has been found that the optical band gap in sample developed by green synthesis is lowered considerably over that in the chemically synthesized sample. The green agencies used in this work are Jatropha latex [45] and dilute Garlic extracts, both are enriched in sulphur and other organic polymeric molecules.

4.2.1 Sample Preparation

The Gadolinium (III) acetate hydrate, analytical grade (Alfa Aesar) was heated about 2000C for 8h with latex of jatropha to prepare Gadolinium Sulfide powder. Gadolinium Nickel Sulfide complex sample were prepared by solid-state reaction method using high purity precursor materials of Gadolinium Sulfide and NiO. Stoichiometric proportion of the powders were thoroughly mixed and heated at temperatures about 3000C for 20h. The Cobalt Sulfide, Nickel Sulfide and Titanium Sulfide are prepared by thermal dissociation with latex of jatropha of respective acetate hydrate. The developed sample was grinding and heated about 3000C for 20h. After heating, a pellet formed by mechanical pressing at pressure 12 ton/cm^2. This applied pressure makes the specimen shiny enough to achieve optical reflection.

4.2.2 Experimental Details

The optical reflectance measurement was carried out using specially designed optical spectrometer, an indigenous set up in which a monochromatic He- Ne LASER (wave length 633 nm) was used as a source and a polarizer was used at the collimator end of the spectrometer to get plane polarized light. The cross-wire of the spectrometer was replaced by a photo transistor to produce equivalent current proportional to the light intensity. The electric current equivalent of the reflected light intensity for different angle of incidence (at angular resolution of 20") of the plane polarized light was recorded by photo transistor based high sensitive detector along with Keithley 2400 (USA) source meter. Experiment was carried out for in plane polarized light namely polarization parallel to the plane of incidence. All measurements were done at room temperature, 300 K.

The developed pellet was sandwiched between two high polished copper plates to form experimental parallel plate capacitor with known geometry. The measurement was done at room temperature (RT) with HIOKI 3522-50 LCR Hi TESTER(JAPAN). DC current voltage characteristics of Gadolinium Nickel Sulphide complex, Cobalt Sulphide, Nickel Sulphide and Titanium Sulphide is measured by Keithley 2400 (USA) source meter.

4.2.3 Results and Discussions

The optical reflectance measurements using the mentioned set were carried over the developed DMD specimens at different external fields. Figure 4.4 Shows the variation of $\mu_r(H)/\mu_r(0)$ with H. The overall variation nature is that of Ferro-magnetic/superparamagnetic[49] material.

A knowledge of $\mu_r(0)$ or ε_r may be used in evaluation of $\mu_r(H)$. The same may be applied by neglecting small contribution from cross coupling effect. The results of variation of $\mu_r(H)/\mu_r(0)$with H, shows the typical character of ferro-magnetic /superparamagnetic material.

Fig.4.4a exhibits a very clear signature of ferro-magnetic/ superparamagnetic nature of the material which may be obtained from derivative of magnetization curve. The graph also shows the tendency to assume the magnetic saturation of the material at low field. This nature is also observed in Fig 4.4b and Fig.4.4c but saturation at relatively higher field compared to that in Fig. 4.4a. The material corresponding to Fig.4.4d exhibits a typical nature for ordinary paramagnetic material. They are relatively good candidates for DMD system. The experimental analysis indicates that obtained magnetism is mostly due to the surface magnetism [50] which is very interesting for topological crystalline insulators [51]. Following Stoner criteria and beyond it may be emphasized that surface magnetism is supposed to be more pronounced over Bulk counterpart due to enhanced moment at the surface. Surface magnetism of nano-structured material exhibits many interesting features [52].

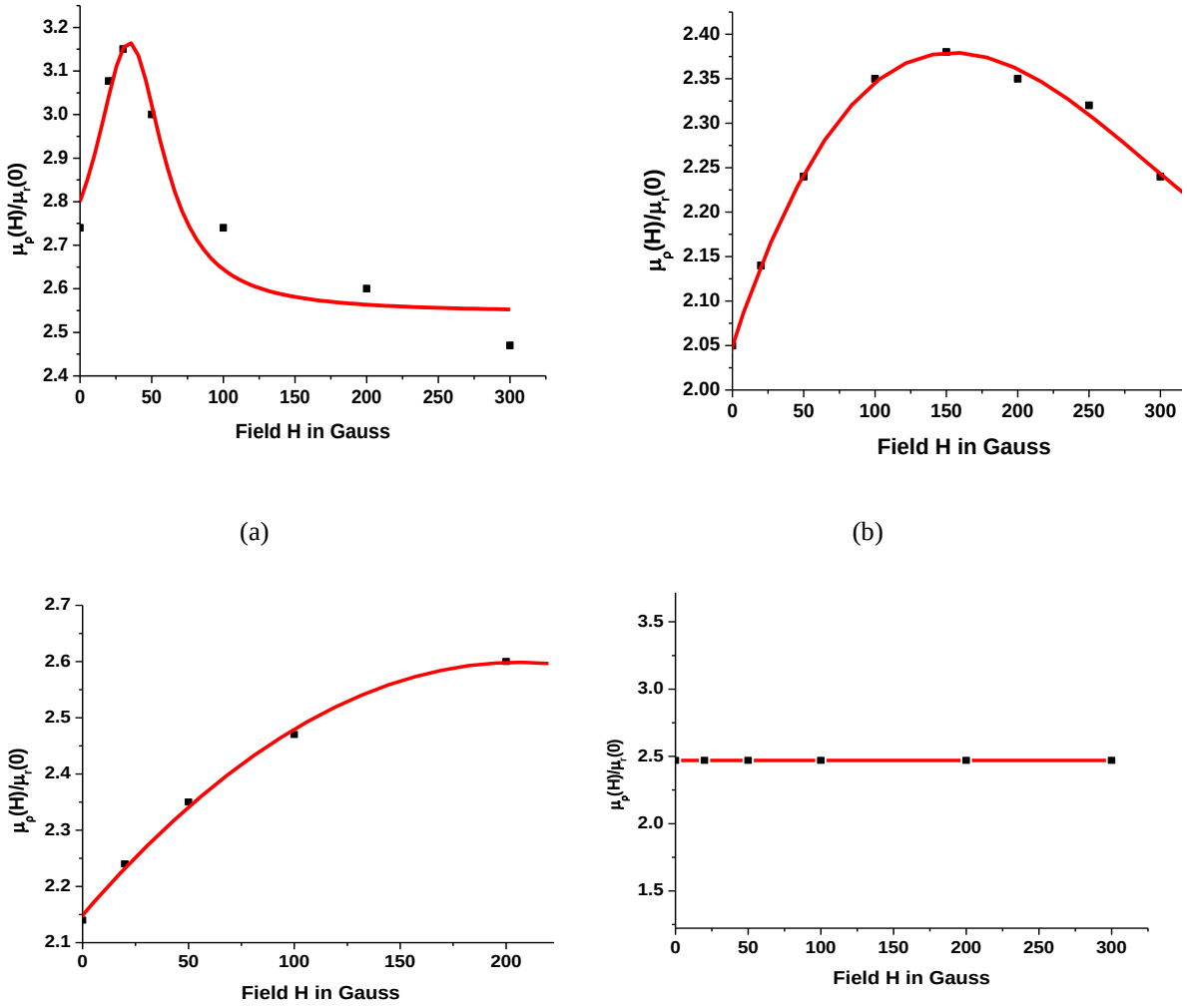

Figure 4.4 Plot of variation of $\mu_r(H)/\mu_r(0)$ of the specimen with external field (a) Gadolinium Nickel Sulfide complex(1.51mm),(b) Cobalt Sulfide(1.54mm),(c)Nickel Sulfide(1.56mm) and (d)Titanium Sulfide(1.52mm). Dots are the experimental points and solid red line is best fit curve for the relation.

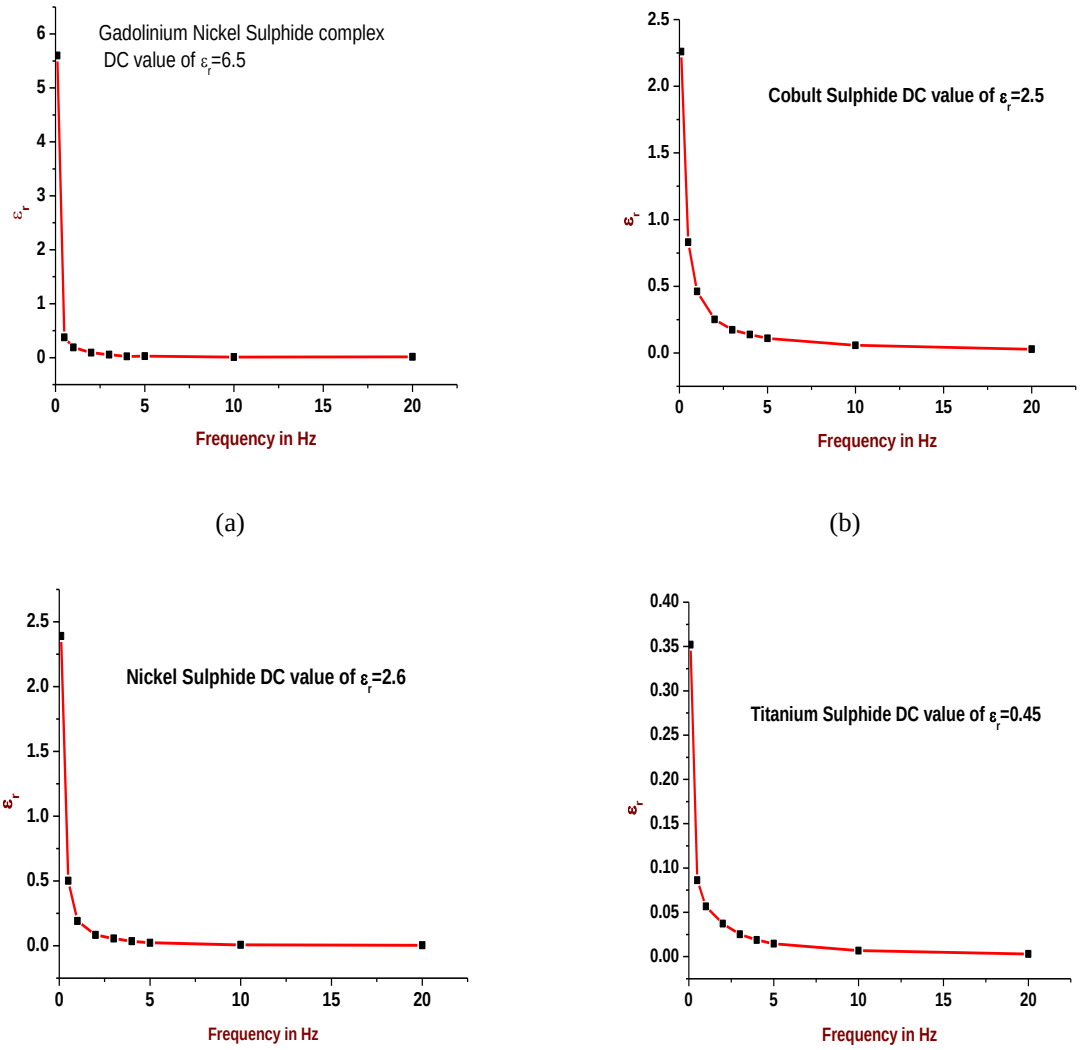

Figure 4.5 Plot of variation of relative ε with frequency of impressed a.c. signal. (a) Gadolinium Nickel Sulfide complex, (b) Cobalt Sulfide, (c) Nickel Sulfide and (d) Titanium Sulfide

Fig.4.5 (a, b and c) show the variation of relative ε with frequency of impressed a.c. signal. They exhibit a strong dielectric nature of materials. The extrapolated dc vale of ε decreases for material corresponding to Fig.4.5a to Fig.4.5d. Fig.4.6 shows the dc volt-ampere characteristics of Gadolinium Nickel Sulfide complex, Cobalt Sulfide, Nickel Sulfide and Titanium Sulfide.

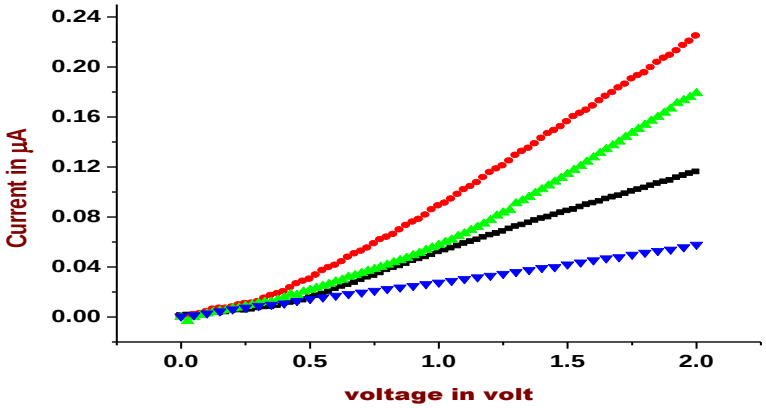

Figure 4.6 Plot of variation of dc current voltage characteristics of (a) Gadolinium Nickel Sulfide complex(black),(b) Cobalt Sulfide(red),(c)Nickel Sulfide(green) and (d)Titanium Sulfide(blue).

Table 1 – Computed value of dc conductivity unit=µ S/cm from linear part of respective curves from Fig.4

Cobalt Sulfide	Nickel Sulfide	Gadolinium Nickel Sulfide complex	Titanium Sulfide
5.88211E-4	3.19E-4	2.87064E-4	1.06E-4

Computed value of dc conductivity from linear part of respective curves in Fig.4.6 shown in Table I and it shows that Titanium Sulfide has lowest electrical conductivity hence poorest among the developed DMD.

The variation of Brewster angle with external field on the developed DMD was recorded successfully. The experimental DMD has a Ferro-magnetic or super-paramagnetic nature at room temperature, an improved version of the instrumentation could be a cost effective one for determination magnetism in such DMD specimens. The overall success of this investigation is found to be good and concise.

CHAPTER 5

LOW TEMPERATURE STUDY OF DMD SYSTEM USING SQUID MAGNETOMETRY

It has been found that several experimental studies [53-54] have been carried out at finite temperature on the nature of magnetism in the elemental ferromagnetism. Rare earths provide apparently a simple case for these studies where the magnetism appears due to indirect exchange coupling between localized 4 f moments via the highly delocalized (5d 6s)-valence states [1]. Gd is the most investigated case, being a prototype Heisenberg ferromagnet with a large moment (S=7/2) in the half-filled 4f levels. Various investigations [54–56] report that the exchange splitting of the bulk valence bands vanishes at the Curie temperature (TCb =293 K) as also observed in other rare earths [57-58]. While most attention has been paid to the surface states magnetism [74], the bulk [75] bands have been until now indisputably believed to follow a Stoner behavior. A comprehensive summary is also provided In a recent development [59].

Author performed SQUID-magnetometry for magnetic measurements. From the magnetic measurements observed magnetic ordering cannot be explained by conventional ferromagnetism. They concluded that the Gd is essential for the magnetic behavior but an additional contribution has to be considered. In their time and temperature dependent SQUID measurements, they deduced a metastable magnetism and memory effects, i.e., the magnetization loops depend on the history of the sample. These observations cannot be

explained by common ferromagnetism, superparamagnetism, or spinglass behavior. In consideration the claim of ferromagnetism at room temperature has to be slightly put into perspective. The hysteresis in the SQUID magnetization loops might not point to common ferromagnetism but anyway to an interesting physical phenomenon.

5.1 Experimental Details

In this work authors have investigated magnetic response for three specimens namely Gadolinium oxide, Gadolinium sulfide, Gadolinium sulfide by green synthesis. Later process provides good stability of the nano clusters (NC) due to in-situ capping of sample NC. It has been found that the optical band gap in sample developed by green synthesis is lowered considerably over that in chemically synthesized sample. The green agencies used in this work are Jatropha latex and dilute Garlic extracts, both are enriched in sulphur and other organic polymeric molecules. In this paper magnetocalcaloric effect is also shown from SQUID-magnetometry. Magnetocaloric effect (MCE) is defined as the heating or cooling of the magnetic materials due to a varying magnetic field. It is due to the coupling of the magnetic sublattice with the magnetic field, which changes the magnetic part of the entropy of a solid. Magnetic refrigeration [60-61] is an environment-friendly technology based on a magnetic solid that acts as a refrigerant by magneto-caloric effect (MCE). In the case of ferromagnetic materials MCE is a warming as the magnetic moments of the atom are aligned by the application of a magnetic field, and the corresponding cooling upon removal of the magnetic field. Magnetic refrigeration is an emerging technology alternative to the conventional gas-compression refrigeration in food preservation and air conditioning applications. Importantly, solid state-cooling offers noise-free and energy efficient refrigeration suitable for room temperature cooling and cooling of microelectronic components [61,63]. Solid state cooling is essential for the growing needs of low temperature applications in space, particle detectors, and medical applications [60-61,64-66]. Liquefaction of H2 (20 K) by magnetocaloric method has been reported to be cost effective and could render hydrogen to be a competitive alternative fuel [60]. To achieve cooling below 1 K, the adiabatic demagnetization refrigeration is an attractive process compared to 3He/4He dilution refrigeration because of the growing cost of helium and scarcely available 3He isotope. For low temperature magnetic refrigerant materials, it is important to have: (i)

large effective spin quantum number, (ii) low magnetic anisotropy and low magnetic ordering temperature, (iii) small specific heat (iv) large magnetization under magnetic field, and (v) weak magnetic exchange interactions [68]. In magnetic refrigeration technology, Gd and Gd based alloys [69-70], large molecular materials [71] have continued to receive large attention because large magnetic moment of Gd. In this work authors have investigated magnetic response for three specimens namely Gadolinium oxide, Gadolinium sulfide, Gadolinium sulfide by green synthesis. Later process provides good stability of the nano clusters (NC) due to in-situ capping of sample NC. It has been found that the optical band gap in sample developed by green synthesis is lowered considerably over that in chemically synthesized sample. The green agencies used in this work are Jatropha latex and dilute Garlic extracts, both are enriched in sulphur and other organic polymeric molecules.

5.1.1 Sample Preparation

The Gadolinium (III) acetate hydrate, analytical grade(Alfa Aesar) was heated (about 200^0 C) for 8h to prepare Gadolinium oxide powder (namely S1). The developed powder was grinding and heated (about 300 ^{0}C) for 20h. The Gadolinium (III) acetate hydrate, analytical grade (Alfa Aesar) was heated about 200^0C for 8h with sodium sulfide to prepare Gadolinium Sulfide powder (namely S2).The Gadolinium (III) acetate hydrate, analytical grade (Alfa Aesar) was heated about 200^0C for 8h with latex of Jatropha and dilute Garlic extracts to prepare Gadolinium Sulfide powder (namely S3).

5.1.2 Measurement Details

Magnetic measurements were done with an Ever Cool Quantum Design SQUID-VSM magnetometer (USA). Temperature dependent magnetization, M (T) in field-cooled (FC) modes with 0.01 T DC field for all the samples are measured from 10K to 350K. Isothermal field-dependent magnetization i.e., M (H) of all samples at 10 K, 100K, 300K is measured up to 7 Tesla.

5.2 Results and Discussions

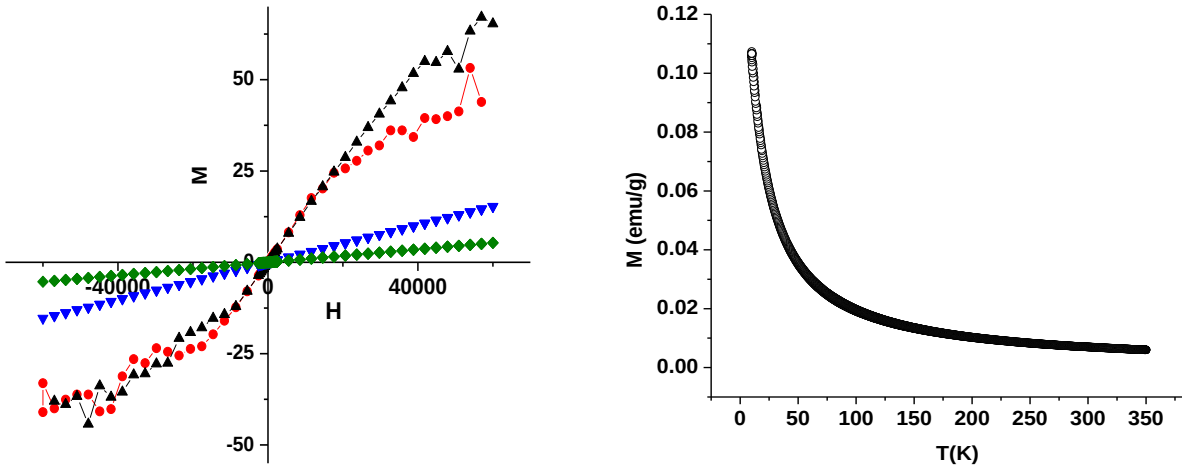

(a) (b)

Figure 5.1: (a) M(μ_B/f.u.)-H (Oe) curve, Magnetization loops obtained for sample S1 at 10 K (black and red line),100K (blue line), and 300 K (green line). (b)Temperature dependence of magnetization at field-cooled (FC) conditions at a magnetic field of 100 Oe for sample S1.

Gadolinium oxide is highly sensitive to its purity in environment. The most general form of Gd_2O_3 in general ($Gd_{2+x}O_{3-x}$), x varies in oxygen concentration; very smsll variation in x may change drastically. In this present experiment it is difficult to control x that causes apparent anomalous result. On the other hand Gadolinium oxide nanoparticles play a central role in multimodal imaging, targeting the cancer cells and drug delivery in medical science[72-73]. Magnetic Resonance (MR) images with higher resolution can be obtained with the help of contrast agents. Contrast agents are magnetic materials, either superparamagnetic or paramagnetic nanoparticles, which increases the MRI signal intensity. Among the various types of MRI contrast agents, gadolinium oxide nanoparticles are well suited for MR Imaging. Gadolinium oxide nanoparticles are positive contrast agents which can reduce the proton's spin-lattice (T1) relaxation time and increase the MR signal intensity.

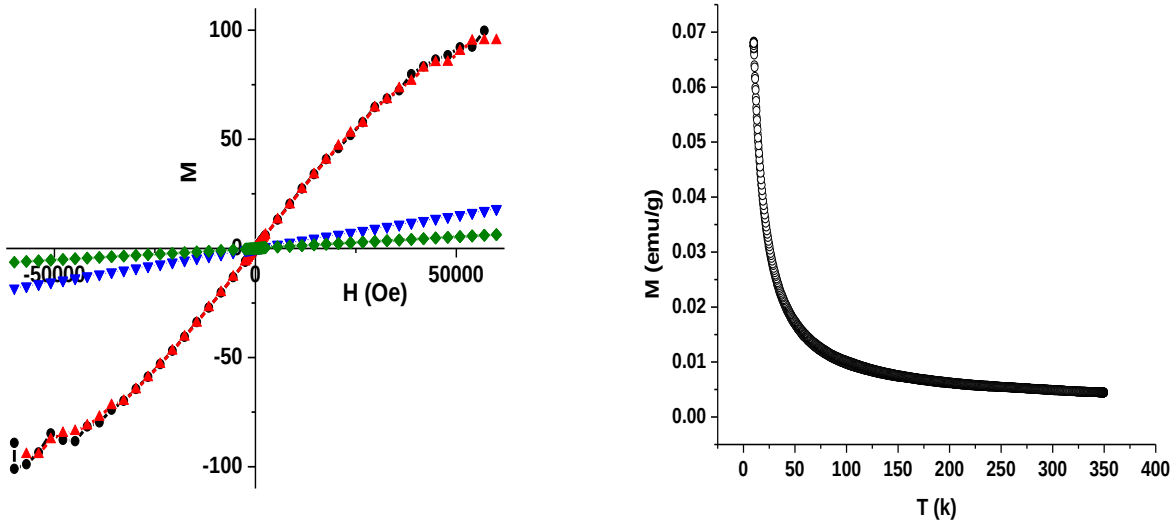

(a) (b)

Figure 5.2 :(a) M(μ_B/f.u.)-H (Oe) curve, Magnetization loops obtained for sample S2 at 10 K (black and red line),100K (blue line), and 300 K (green line). (b)Temperature dependence of magnetization at field-cooled (FC) conditions at a magnetic field of 100 Oe for sample S2.

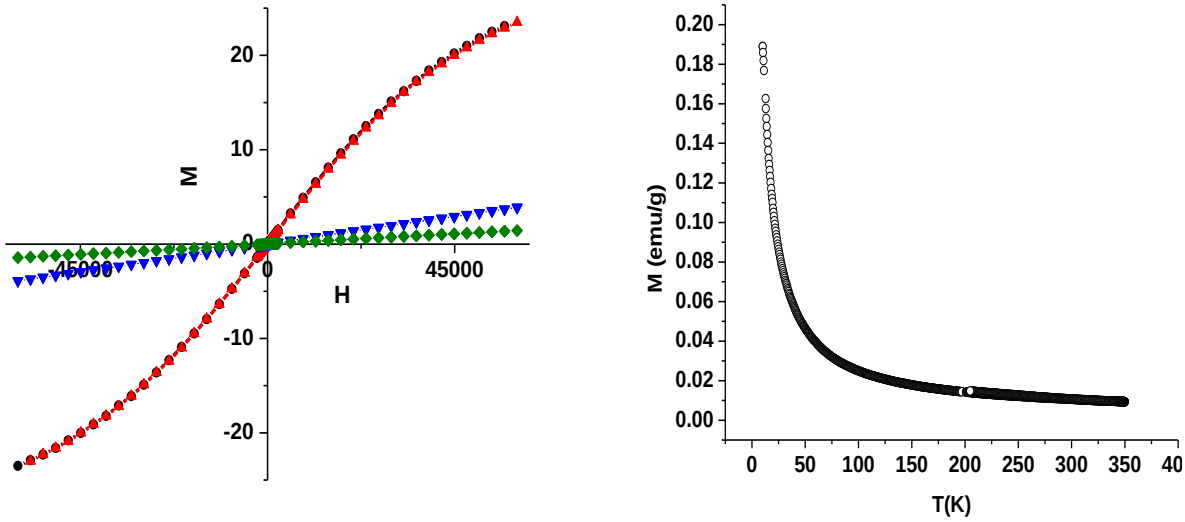

(a) (b)

Figure 5.3: (a) M(μ_B/f.u.)—H (Oe) curve, Magnetization loops obtained for sample S3 at 10K (black and red line), 100K (blue line), and 300 K (green line). (b)Temperature dependence of magnetization at field-cooled (FC) conditions at a magnetic field of 100 Oe for sample S3.

Isothermal field-dependent magnetization i.e., M (H) of specimen S1,S2and S3 samples at 10 K,100K, 300K up to 7 Tesla(70000 oe) is shown in the Fig1(a),Fig 2(a),Fig 3(a). All three samples show no hysteresis and such kind of magnetic reversibility in M (H) is beneficial for the solid-state magnetic refrigeration. We have observed no bifurcation in between field-cooled cooling and field cooled warming modes of magnetization that suggests the absence of thermal hysteresis in both the samples. M vs. T (K) data in FC (open symbol) modes for 0.01 T field for the sample S1, S2, S3 is measured.

Incomplete saturation of magnetization in specimen can be related to the presence of significant 3d-4f negative AFM exchange correlations. With this data, we have calculated MCE using Maxwell's relation [69],

$$\Delta S_M(T,M) = \int_0^H \left(\frac{\partial M}{\partial T}\right)_H dH \qquad (5.1)$$

Since, isothermal M (H) curves are measured by discrete field changes, the following expression is used,

$$\Delta S_M = \sum \frac{M_i - M_{i+1}}{T_{i+1} - T_i} \Delta H_i \qquad (5.2)$$

Here, Mi and Mi+1 are initial magnetization values at Ti and Ti+1 respectively for a field change of ΔH_i. In this method, the magnetic entropy change corresponding to the average temperature T (= (T1+T2)/2) is given by the area enclosed by two consecutive isothermal M (H) curves at T1 and T2 divided by ΔT = T2-T1 (T2 > T1). We have calculated magnetic entropy change ($-\Delta SM$) using Eqn. (5.2) and is plotted with temperature for different magnetic fields as shown in the Fig4. The value of $-\Delta S_M$ is positive in the entire temperature region and increases with the magnetic field; this indicates that the magnetic field favors FM ordering. $-\Delta S_M$ increases with the decrease of temperature and a maximum change of entropy of ~ 21.8 J Kg-1 K-1 for the sample S3 and 14.4 J $Kg^{-1}K^{-1}$ for the sample S2 is observed.

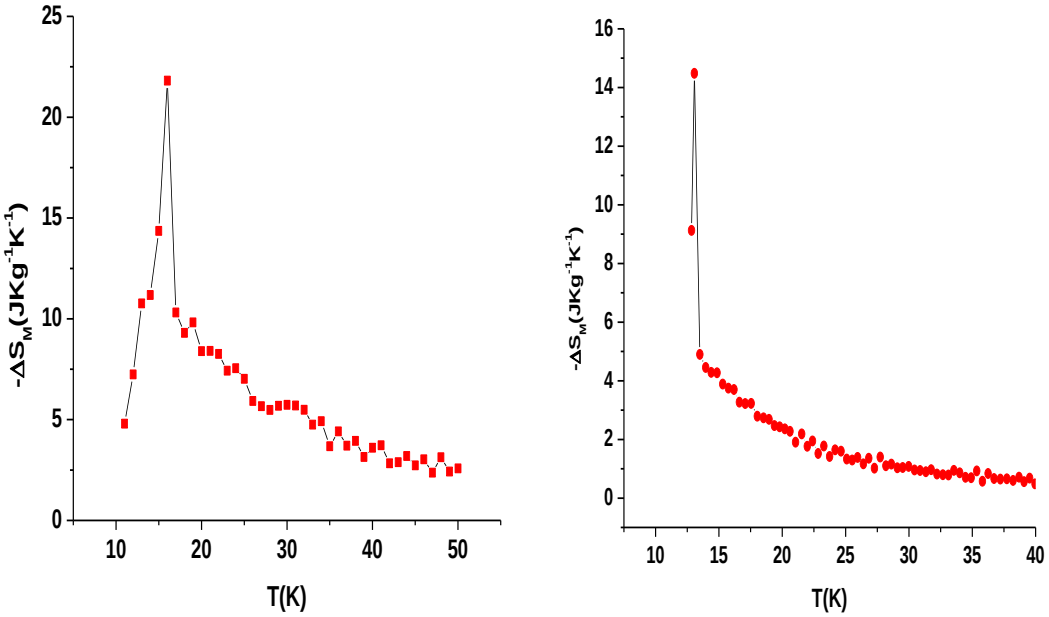

Figure 5.4 -ΔSM vs. T (K) curves measured from the magnetization curves of sample S3and S2

We have measured the electrical resistivity in these samples, and it is of the order of 10^6 Ωm at room temperature. Particularly, for low temperature refrigeration, high electric resistivity is desirable as the low resistivity of the materials can induce significant eddy current loss that limits the cooling efficiency of magnetic refrigeration process [66].

In summary, we have prepared three samples by simple solid-state reaction method and studied their magnetocaloric properties. Magnetic measurements on three sample has revealed a superior magnetocaloric performance of ΔS_M~ 21.8 KJ $g^{-1}K^{-1}$ for the sample S3 and 14.4 J $Kg^{-1}K^{-1}$ for the sample S2. Further, simple synthesis, high chemical stability, absence of magnetic and thermal hysteresis and insulating nature suggest them as potential magnetic refrigerants below the liquid hydrogen temperatures.

OVER ALL CONCLUSION

The central theme of the thesis is to investigate electromagnetic response function for dielectric material. The simplest form of the linear response is the pioneering Debye response theory. Later many prominent phenomenological non-Debye responses have been proposed. A simple form of nonlinear dielectric response function is proposed in this work. The proposed form is an extension of Debye linear response and simple one following L-C-R electric analogue of material to depict a non-Debye response function. The function of dielectric response is capable to reproduce other existing response function along with some new features. Hence, following Maxwell Granett Theory (MGT) and using the modified Clausius-Mossotti relation, the effective relative permittivity of the composite medium is formulated. Effect of electro-magnetic coupling in case of metal dielectric composite like Dilute Magnetic Dielectric (DMD) is introduced. It has found that in magneto-electric, ferroic, and chiral materials the application of magnetic fields can produce a dielectric response and the application of an electric field can produce a magnetic response. These cross coupling behaviors can be found to occur in specific material lattices, layered thin films, or by constructing composite materials. An origin of the intrinsic magneto-electric effect is from the strain-induced distortion of the spin lattice upon the application of an electric field. When a strong electric field is applied to a magneto-electric material such as chromium oxide, the lattice is slightly distorted, which changes the magnetic moment and therefore the magnetic response. Variation of real and imaginary part of dielectric constant as a function of frequency is measured at different d.c. Magnetic field (H). The results show that a substantial change in real and imaginary part of dielectric constant under variation of H in the measured frequency rage. The proposed theoretical formulation of DMD like composites (pearl and mica) and its comparison with experimental result by UV-VIS

spectroscopy shows a good qualitative agreement. Magnetoresistance, which change under the application of an external magnetic field, is also measured for DMD (NiO and CoO) systems. In this work another indigenous optical experimental setup for investigation of magnetism in a DMD is attempted. The technique exploited the Maxwell's EM theory. DMD with good reflecting surface to exhibit zero/ minimum reflectance of incident in plane polarized light. The corresponding angle of incidence is the Brewster angle. The influence of external out of plane magnetic field is to cause the variation of the Brewster angle due change in magnetism of the specimen. Authors have investigated dielectric response for four DMD (sulfide) sample i.e. Gadolinium Nickel Sulfide Complex, Cobalt Sulfide, Nickel Sulfide and Titanium. All samples were synthesized following chemical and green techniques. Later process provides good stability of the nano clusters (NC) due to in-situ capping of sample NC. All samples were synthesized following chemical and green techniques. Later process provides good stability of the nano clusters (NC) due to in-situ capping of sample NC. It has been found that the optical band gap in sample developed by green synthesis is lowered considerably over that in the chemically synthesized sample. The green agencies used in this work are Jatropha latex and dilute Garlic extracts, both are enriched in sulphur and other organic polymeric molecules.

The experimental DMD has a Ferro-magnetic or super-paramagnetic nature at room temperature. The experimental analysis indicates that obtained magnetism is mostly due to the surface magnetism which is very interesting for topological crystalline insulators. An improved version of the instrumentation could be a cost effective one for determination magnetism in such DMD specimens. Finaly, to investigate the magnetic nature of Dilute Magnetic Dielectrics (DMD) at low temperature, SQUID-magnetometry is used over the developed nano sized Gadolinium oxide, Gadolinium Sulfide and Gadolinium sulfide made by green synthesis. Gadolinium oxide nanoparticles play a central role in multimodal imaging, targeting the cancer cells and drug delivery in medical science. Magnetic Resonance (MR) images with higher resolution can be obtained with the help of contrast agents. Contrast agents are magnetic materials, either superparamagnetic or paramagnetic nanoparticles, which increases the MRI signal intensity. In this work magnetic moment is measured and magnetocalcaloric effect is also shown. Further, simple synthesis, high chemical stability, absence of magnetic and thermal hysteresis and insulating nature suggest them as

potential magnetic refrigerants below the liquid hydrogen temperatures. The presented optical indigenous experimental setup on DMD system is found to be successful one. The overall results on the study of electromagnetic response over DMD system are found to be good and consistant.

REFERENCES

[1] A.J.Dekker, solid state physics, PrenticeHall, Inc,USA(1958)

[2] E Thoms, P Sippel, "Dielectric study on mixtures of ionic liquids". *Sci. Rep*. (2017).

[3] C. Kittel, Introduction to Solid State Physics, 6th Edition, JohnWiley, NY (1986).

[4] N. W. Ashcroft and N. D. Mermim, Solid State Physics, Saunders College, Philadelphia (1976).

[5] C. J. F. Bottcher and P. Bordewijk, Theory of Electric Polarization, Vol. I and II, Elsevier, NY (1978).

[6] P T. van Duijnen, A. H. de Vries, M. Swart, and F. Grozema,Polarizabilities in the condensed phase and the local fields problem: Adirect field formulation, J. Chem. Phys. 117, 8442-8453 (2002)

[7] M. Kuhn and H. Kliem, Local field in dielectric nanospheres from a microscopic and macroscopic point of view, IEEE

[8] G. G. Raju, Dielectrics in Electric Fields, 1st Edition, Marcel-Dekker, Inc., NY (2003). http://dx.doi.org/10.1201/9780203912270

[9] C.J.F. Bottcher, P. Bordewijk, Theory of Electric Polarization,vol. 2, second ed., Elsevier, Amsterdam,(1992). http://dx.doi.org/10.1063/1.1512278

[10] N.E. Hill, W.E. Yaughan, A.H. Price, M. Davis, DielectricProperties and Molecular Behavior, Van Nostrand,London, (1969).

[11] B.K.P. Scaife, Principles of Dielectrics, Oxford UniversityPress, Oxford, 1989.

[12] S.R. Elliott, *Solid State Ionics*, 27, p131,(1988).

[13] H. Sch€afer, E. Sternin, R. Stannarius, M. Arndt, F.Kremer, *Phys. Rev. Lett.* 76, 2177. (1996)

[14] A. Bello, E. Laredo, M. Grimau, *Phys. Rev. B* 60 12764. (1999)

[15] S. Havriliak, S. Negami, *J. Polymer Science*: Part C 1499(1966).

[16] K.S. Cole, R.H. Cole, *J. Chem. Phys*. 9 341(1941).

[17] D.W. Davidson, R.H. Cole, *J. Chem. Phys*. 19 1484 (1951)

[18] A.K. Jonscher, Dielectric Relaxation in Solids, ChelseaDielectric Press, London, 1983.

[19] A.K. Jonscher, Universal Relaxation Law, Chelsea DielectricPress, London, 1996.

[20] H.L. Liu et al Ann. Phys. (Leipzig) 15, No. 7 – 8, 606 – 618 (2006).

[21] M. Dressel and M. Scheffler, Ann. Phys. (Leipzig) 15, No. 7 – 8, 535 – 544 (2006)

[22] K. Gilmore, Y. U. Idzerda, and M. D. Stiles, Identification of the dominant precession-damping mechanism in Fe, Co, andNi by first principles calculations, Phys. Rev. Lett. 99, 027204 (2007).http://dx.doi.org/10.1103/PhysRevLett.99.027204

[23]D. D. Awschalom and M. E. Flatte, Challenges for semiconductor spintronics, Nature Physics 3, 153-156 (2007).http://dx.doi.org/10.1038/nphys551

[24] J.A. Kong, Electromagnetic wave theory,(John Wiley & Sons,1986), USA

[25] J.D.Jackson , Classical Electrodynamics, 2nd Ed., Wiley Eastern Limited, India

[26] C Roychoudhuri , AF Kracklauer, K Creath . The nature of light: What is a photon. CRC Press; NY(2008). http://dx.doi.org/10.1201/9781420044256

[27] G Smith. Introduction to Classical Electromagnetic Radiation. Cambridge University Press; Cambridge, UK: 1997

[28] J C Maxwell Garnett, Phil Trans R Soc London, vol. 203,385–420, 1904.

[29] F Nasirpouri and A Nogaret, Nanomagnetism and Spintronics, World Scientific, Singapore, 2011

[30] A. H. Sihvola, J. Electromagn. *WavesAppl*.**6** 1177 (1992)

[31] E. U. Condon, *Rev. Mod. Phys*. **9**, 432 (1937)

[32]9. G. T. Rado, et al . *Phys. Rev*.**88**, 909-915 (1952) http://dx.doi.org/10.1103/PhysRev.88.909

[33] J.K.Furdyna, "Diluted magnetic semiconductors". *J. Appl. Phys*. **64** (1988). doi*:*10.1063/1.341700

[34] H Ohno, "Making Nonmagnetic Semiconductors Ferromagnetic". Science. **281**: (1998).. doi:10.1126/science.281.5379.951.

[35] S B Ogale, "Dilu9te doping, defects, and ferromagnetism in metal oxide systems". *Advanced Materials*. **22** (29): 3125–3155. (2010). doi:10.1002/adma.200903891..

[36] M.H.N Assadi, D.A.H Hanaor, "Theoretical study on copper's energetics and magnetism in TiO_2 polymorphs" *Journal of Applied Physics*. **113** (23) (2013) :233913. arXiv:1304.1854 . doi:10.1063/1.4811539.

[37] K. Kikoin and V. Fleurov Superexchange in dilute magnetic dielectrics: Application to (Ti,Co)O2 *Phys. Rev. B* 74, 174407

[38] Prestgard, M.C.; Siegel, G.; Ma, Q.; Tiwari, A. *Appl. Phys. Lett*., 103, 102409. DOI: 10.1063/1.4820145. 2013)

[39] P Misra, M *Dubinskii,. Ultraviolet Spectroscopy and UV Lasers. New York:* r. ISBN 0-8247-0668-4. (2002).

[40] Skoog, Douglas A.; Holler, F. James; Crouch, Stanley R. *Principles of Instrumental Analysis* (6th ed.). Belmont, CA: Thomson Brooks/Cole. pp. 169173. ISBN 9780495012016. (2007).

[41] 'Magnetic Property Measurement System' SQUID VSM User's Manual (2009).

[42]F. Jansson,M. Wiemer, A. V. Nenashev, P. J. Klar Petznick *Journal of Applied Physics* 116, 083710 (2014); doi: http://dx.doi.org/10.1063/1.4894236

[43] David J Griffiths,Introduction to electrodynamics/. David J. Griffiths, Reed College. – third edition 2000

[44] A.Banerjee and A. SarkarVariation of effective dielectric constant of dilute magnetic dielectrics with magnetic field *AIP Conference Proceedings***1591**, 1583 (2014); doi: 10.1063/1.4873042

[45] Somnath Paul and A. Sarkar Anomalous conduction in pure and Mn doped Gd2O3,*AIP Conf. Proc*. 1536, 587 (2013); doi: 10.1063/1.4810363

[46] Y. Tamayama, 101001T. Nakanishi, 101001K. Sugiyama, 101001M. Kitano, *phys.Rev.B* 73, 1931(2006)arxiv:physics/0511005 [physics.optics]

[47] J Hamrle, et al. (2007). "Huge quadratic magneto-optical Kerr effect and magnetization reversal in the Co_2FeSi Heusler compound". *J. Phys. D: Appl. Phys*. **40**: 1563. arXiv:cond-mat/0609688

[48] F Huang, M T Kief, G J Mankey and R F Willis *phys.Rev.B* ,(1994)3962

[49] M Benz, *Superparamagnetism:Theory and Application.* 2012.

[50] G Mathias, *Surface magnetism* , Springer, Heidelberg, NY, 2010

[51]H A Fertig, L Brey and S Zhang, *Phys. Rev. B* **96**,p 201111 (R), 2017.

[52] A Enders, R Skomski and J Honolka, *J. Phys.: Condens. Matter* **22** (2010) 433001 (32pp) doi:10.1088/0953-8984/22/43/433001

[53] K Maiti et al, Phys. Rev. Lett. 86, 2846 (2001)

[54] D Li, J Zhang, P A Dowben and M Onellion, Phys. Rev. B45, 7272 (1992)

[55] B Kim et al, Phys. Rev. Lett.68, 1931 (1992)

[56] M Donath, B Gubanka and F Passek, Phys. Rev. Lett. 77, 5138 (1996)

[57] M Bode et al, Phys. Rev. Lett.83, 3017 (1999)

[58] C Schussler-Langeheine et al, Phys. Rev. Lett.84, 5624 (2000)

[59] A Banerjee, A Sarkar, Investigation of Effective Permeability and dielectric aspect of Dilute Magnetic Dielectrics by Optical Method

[60] Tishin A M and Spichkin Y I, The Magnetocaloric Effect and its Applications (Taylor & Francis) (2003).

[61] K A GschneidnerJr, V K Pecharsky and A O Tsokol *Rep. Prog. Phys*. 68, 1479 (2005)

[62] B F Yu, Q Gao, B Zhang, X Z Meng and Z Chen *Int. J. Refrigeration* 26, 622,(2003)

[63] V Franco , J S Blázquez, B Ingale and A Conde Ann. *Rev. Mater. Res*. 42, 305,(2012)

[64] Hagmann C and Richards P L, *Cryogenics* 35, 303 ,(1995)

[65] A Kushino, Y Aoki, N Y Yamasaki, T Namiki, Y Ishisaki,T D Matsuda, T Ohashi, K Mitsuda and T J Yazawa *Appl. Phys*. 90, 5812 ,(2001)

[66] A M Tishin and Y I Spichkin *Int. J. Refrigeration* 37 223.(2014)

[67] L Zhang, S A Sherif, A J De Gregoria, C B Zimm and T N Veziroglu

Cryogenics 40, 269, (2000)

[68] Dankov S Y, Tishin A M, Pecharsky V K and Gschneidner K A, *Phys. Rev*. B 57, 3478,(1998)

[69] Pecharsky V K and Gschneidner J K A *Phys. Rev. Lett*. 78, 4494,(1997)

[70] R Sessoli Angew. *Chem. Int.l Ed*. 51,43. (2012)

[71] V K Pecharsky and K A Gschneidner J. Appl. Phys. 86, 565 (1999)

[72] Z. Y. Chen, Y. X. Wang, Y. Lin, J. S. Zhang, F. Yang, Q. L. Zhou, and Y. Y. Liao,*BioMed. Res. Int.* 2014 (2014).

[73] H. Yim, S. Seo, and K. Na, *J. Nanomat*. 2011, 19 (2011).

[74] Ananya Banerjee and A.Sarkar Investigation of Effective Permeability and dielectric aspect of Dilute Magnetic Dielectrics by Optical Method *Indian Journal of Physics* (communicated) 2019.

[75] Ananya Banerjee S Paul and A.Sarkar Low Temperature Study of Magnetism in system using SQUID magnetometry, *Adv.in App Sc Research*, (communicated) 2019.